Quantifying the Infilling of Mekong Floodplains in Cambodia using DEM Differencing

Submitted by Kieran David Cyan Bird to the University of Exeter as a thesis for the degree of Masters by Research in Physical Geography in September 2020.

I certify that all material in this thesis which is not my own work has been identified and that no material has previously been submitted and approved for the award of a degree by this or any other University.

Signature: ……

Abstract

Global sand and gravel (aggregate) extraction is changing landscapes, with 29,375x$10^6$$m^3$ to 36,875x$10^6$$m^3$ globally mined each year (Steinberger et al, 2010). Rapid economic development in South East Asia has markedly driven demand for sand in the Mekong River basin (Hackney et al, 2019). The Mekong River, a convenient source of high-quality aggregate, is the main source of sediment in the region (Kondolf, 1994; Bravard et al, 2013). Aggregate is used in the burgeoning construction industry, reclamation projects, and infilling of land along the Mekong's low-lying floodplains (Pierdet, 2008; Doyle, 2012; Mailhe et al, 2019). Questionnaire-based research found all countries that the Mekong flows through extracted material during 2010-11, of these Cambodia extracted the largest volume of at least 21x$10^6$$m^3$$yr^{-1}$ of Mekong River sediment (Bravard et al, 2013). However, the study timeframe was limited, and specific destinations of this sand were not mapped or quantified with field measurements.

This research develops differencing methods that tie the datasets together to facilitate direct comparisons between the 2000 (NASADEM) and 2013 (TanDEM-X) global elevation DEMs, a promising new approach that could be applied globally. For the Cambodia study area over 183±18 x10^6 m^3 of floodplain infill (FPI) occurred, identifying FPI the likely biggest demand for sand along the Cambodian Mekong River. Timing of FPI can be determined with annual high-resolution imagery, with peak infill activity occurring between 2010 and 2011. FPI volumes measured in this period were over 4±2x$10^6$$m^3$ greater than estimates of sediment extraction from the Mekong during 2011 (Bravard et al, 2013). FPI decreases flood risk, bringing economic and social advantages to property owners in the basin (Pierdet, 2008). But rising demand for sand in the basin has caused local channel changes and a sediment deficit being supplied to the delta, causing delta retreat and flooding, which has displaced people (Orr et al, 2012; Jordan et al, 2019). The timing and enormous scale of FPI quantified in this paper can inform future frameworks and policies, and the novel techniques provide a pathway to expanding this research elsewhere.

List of Contents

List of Tables

NO TABLE OF FIGURES ENTRIES FOUND.

List of Figures

1. Introduction

1.1 The Mekong River Basin

The Mekong River is a 4,800 km long Transboundary river, from its source in the Tibetan Highlands in China, into Myanmar (Burma), Lao PDR (Laos), Thailand, Cambodia and finally the delta in Vietnam where it meets the South China Sea (Figure 1-1) (Kondolf et al, 2018). The river initially flows for around 4000km over Palaeozoic, Mesozoic, and Granitic rocks until it reaches the alluvium of Cambodia and Vietnam, allowing it to move freely (Gupta & Liew, 2007). The Mekong basin covers 795,000 km^2, referred to as the Upper Mekong River Basin in China and Myanmar, and the Lower Mekong River Basin (LMB) spanning Laos, Thailand, Cambodia, and Vietnam (Kondolf et al, 2018).

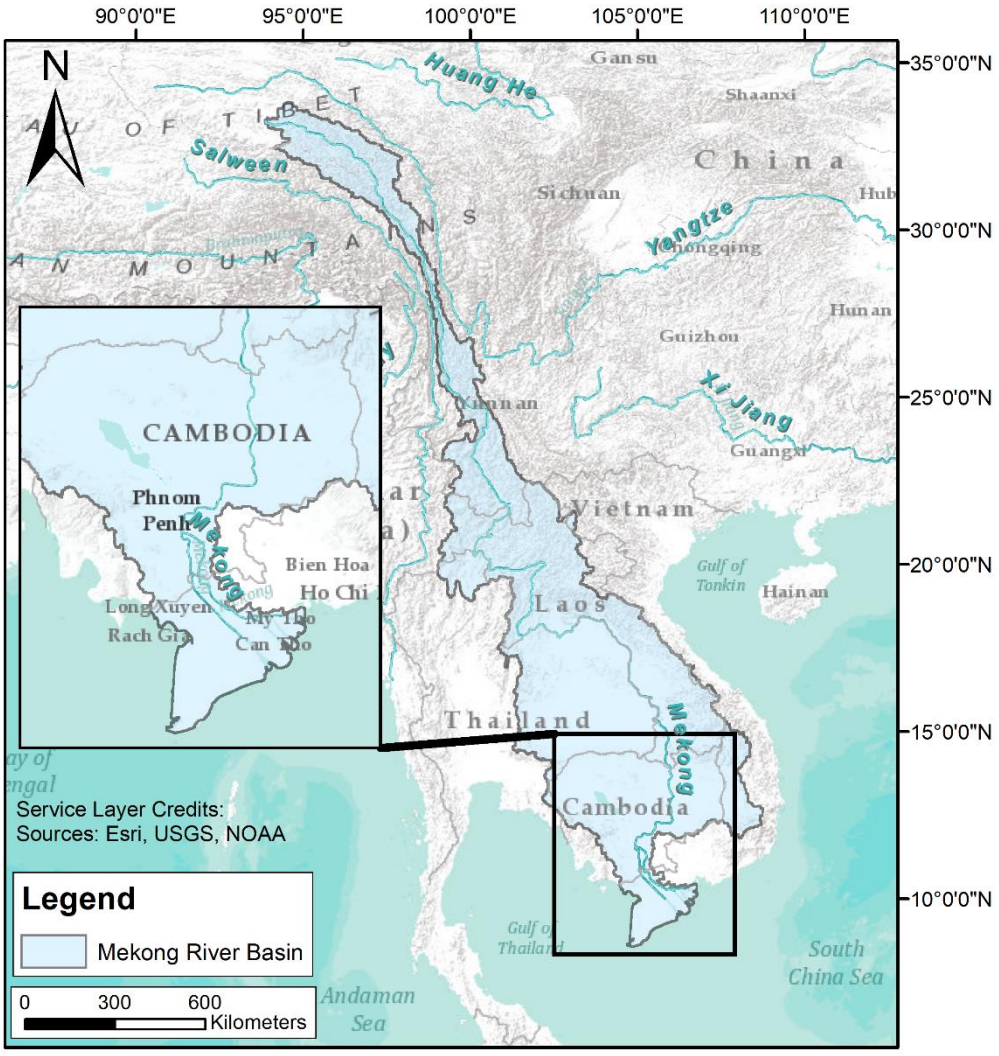

Figure 1-1: The MRB, with focus on the basin in Cambodia and the delta.

The LMB has a monsoon summer, experiencing 85-90% of annual rainfall between the months of June and October (Gupta & Liew, 2007). This causes around 130 days of monsoon flooding in the Mekong basin, which in the lower Cambodian floodplain averages a total volume of 350 billion m^3 (Bravard et al, 2013). Flooding poses a significant risk to the 70 million people that live within the LMB, therefore flood protection projects including levees and floodplain infill (FPI) have been used for decades to raise land above flood levels (Doyle, 2012; Piesse, 2016).

The Mekong River's average suspended load ranks 10th for rivers globally, estimated to be roughly 160 million tonnes per year (Meade, 1996; Bravard et al, 2013). High volumes of sediment supplied the formation of the Mekong Delta during the late Holocene, which now extends out from Phnom Penh in Cambodia through Vietnam to the South China Sea (Figure 1-1) (Nguyen et al, 2000). However economic development in the basin has increased the demand for sand. This has fuelled industrial scale extraction of sand from the Mekong River of around 50 $Mt\,yr^{-1}$, which greatly exceeds the current sand flux to the delta of $6.18 \pm 2.01\ Mt\,yr^{-1}$ (Hackney et al, 2020).

1.2 Mekong River sediment

In the LMB, downstream of Kratie in Cambodia the river has a free alluvial channel (Gupta & Liew, 2007). The thickness of sand under the riverbed is greatest around 45m near Kampong Cham in Cambodia and is around 25m south of Phnom Penh. This data was collected using coring and seismic survey methods (Kubo, 2008; Uhlemann et al 2017; Hackney et al, 2020). Sand reserves are important to the health of the river as a whole and are particularly crucial for sustaining sediment supplies to the Mekong Delta, to balance subsidence and maintain the shoreline. Sand mining is also responsible for enhancing salt-wedge intrusion on the Mekong Delta during the dry season, which increases salinization of cultivated land and damages the domestic water supply (Torres et al, 2017). The Mekong Delta is the third largest delta in the world, it is home to a population of around 20 million people and is crucial for food security as it provides half of Vietnam's food (Anthony et al, 2015). In spite of such vulnerability extraction of

sand from the Mekong river currently exceeds the sand supply to the delta by between 31 and 56 $Mt\,yr^{-1}$, resulting in a deficit in the sediment budget of the Mekong River Basin (MRB) (Hackney et al, 2020).

1.3 Aggregate demand in South East Asia

Economic development results in rapid urban expansion, which uses large volumes of aggregate for building materials such as concrete and glass, of which sand is a key ingredient (Torres et al, 2017). Fluvial sand is particularly desirable because it is a high-quality source of sediment which is often conveniently located close to areas of expansion, putting a strain on sand resources of rivers across the world (Kondolf, 1994). Worldwide cement production has multiplied three-fold in the past couple of decades, with the majority of growth experienced in Asia (Peduzzi, 2014). Singapore is the largest imported of sand in the world, mostly using aggregates to reclaim land, which has increased its land area by 20% in the last 40 years (Peduzzi, 2014). Initially much of the sand was sourced in Indonesia. However, since the turn of the century Thailand, Cambodia and Vietnam, all countries within the MRB, have made up a large quantity of Singapore's sand imports (Franke, 2014; Koehnken & Rintoul, 2018).

Rapid economic expansion within the MRB has enabled the planning and construction of hundreds of large capacity hydropower dams, which has caused international concern over the environmental impacts (Anthony et al, 2015). As sediment trapping by dams would decrease sediment supply to the delta, resulting in recession of the delta and mangrove removal along the coast (Anthony et al, 2015). Pressure from development in the basin has spurred large scale sand mining from the Mekong riverbed, which in addition to the construction of dams, will contribute to the reduction of the sediment supply of the Mekong River (Bravard et al, 2013; Anthony et al, 2015). Economic development in South East Asia has fuelled the demand for sand in the LMB, resulting in large scale trade at regional, national, and international scales (Peduzzi, 2014; Bravard et al, 2013).

1.4 Sand use in Cambodia

Cambodia's economic growth rates have been increasing 7% per year since the turn of the century (Un, 2011; Mailhe, 2019). Such economic development has enabled a six-fold increase in the construction industry between 2003 and 2008, this would have created a large demand for sand and aggregate (Nam, 2017). Fluvial sediment would be desirable for construction projections because it is high quality and convenient, as the capital city (Phnom Penh) and Kampong Cham built along the riverbanks (Kondolf, 1994). Within the MRB, Cambodia has been identified as the largest excavator of sediment, this is particularly evident downstream of Kampong Cham where the river has a free alluvial channel (Table 1-1) (Gupta & Leiw, 2007; Bravard et al, 2013). Of all the consumption of aggregate in Cambodia, floodplain infill activity has been uniquely identified as the largest consumer of sand drawn directly from the riverbed (Bravard et al, 2013).

Table 1-1: Volumes of sediment, divided into material type, extracted from 6 sections along the Mekong River (Bravard et al, 2013).

Reaches	**Thousands of cubic metres per year**			
	Sand	**Gravel**	**Cobbles**	**Total**
Upstream of Vientiane	87	0	7	94
Vientiane - Savannaketh	4,154	1,107	367	5,628
Savannaketh - Champasak	341	29	80	450
Cambodia upstream of Kompong Cham	580	2,038	0	2,618
Kompong Cham - Vietnamese border	18,160	7	0	18,167
Delta, Vietnam (Bassac + Main channel)	7,750	0	0	7,750
Total	31,072	3,171	454	34,707

Within the MRB, the largest consumer of sand excavated directly from the riverbed has been identified as floodplain infill (FPI) (Bravard et al, 2013). FPI is used to elevate the land, in the natural depressions surrounding the Mekong, above the seasonal flood levels within the basin (Figure 1-2). Phnom Penh, the capital of Cambodia, has been a hotspot for FPI activity since French Colonials introduced infill methods in the 1860's in order to expand the city from the Mekong banks across the seasonally flooded depressions (Doyle, 2012). In modern times FPI is used in the same way to elevate land above flood levels, and has been said to increase the value of land by up to five times, due to the increased protection and security from flood risk (Pierdet, 2008). In Phnom Penh multiple projects have infilled lakes to reclaim land for valuable development in densely populated urban areas (Figure 1-2) (Schneider, 2011). FPI therefore continues to play a vital role in protecting infrastructure in the low-lying floodplains on the LMB, however such activity increases the demand for sand in the basin (Bravard et al, 2013). This process has put strain on the main source of sand in the basin; the Mekong riverbed (Kondolf, 1994).

Figure 1-2: Photograph of infill activity in Boeng Kak Lake in Phnom Penh, Cambodia (Schneider, 2011).

Large scale sand mining in the Mekong River, to fuel this demand for sand, has been shown to have detrimental geomorphic, environmental, and human impacts (Brunier et al, 2014; Piesse, 2016; Kondolf 2018). Sand mining has been shown to affect the geomorphology of the Mekong as a result of bed lowering, which induces bank instability and erosion, eventually impacting infrastructure along the rivers banks (discussed in section 2.2) (Kondolf, 1994; Brunier et al, 2014). The Mekong River delta is also vulnerable to reductions in sediment supply caused by a combination of sand mining and dam construction, also further impacted by projected sea level rise (Kondolf, 2018). Environmentally, sand mining impacts the instream and riparian habitats, which affect fish stocks and reduce biodiversity (Padmalal et al, 2008). Each of these impacts are exacerbated by additional anthropogenic forcing within the MRB including dam construction and irrigation (Anthony et al, 2015). Nearly 10 million households rely on the Mekong river for their livelihoods and food, with such impacts putting stress on them (Piesse, 2016). On the delta outmigration of residents has already begun, from a combination of many impacts, illustrating the local understanding of the environmental risk which has been induced (Szabo et al, 2016).

1.5 Research focus on floodplain infilling

Research by Bravard identified Cambodia as the largest excavator of sediment per year in the 2011 to 2012 period within the MRB (Bravard et al, 2013). However, to understand the scale of the sand industry within Cambodia, it is important to understand the main driver for the demand for sand. Therefore, this paper will aim to quantify the scale of FPI within the study area in Cambodia (Figure 1-3), in order to fill a gap in the scientific knowledge of the drivers in the demand for sand in the Mekong Basin (Bravard et al, 2013). This knowledge of the scale of FPI can ultimately help understand the main driver for the demand for sand, and aid policymakers in making sand extraction and trade sustainable within the basin. This paper will not quantify the consumption of sand used in building materials by the construction industry, or land reclamation, and other uses of sand which all accumulate to increase the demand for sand. Instead this paper aims to put floodplain infill (FPI) under the microscope, to improve understanding of sand consumption in Cambodia. Understanding the drivers of

sand extraction is an important step in creating and enforcing regulatory frameworks which reduce sand extraction from rivers, to establish a sustainable balance between the sediment storage, supply, and mined material (Hackney et al, 2020).

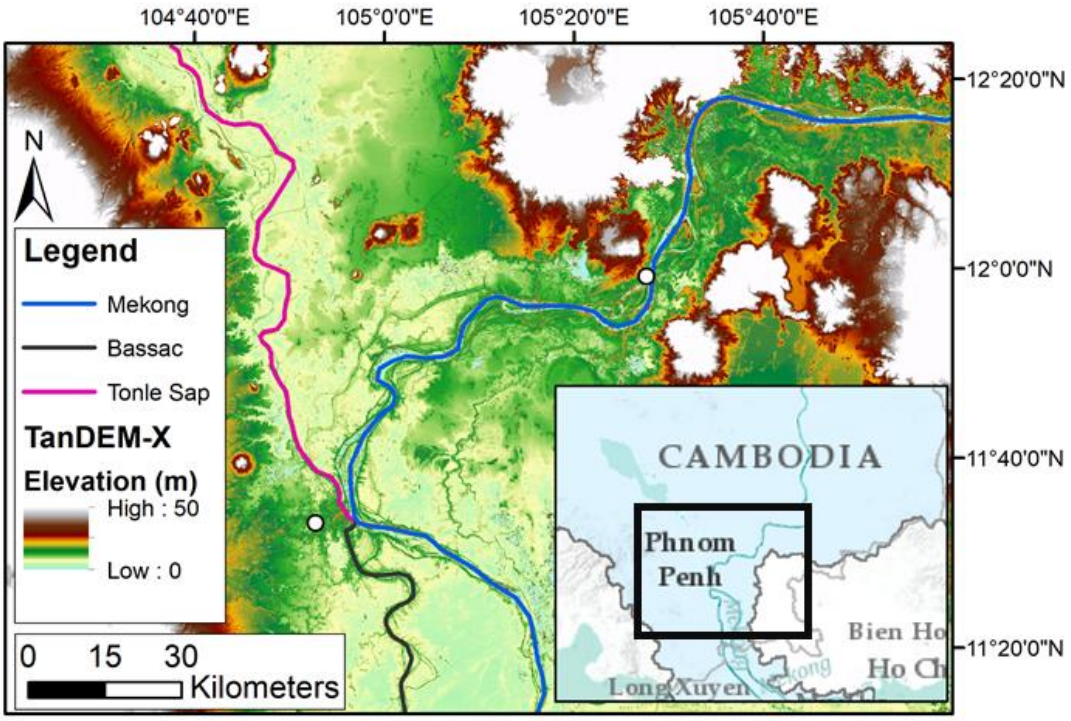

Figure 1-3: Site study map, with each of the main rivers overlaid on TanDEM-X elevation data.

1.6 Digital Elevation Models for Cambodia

Remote sensing techniques provide a view of land surfaces, enabling measurements of surface changes to be made which can be used in river basin management, without ever coming into contact with it (Lillesand et al, 2004). Digital Elevation Models (DEM) can be derived from active or passive remote sensing techniques. Passive techniques can include structure from motion photogrammetry (Díaz-Varela, 2015). Whereas active derived DEMs use instruments emit radar signal towards the earth and measure the reflected signal. Radar can penetrate cloud cover and as it does not rely on sunlight, can be effectively acquired at any time of day unlike some passive remote sensing techniques (Musa, Popescu & Mynett; 2015).

The Shuttle Radar Topographic Mission (SRTM) provided a global dataset of 1 arc second resolution (Nominally 30m) DEMs, captured in February 2000 (Hayakawa et al, 2008). SRTM has had numerous succeeding releases, up to the most recent floating point reprocessed NASADEM release, with 1 arc second resolution (Crippen et al, 2016; Purinton & Bookhagen, 2018). SRTM was collected using radar interferometry, which has been enhanced in NASADEM using Ice, Cloud, and Land Elevation Satellite (ICESAT) ground control points to improve the surface elevation data (USGS, 2020). An along-track filtering approach used differences between the SRTM heights and ICESat GLAS elevation data to correct the SRTM strip DEMs, including reductions in height ripple error (Buckley et al, 2020). The original SRTM dataset was shown to have a significant stripping pattern across the Mekong Delta, originating from uncompensated shuttle boom motion and other systematic height errors (Minderhoud et al, 2019). However, the Height Ripple Error Correction used in NASADEM mitigated such systematic errors to 'nearly eliminate' their impact (Buckley et al, 2020). The enhanced SRTM dataset: NASADEM was used in the research for this thesis, referred to as NASADEM. There are alternatives such as Terra Advanced Spaceborne Thermal and Reflection Radiometer (ASTER) produced DEMs from optical sensors, however it is documented that these DEMs have worse vertical accuracies than radar, and persistent high frequency artefacts in the data (Tachikawa et al, 2011; Purinton & Bookhagen, 2017).

TanDEM-X was a more recent global DEM mission collected from 2010 to 2015 using radar techniques, to produce 0.4 and 1 arc second resolution DEMs (~ 12 and ~ 30 m respectively) (Purinton & Bookhagen, 2018). Elevation difference studies revealed that SRTM showed a high level of consistency with TanDEM-X data, however there are errors in ASTER data resulting from mismatches in adjacent scenes in the photogrammetric process (Grohmann, 2018). DEM differencing between SRTM (2000) and TanDEM-X (2013) has been shown to be effective in measuring natural and human changes in land elevation and can be repeated across the global coverage of the two datasets (Grohmann, 2018; Purinton & Bookhagen, 2018). The scalability of SRTM and TanDEM-X differencing has been proven with accuracy, and effectiveness, making it an

appropriate methodology to look at recent changes over the large areas of the Mekong River Floodplain in Cambodia (Purinton & Bookhagen, 2018).

It is important to discuss the vertical accuracies of both NASADEM and TanDEM-X as this will induce uncertainties in the results comparing the two datasets. The original SRTM dataset (from which SRTM was derived), had a standard accuracy value of 16m in its specification, however comparisons with CGIAR field datasets in neighbouring country Thailand (Phuket) showed average vertical errors of 7.58 ± 0.60 m (Gorokhovicha & Voustianiouk, 2006). In this work greater error values were associated with rugged terrain, as slope and aspect have a negative impact on the accuracy of the SRTM dataset (Gorokhovicha et Voustianiouk, 2006). Recent TanDEM-X specifications set a target absolute vertical accuracy of 10m, with a 2m relative accuracy for slopes <20% (Hawker et al, 2020). Benchmarking testing of TanDEM-X and SRTM against high resolution airborne LiDAR (Light Detection and Ranging) DEMs which typically has a vertical accuracy of <20cm to fulfil accuracy assessments at a large scale, have been carried out for 32 floodplains globally, including the Mekong (Hawker et al, 2020). Using nearly 64,000 reference points the average vertical accuracy (RMSE) was 1.09m for TanDEM-X and 2.57m for SRTM (Hawker et al, 2020). Such vertical inaccuracies will therefore have an impact on the accuracy of the comparisons between the two datasets, which has tried to be accounted for using bare earth control methods tie the elevation datasets together to minimise relative differences.

TanDEM-X was created using the X-band signal with a 3.1cm wavelength, which is reflected from a surface (such bare earth, building or a tree). The X-band signal can partially penetrate vegetation with the scattering properties dependant on the species (Purinton & Bookhagen, 2018; Hawker et al, 2020). The SRTM, most recently floating-point-reprocessed for NASADEM, produced the interferometric synthetic aperture radar (InSAR) DEM from C-band radar, with a 5.6 cm wavelength (Purinton & Bookhagen, 2018). TanDEM X-band and SRTM C-band radar have different penetration depths in dense vegetation (Purinton & Bookhagen, 2018). The different interactions with the ground surface of C-band and X-band result in biases in elevation at different land surfaces, as shown when comparing SRTM (C-band) and TanDEM-X (X-band) with LiDAR data in 32 floodplains across the earth (Table 1-2).

In principle the radar would have been on a Satellite in the case of SRTM and TanDEM-X, each time energy is sent by the imaging radar a radar footprint is formed on the ground, which is made up of many small cells (Figure 1-4). At each ground cell the echo is backscattered then received and recorded as a pixel in the image plane according to the slant range between the antenna and the ground cell (Chen et al, 2000). Backscattering is dependent on the land surface, for example water surfaces have a low backscatter which means elevation values are very noisy (UN, 2020; Hawker et al, 2020).

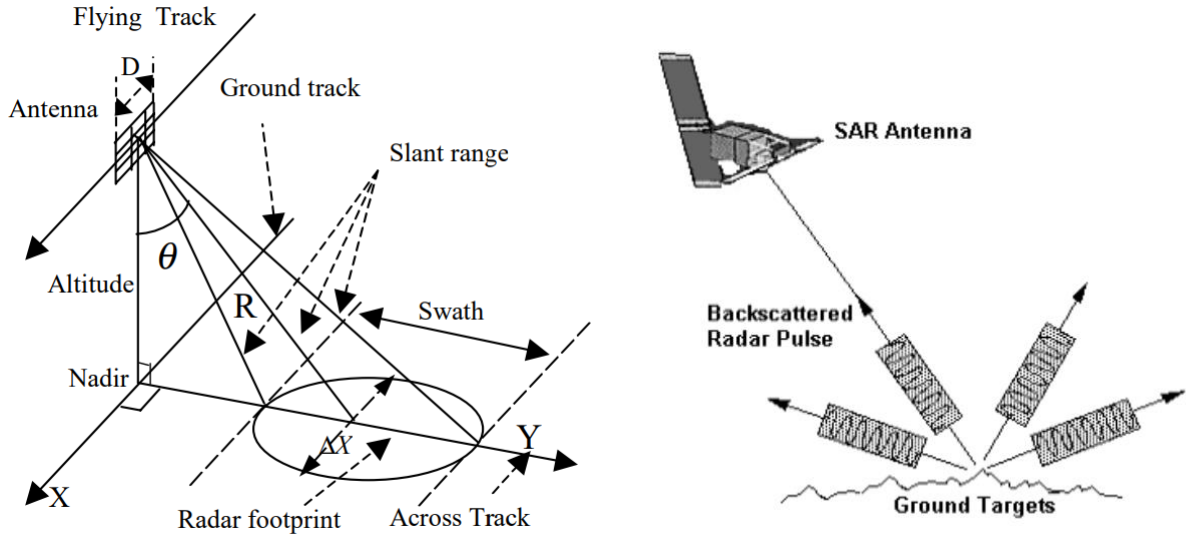

Figure 1-4 – On the left the Radar geometry principles (Chen et al, 2000) and on the right showing the backscattered to the Antenna by the ground surface (UN, 2020).

Table 1-2: DEM dataset vertical accuracy based on root mean square error (RMSE) calibration with LiDAR datasets across 32 floodplains globally (Hawker et al, 2020).

Land Surface	DEM	No. of Reference Points	RMSE (m)
Bare	SRTM	6860	2.99
	TanDEM-X (90)	6619	2.04
Short Vegetation	SRTM	769432	3.07
	TanDEM-X (90)	762798	2.12
Tree Cover	SRTM	291352	6.04
	TanDEM-X (90)	251150	5.68
Urban	SRTM	107958	3.14
	TanDEM-X (90)	149233	2.38

The non-void filled (SRTM data only) NASADEM was used to ensure consistency of the original data source. rather than being void filled from other data sources such as ASTER, which would have differing dates of collection and processing methods (Purinton & Bookhagen, 2018). The non-void filled NASADEM dataset is also referenced to the WGS84 ellipsoid vertical datum, the same as TanDEM-X, whereas previous SRTM data were refenced to EGM96 (Purinton & Bookhagen, 2018).

1.7 Volumetric change measured by DEM differencing

To assess national scale changes in the land surface, remote sensing methods have been adopted as this allows for analysis of a greater area, over a relatively longer period of time than could be achieved by fieldwork. In the past couple of decades multiple DEMs with global coverage have been produced, notably SRTM in 2000, ASTER in 2008 and TanDEM-X in 2014 (Hayakawa, Oguchi & Lin, 2008; EO, 2020). As such datasets have been released, DEM differencing methods have started to be used to measure volumetric changes of other processes which change the earth's surface, including landslides and of lava flow (Bagnardi et al, 2016; Purinton & Bookhagen, 2015). Such methods allow analysis of large-scale study areas, without ever coming into contact the study site. This makes them easily accessible across the world, and with global coverage of the DEM datasets it is possible to repeat all over the earth. These benefits come with greater uncertainty than physical surveying techniques, due to the way the data is collected, and the radar interacts with the land surface (as described in section 1.6) (Purinton & Bookhagen, 2015; Hawker et al, 2020). This paper will use DEM differencing methods due to the feasibility and benefits of assessing a large study site, but this will come with significant uncertainty. The DEM differencing will measure anthropogenic changes to land elevation, from floodplain infill. The NASADEM and TanDEM-X datasets will be tied together using control areas of bare earth to minimise the relative differences, bare areas are used as they have been shown to have the better vertical accuracy (of around 2-3m for SRTM and TanDEM-X) compared to vegetated areas and tree cover (Table 1-2Table 1-2: DEM dataset vertical accuracy based on root mean square error (RMSE) calibration with LiDAR datasets across 32 floodplains globally

(Hawker et al, 2020). The absolute accuracy of the elevation of both datasets will not improve through this method, however this is not a requirement for the volumetric measurements between NASADEM and TanDEM-X in this research.

1.8 Societal impacts in the Mekong Basin

There are multiple integrated natural and anthropogenic forcings on the Mekong River sediment budget, upon which many of the ecosystems in the basin rely (Kondolf et al, 2018). The largest cumulative threat is in the Lower Mekong Basin (LMB) and the delta, with populations of over 70 million and 17 million respectively (Piesse, 2016; Kondolf et al, 2018). It is estimated that 80% of these populations are directly dependent on the Mekong River for their livelihoods and food (Piesse, 2016). It is important to understand the processes which impact the MRB, and the ways in which they can increase vulnerability in the future.

Climate change poses a critical threat to the MRB safety and sustainability (Hoang et al, 2016). Environmental change is expected to alter the monsoon rain's timing and intensity in the MRB, noticed in recent years, resulting in more frequent high discharge events and exacerbate flood risks in the basin (Hoang et al, 2016; Pokhrel, 2018). In turn this flooding will considerably modify aquatic ecosystems and devastate crops, disturbing the reliant populations (Piesse, 2016).

Sea level rise projections are also likely to impact the Mekong Delta, causing saltwater intrusion which will affect crops and drinking water sources (Pokhrel, 2018). Additionally, coastal erosion and flooding is a likely impact of sea level rise, which may mean inhabitants are forcibly displaced from the delta, resulting in climate change refugees (Orr et al, 2012; Anthony et al, 2015; Jordan et al 2019). The natural ecosystems in the Mekong Basin, are forced to co-evolve under rapid human development, which has been seen to cause many issues (Pokhrel, 2018).

Within the Mekong Basin in the past few decades the greatest human processes impacting the river have been identified as construction of hydropower dams, land use change, irrigation and sediment extraction (Bravard et al, 2013; Anthony et al, 2015; Kondolf et al, 2018). Each of these processes integrate together,

combined with natural forcings, to put extreme stress on the geomorphology, ecosystems, and people within the MRB; with the greatest vulnerabilities in the LMB and the delta (Pokhrel, 2018). Anthropogenic processes within the basin provide economic or security benefits to benefactors of each project, however the long-term negative impacts throughout the system as a whole are undervalued at the planning stage.

In the LMB there has also been an increase in deforestation to turn areas into urban and agricultural land, caused by socio-economic development (Costa-Cabral et al, 2008). Increases in agricultural areas adversely affects the surface roughness and albedo of land. Plus, irrigation supplies extra water, which can alter both the energy and water balance (Pokhrel et al, 2018). The expansion of urban areas within the basin, in conjunction with climatic changes in precipitation and projected sea level, rise has been determined to result in significant increase in flood risk in Vietnam on the delta (Huong & Pathirana, 2012).

Construction of hydropower dams have a huge potential to provide up to 53,0000 MW of power to the region, due to the Mekong Basin's strong topographic gradient and high flow volumes providing ideal engineering conditions for dam construction (Stone, 2011). China has been developing hydropower dams in the Upper Mekong (Lancang River), creating a cascade of six mega dams, with an additional 12 planned or under construction (Magee, 2011). Laos, Thailand and Vietnam have also tapped into the hydropower potential of the Mekong, and there are dams under construction and planned in all of the countries that make up the Mekong Basin (Figure 1-5) (Hecht et al, 2019). Existing dams in the Mekong have already caused trans-boundary impacts at a large scale, and the construction of additional dams is expected to compound these impacts. Such as blocking fish migration, changing water levels, and impeding sediment delivery to the Mekong delta (Kummu et al, 2010; Stone, 2016; Kondolf et al, 2018). Reductions to the sediment supply and resources in the Mekong are exacerbated by sediment extraction from the river channel, which directly reduces the volume of sediment within the river system (Bravard et al, 2013; Kondolf et al, 2018).

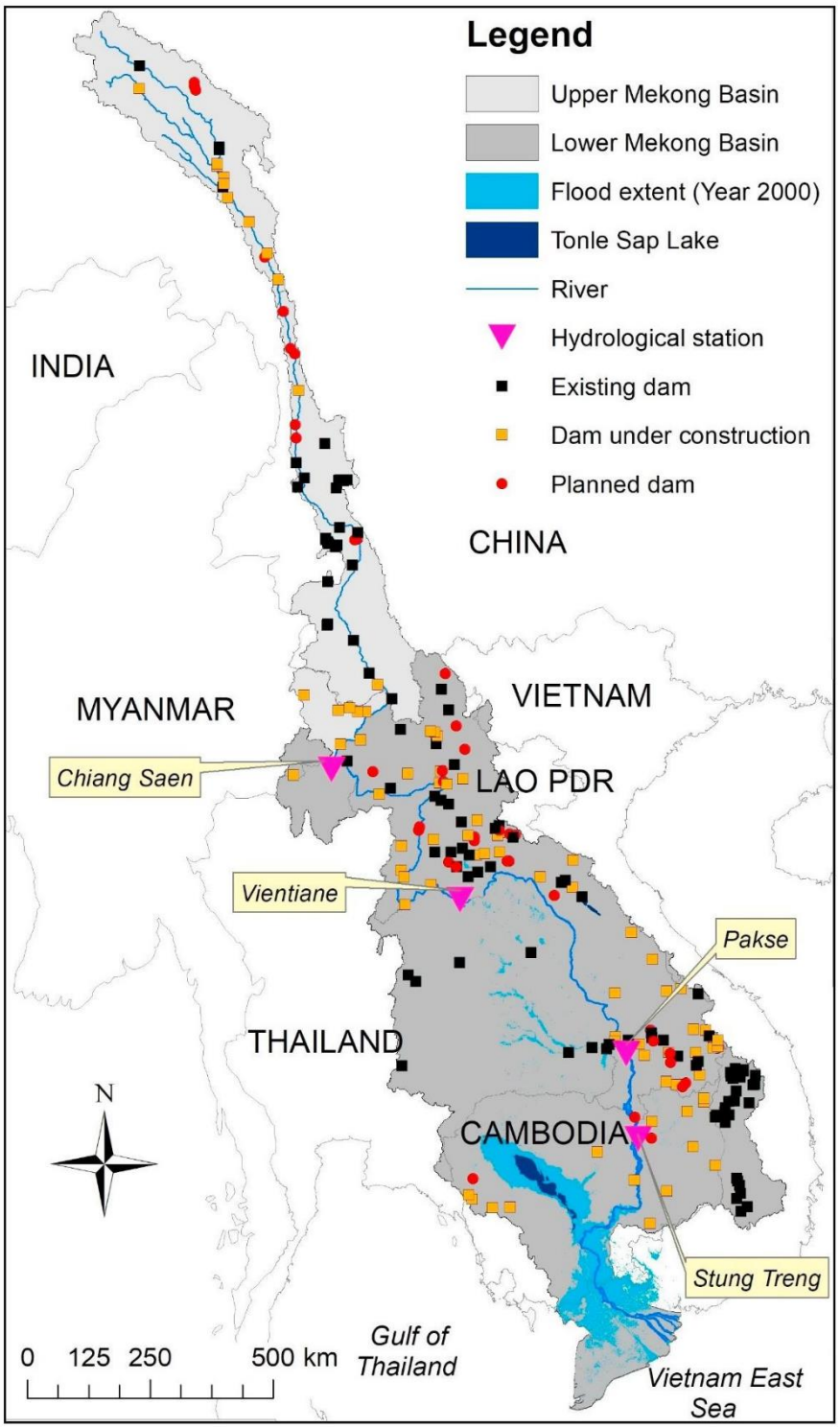

Figure 1-5: Hydropower dams within the MRB, and the flood extent in the year 2000 (Hecht et al, 2019).

1.9 Sand mining in the MRB

In the MRB rapid economic development over the past few decades has fuelled the demand for sand, and riverbeds are often convenient sources of high-quality aggregate (Kondolf, 1994; Hackney et al, 2019). Recent investigations have shown that the current rates of sand extraction (50 Mt yr^{-1}) exceed the total sediment flux being delivered to the Mekong delta (6.18 ± 2.01 Mt yr^{-1}) by over 40 Mt yr^{-1} (estimated bulk density of 1600 kg/m^3 for sand) (Bravard et al, 2013; Hackney et al, 2020). Under such rates of extraction riverbed levels have been shown to lower, inducing bank instability, which can ultimately damage infrastructure (Brunier et al, 2014; Hackney et al, 2020). Sediment extraction has already been identified as a main reason for shoreline erosion of the Mekong Delta measured between 2003 and 2012, combined with dam retention of sediment and subsidence just to groundwater extraction (Anthony et al, 2015). These impacts highlight that the Mekong delta and the LMB are the areas of greatest vulnerability, and also the areas where the largest volumes of sediment extraction take place (Bravard et al, 2013; Pokhrel, 2018).

In the LMB the largest consumer of sand extracted directly from the riverbed has been identified as FPI, where the sediment is used to fill the low-lying floodplains above flood levels (Bravard et al, 2013). It is therefore vital to have a better understand of the scale of FPI activity in the basin, where there is currently a gap of understanding in the scientific literature. By filling this gap this paper will aim to help advise policymakers on FPI and give them a better understanding of the drivers behind sediment extraction. This will enable regulatory frameworks to be established which will enforce sustainable FPI practices and consequently reduce the demand for sand in the basin, ultimately helping the balance between sediment extraction and the natural supply to become sustainable (Hackney et al, 2020). This is necessary in order to protect the health of the MRB from detrimental damage to the geomorphology, ecosystems and to the millions of people who rely upon it (Brunier et al, 2014; Piesse, 2016; Pokhrel, 2018). In order for this to be achieved, this paper will first use DEM differencing methods to measure the volumes of FPI from 2000 (NASADEM) to 2013 (TanDEM-X within the study site) for the Cambodian Mekong River Basin near Phnom Penh. Then this data will be compiled over time and location to explore any patterns of

FPI needed to better understand the temporal and spatial scales of the main driver for sediment extraction.

1.10 Research aims

The overarching aim of this thesis is to improve the understanding of the volumes of sand used in Floodplain Infill (FPI) activities in Cambodia. This can be broken down into the following smaller research aims:

- Identify areas of FPI within the study site in Cambodia.
- Develop a robust approach by reducing relative differences and exploring uncertainties in datasets to measure the volumetric changes in the areas of FPI.
- Compile and analyse the scale of FPI over time and space.
- Quantify likely sources of FPI material.

Understanding the source of sediment is vital in understanding the sustainability of the aggregate used in FPI activities in Cambodia. Possible sources that will be investigated include imported sand, quarried material, and fluvial aggregate.

2. Literature Review

2.1 Understanding the impacts of sediment extraction

In the 1970s sand and gravel mining had become the largest non-fuel industry in the United States, in 1972 alone 913 million tonnes were produced to fuel growth in the construction industry (Bull & Scott, 1974; Newport, 1974). During this expansion large amounts of sand and gravel were extracted from river channels, as the aggregate is of high quality and convenient (Newport, 1974). With these large-scale operations, insight into the potential impacts on river systems has become an important area for academics to study. Thus, understanding the drivers of the increase in the demand for sand is of paramount importance to be able to reduce excavation and the effects this has on river systems globally.

2.2 Geomorphic impacts

During the early stages of research, examples began to show that bed lowering from sediment extraction made riverbanks more susceptible to erosion, resulting in increased potential of undermining nearby infrastructure (Bull & Scott, 1974). It was initially recorded by Bull & Scott that pits created from sediment excavation result in upstream scour for long distances. This was further supported by subsequent research showing that pits can act as knickpoints which erode upstream in a process called ‘headcutting’ (Bull & Scott, 1974; Kondolf, 1997). Such observations of upstream erosion of excavated pits have been documented in subsequent investigations. More recent research introduced the idea of downstream propagation of incised pits, as the sediment load is reduced but the river still has the capacity to transport sediment, causing downstream erosion (Kondolf, 1994; Kondolf, 1997). Kondolf has been able to clearly visualise all of these geomorphic impacts to the river channel when sediment is extracted from the bed (Figure 2-1).

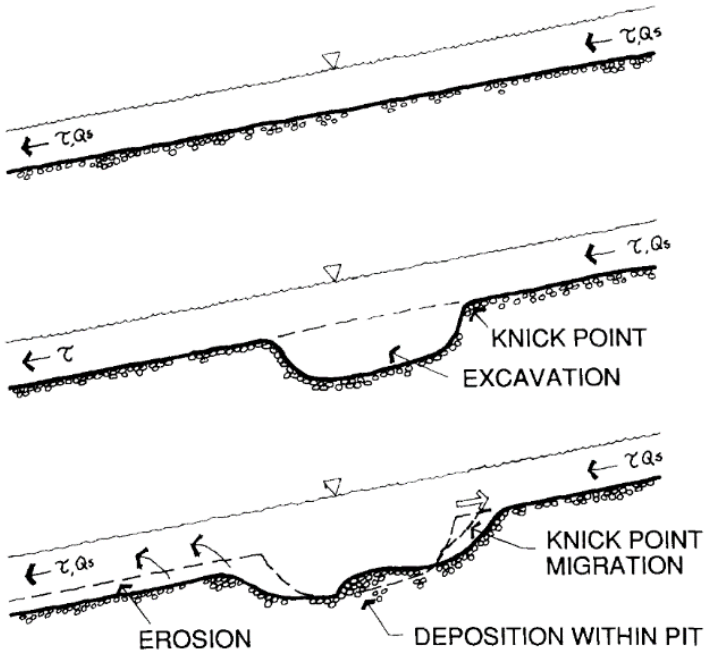

Figure 2-1: The impacts of instream sand mining on long profile sections of a riverbed. The top shows no sand mining activity, the middle shows recent excavation creating a pit, and the bottom of the diagram shows the upstream and downstream propagation of the pit from erosional and depositional processes (Kondolf, 1994; Kondolf, 1997).

In areas where riverbeds have deepened due to sediment excavation, theories of bank instability began to be conceptualised. This was supported by research on the San Juan Creek and Stony Creek in California where increased channel instability caused undercutting of banks making the channels wider. Channel instabilities in Stony Creek undercut a highway bridge, which cost over US $1.5 million to repair (Kondolf, 1994). This highlights that a large economic cost was another important step in getting business operations and decision makers to take the effects of sediment extraction more seriously. Bank instability has also been observed due to sediment extraction from rivers with much larger catchment sizes. In Italy damage to bridge structures was observed along the banks of The River Arno which has a catchment area, over four times the size of the previously mentioned creeks, of 8,228km^2 (Rinaldi et al, 2005).

Much larger rivers in the developing world have started to see the effects of sediment excavation since the 1990s. The mid-lower Yangtze River in China has been heavily impacted by sand mining, with approximately 26 Mt/yr extracted in the 1980s rising to 80 Mt/yr by the end of the 1990s. The Yangtze River has also been impacted by the construction of at least 50,000 dams including the Three Gorges Dam, which combined with sediment extraction has had a tremendous impact on the sediment supply from $466x10^6\ yr^{-1}$ in 1978 to 294Mt/yr in 1998. This has decreased progradation rate of the delta and caused erosion in some areas (Du et al, 2016). Since 2000 sand mining has been banned in the Middle and Lower reaches of the Yangtze River, however these localised bans mean that excavation operations have moved rather than ceased. Poyang Lake, which feeds into the Yangtze River, has since become home to sand mining at an unprecedented scale with estimated $236x10^6\ m^3yr^{-1}$ extracted between 2005 and 2006 (Leeuw et al, 2009; Zhao et al, 2017). Leeuw revealed this by analysing high-resolution ASTER imagery, initiating opportunities for studying sand mining with remote sensing techniques (Leeuw et al, 2009).

The Mekong River has also been impacted by sand mining and the construction of dams, and similar to the Yangtze River, it has a delta which is home to nearly 20 million people (Orr et al, 2012). On the Mekong Delta in Vietnam channel deepening has been measured between 1998 and 2008 using bathymetric data, as a direct result of large-scale sediment excavation by Brunier. Abnormally deep pits existing pre-1998 that had propagated by 2008 so additional large and irregular incisions were abundant (Brunier et al, 2014). The pits created by sand mining were further eroded by the flow of the river meaning they increased in size, propagating up and downstream as was theorised by Kondolf (Kondolf, 1994; Brunier et al, 2014). Brunier is also in agreement with earlier studies that channel deepening caused by in channel excavation increases bank instability, supported by observations of channel widening for the first time in a significantly larger river channel (Brunier et al, 2014).

In recent years Kondolf has focused his research on the Mekong River, looking into the cumulative impacts on the sediment budget due to the vulnerability of the Lower Mekong Basin and Delta. Kondolf stated the main anthropogenic pressures on the Mekong River include dams sand mining, construction of

infrastructure on the delta and global climatic changes. Although it is difficult to determine the exact contribution of sediment extraction among these factors, sand mining can be attributed to causing damage to infrastructure through bank collapse and retreat of the delta coastline (Kondolf et al, 2018). Fears of delta instability have been further compounded by research by Hackney who demonstrated that currently the total sand flux to the Mekong delta (6.18 ± 2.01 Mt yr^{-1}) is far less than sand extraction rates (50 Mt yr^{-1}) (Hackney et al, 2020). This deficit of sediment being supplied to the delta support Kondolf's ideas of the recession of the delta coastline, which would be exacerbated by the combined impact of dam sediment retention (Kondolf et al, 2018; Hackney et al, 2020). Findings from these key academic papers looking at the impacts of sediment extraction are summarized below (Table 2-1).

Table 2-1: Key studies over time of the impacts of sediment extraction on water bodies around the world. Information about sediment extraction is outlined alongside additional disturbances referred to which would have had a combined effect. The impacts on each river are then defined generally based on morphological, environmental and structural impacts where appropriate.

River/ waterbody and region	Watershed features	Sediment excavation	Additional disturbances	Impacts	References
River in Tuscon, Arizona	7.6m sandy gravel bed in area of bridge	Between 1965 and 1973, sandy gravel above the base of bridge lowered by 4m	None documented	Bed lowering, bank instability and increased potential of undermining bridges	Bull & Scott, 1974
San Juan Creek, California	347 km^2 basin size river	Gravel pit excavated	None documented	Channel incision which cause channel widening from undercutting of banks	Chang, 1987 cited in Kondolf, 1994
Stony Creek, California	2,010 km^2 basin size river	Sediment excavation incised channel which migrated laterally	Black Butte Dam construction in 1963	Channel instability that undercut highway bridge costing over US $1.5 million	Kondolf and Swanson 1993 cited in Kondolf, 1994
River Arno, Italy	8228 km^2 basin size river	Predominantly gravel bed sediments	Dam construction	Incision which led to damage to bridge structures	Rinaldi et al, 2005
Yangtze River, China	9th largest catchment basin in the world (1.8 million km^2) with delta	Developed in the middle and lower reaches in the 1990s, subsequently banned in 2000	Dam construction and soil conservation	Combined reduction of sediment supply, which has triggered erosion at the front of the delta	Du et al, 2016
Poyang Lake, China	Largest freshwater lake in China, includes six protected areas	Started in 2001 after sand mining in Yangtze river was banned, calculated rate of sand extraction of 236 million m^3 $year^{-1}$ in 2005–2006	Water impounding and sediments trapping from dams	Highly turbid waters, with fears of effecting biodiversity which would affect millions of wintering birds (further environmental impact assessments needed)	Leeuw et al, 2009; Zhao et al, 2017
Mekong River, South East Asia	795,000 km^2 drainage basin, diverse from mountains to low lying floodplains and delta	Estimated 34,446,983 m^3yr^{-1} extracted in 2011	Construction of dams and irrigation	Significant incision and expansion of pools, average bed deepening of 1.3m in Mekong and Bassac channels on the delta, contributing to bank instability and shoreline erosion of the delta	Bravard, et al 2013; Brunier et al 2014; Kondolf, 2014

2.3 Environmental impacts

Although dredging can be seen as good for keeping rivers and routes navigable and for flood mitigation, there are detrimental impacts from excavating from the riverbed, especially in an uncontrolled mining fashion. Bull & Scott highlighted the importance of monitoring the natural and anthropogenic changes in the physical environment, showing an early consciousness of environmental impacts (Bull & Scott, 1974). Around the same time Newport began to explore the ecological impacts of sediment removal from water bodies, as the removal of bed material is a loss of habitat for aquatic life. Also increased turbidity would affect light penetration which could affect the productivity of plankton and the benthic community which feed the fish population (Newport, 1974). This was revolutionary in a time where sediment extraction was focused on economic development and impacts from bank instability near infrastructure; beginning to give value to the environment of the river system.

In the 1990's Kondolf judged that the environmental costs were still not valued in production costs, so began to evaluate methods of environmental impact analyses. Kondolf reiterated that sand mining would reduce riparian habitat and increase turbidity which would impact benthic invertebrate and shift populations of fish to species tolerant of turbid conditions. Within this paper studies from parts of the Naugatuck River in Connecticut have demonstrated that sand mining has widened the channel in which the water is nearly stagnant during low flows. With low levels of dissolved oxygen creating near unhabitable areas for aquatic life (Kondolf, 1994). However, as Kondolf neglected these points in the conclusive statements, the full potential was not reached. Instead, recommendations could have been given to help learn from such environmental impacts in the future.

In cases where sediment has been excavated to improve channel connectivity for shipping routes, for example on the Niger Delta in Nigeria, other environmental impacts have been observed. Channels were dredged to access oil and gas reserves found in the geological structure of the Delta, and sediment was often abandoned on the banks as the aim of the operations was not to mine the aggregate. Nearly 50 years since dredging began on the delta environmental impacts where assessed by Ohimain, who found alterations to the delta topography and hydrology, as well as acidification and water contamination, all

of which damaged the fragile mangroves and killed fish (Ohimain, 2004). This paper came after nearly half a century of dredging activity on the delta and did an excellent job of looking into the future at how restoration projects can be effective. In this case to the topography and thus the hydrology which allowed mangroves to grow back, showing the bounce back ability of ecosystems when the environment is restored. Ohimain also introduces ideas of management plans and regulations which would ensure the large oil and gas companies would have to carry out Environmental Impact Assessments for their work and mitigate the impacts from dredging on the delta and its ecosystem (Ohimain, 2004).

Poyang Lake ecosystem is rich in biodiversity that has been impacted by large scale sand mining. The lake is a particularly important site for millions of migratory birds, so in order to protect the biological diversity the Poyang Lake National Nature Reserve was established. Leeuw reiterated concerns over the impacts of turbidity in ecosystem productivity, and further introduced fears that noise from mining operations may affect the echolocation of the critically endangered Yangtze finless porpoise (Leeuw, 2009). This raised the importance of protecting such biodiverse ecosystems from the effects of sand mining. A vital step in informing policymakers to control the scale of sediment extraction to sustainable levels. Research into the environmental impacts of sand mining will be needed at each unique site to fully understand what is needed to limit and mitigate the negative impacts.

The environment in the Mekong basin and delta is vulnerable to sand mining as well as dam construction, which both of which have negative impact that can perpetrate throughout the entire river. On the delta there has also been pumping-induced subsidence of up to 3 cm yr^{-1}, and there are fears over sea level-rise (Kondolf, 2018). A combination of these forcing's has increased the environmental hazards in the basin, particularly in the delta where outmigration of residents has begun (Szabo et al, 2016). This illustrates the local understanding of the environmental risk which has been induced. The majority of scientific papers have predominantly focused on the geomorphic impacts of sand mining on the Mekong River, neglecting research into the environmental impacts. Bravard's research aimed to raise awareness of the scale of sand mining operations in the basin, illustrating their importance in management natural

resources and biodiversity conservation (Bravard et al, 2013). Further research has continued to focus on the geomorphic impacts, including Anthony's paper on the rapid erosion of the Mekong River delta due to human activities. In addition, Anthony and a later paper by Torres began to theorise the possible environmental impacts of sediment extraction from the Mekong, which consist of disruptions to the productivity of fish populations that would in turn effect food security. They also described how sand mining enhances salt-wedge intrusion in the dry season, this increases the salinity in the water used for domestic and agricultural use (Anthony et al, 2015; Torres et al, 2018). In 2018 Kondolf gave an excellent overview of the current understanding of the environmental impacts on the Mekong River. Concluding that better understanding of the cumulative impacts on the Mekong basin which support highly diverse ecosystems which many inhabitants' livelihoods rely on, is needed for producing the most effective planning to minimise future impacts on human livelihoods (Piesse, 2016; Kondolf et al, 2018).

2.4 Factors effecting the MRB

Understanding the drivers of change in the MRB is vital to be able to mitigate and manage the river system in a sustainable manner. The delta, which houses the largest population and the greatest agricultural production in the Mekong basin, has been heavily focused on in academic literature. As the delta is affected by the accumulation of upstream factors as well as climatic changes and sea level rise. Without mitigating action, it is likely that by 2100 almost half of the Delta's land surface will be below sea level (Kondolf et al, 2018). In addition, climate change is projected to alter temperature and rainfall. During the wet season in the Mekong Basin much of the sediment load is mobilised, in Kratie for instance almost 1/3 of the suspended sediment load is forced tropical cyclone induced runoff. Therefore, Darby has shown that changes in cyclone peaks will likely have a substantial impact in the suspended sediment of the river system (Darby et al, 2016). Changes to the sediment supply from climatic changes will impact the already vulnerable delta, which will be combined with sediment reduction from anthropogenic activity.

The Lower Mekong Basin has a population of over 70 million people, with 80% of the households in the region directly depending upon the river for their livelihoods and food (Piesse, 2016). This illustrates how there are vulnerabilities within the population from many types of impacts. Research into the vulnerabilities of the largest city on the Mekong Delta, Can Tho, was carried out by Huong and Pathirana, using urban drainage modelling methods to assess the flood hazard resulting from urban growth and projected climatic change (Houng & Pathirana, 2013; Anthony et al, 2015). This research successfully highlighted that flood hazard risk is expected to increase in business as usual scenarios, due to urbanisation, sea level rise and climatic change. However, it failed to mention the impact of contributing factors such as dam construction, sand mining and irrigation.

Environmental and Geomorphic impacts on the Mekong River have been largely driven by sediment extraction and dam construction. In 2008 The Mekong was described as one of the least regulated large river basins, at a time where active reservoir storage amounted to just 2% of its mean annual discharge (Kummu et al, 2010). However, over the past decade and looking into the next decade increases in dam construction mean the active reservoir storage is expected to rise to between 17-23% by 2025. This is also supported by data from the Mekong River Commission (MRC) which expect it to be equal to 19% without the inclusion of numerous dams in the extent of the Mekong in China (MRC, 2011; Hecht et al, 2019). In conjunction with sediment trapping due to dams it was estimated that 34,446,983 m^3yr^{-1} of sediment was extracted from the Mekong between 2011 and 2012, 60% of which in Cambodia (Bravard et al, 2013). This estimate gave the first real quantification of the scale of sediment excavation from the Mekong River, stressing the effectiveness of Cambodia's ban on sand exports which was enforced in 2009 (Global Witness, 2010). Although the survey method used by Bravard allows for underestimates, as mining operations must pay fees for the volumes extracted, so would be inclined to declare excavation data as low as possible. The questionnaire method also fails to quantify all illegal sand mining operations.

2.5 Legislation of sand excavation

Newport outlined the earliest ideas of legislation in the United States of America (USA), where in 1899 the Rivers and Harbours Act was put in place to stop industries discharging matter which would cause obstruction in navigable channels (Newport, 1974). In essence encouraging the removal of sediment from channels to ensure they are navigable. Throughout the 20th Century up to the writing of Newport's paper in 1974, over 100 bills concerned with polluting waterbodies were passed, showing an active commitment to limiting industrial impacts on water quality (Newport, 1974). These bills were simply outlined and written about in terms of general causes of water pollution, leaving the reader to tie the causes of such pollution such as sand mining operations. River aggregate has long been regarded as a source of high-quality aggregate, meaning without proper enforcement of bans, or a reduction in the demand for aggregate, sand mining will continue to thrive (Bull & Scott, 1974).

The demand for sand in South East Asia, stems from economic development which increases construction and land reclamation activity. Over the past two decades Singapore has imported over 500 million tonnes of sand, more than any other nation (United Nations, 2019). Malaysia was one of the fastest nations in Asia to notice the detrimental impacts coastal and fluvial sand mining was having, resulting in the ban of natural sand exports to be placed in 1997 (BBC, 2017). It was also recognised by Vietnamese authorities that sediment extraction from the Mekong River has caused substantial environmental externalities, catalysing the ban of international sand exports in 2000 in Vietnam (Kondolf, 2018). However, Bravard explained how Cambodia then replaced Vietnam in serving Singapore's demand for sand, meaning sediment removal from the Mekong continued (Bravard et al, 2013). This shows the failings of international management in the MRB, as each country only wanted to make the largest economic gain from the natural resources the Mekong provides, without regarding the health of the whole river system. After nine years of exploiting the Mekong for its high-quality aggregate Cambodia followed suit and banned international sand exports. Unfortunately, these bans do not limit sand excavation for national use and bans on export have been shown to be poorly enforced by investigating imports on UNComtrade from countries such as Singapore since 2009 (Peduzzi, 2014).

2.6 Global drivers of sand extraction

Sand mining was first documented in the USA, with demand for high quality aggregates coming from the booming construction industry which accounted for 96% of sand and gravel use. In 1974 Newport gave one of the first in depth insights into the increasing scale of sand excavation since 1950 in USA. He explained expertly how sand excavation had been fuelled by the increased demand and it was this that resulted in the long term trend of increased prices (Figure 2-2) (Newport, 1974). This deeper explanation perfectly illustrates how use of sand in the growing construction industry, increases the demand and in turn the value of aggregates making sand mining profitable. This is a concept that can be applied to the global trade of sand today.

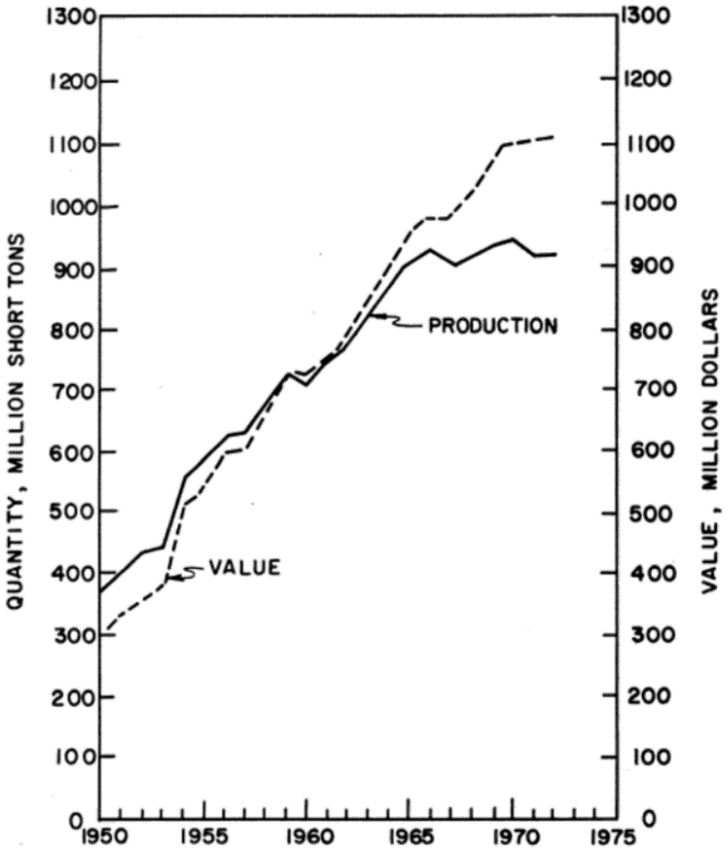

Figure 2-2: The rates of production and the value of sand over time in the United States (Newport, 1974).

Asia has experienced rapid economic growth that triggered the expansion of the construction industry, that requires extremely high quantities of aggregate to create concrete. The Mekong Basin is no exception to this, as the economic development in Cambodia, Thailand and Vietnam has resulted in a high demand for sand (Bravard et al, 2013). In the low-lying floodplains of Cambodia and Vietnam, in order to protect infrastructure, there is a long history of buildings being built on stilts or being infilled in order to raise them above flood levels. In Cambodia floodplain infill (FPI) originated in the capital city, Phnom Penh. FPI began to expand rapidly between 1863 and 1953 when French colonists wanted to expand the capital outwards from the Mekong River's banks onto the wetlands and floodplain (Doyle, 2012). References to FPI in Cambodia have continued to be qualitatively evaluated, describing how the scale continues to increase as more landowners can afford to by sand to elevate their land above flood levels, which Pierdet said can increase the value of the land by up to five times (Pierdet, 2008). With prolonged increases in land value in Phnom Penh, lakes have begun to be infilled with sediment for developments to be built on them (Doyle, 2012; Schneider, 2011). However, due to a lack of bathymetric data the volumes of sand used are unknown. Mialhe's research measured the quantitative increase in Phnom Penh's urban area from 30km^2 in 1973 to 250km^2 in 2015, with FPI, wetland and lake infilling highlighted as key processes in the expanse (Mialhe et al, 2019). The imagery analysis of surface area within this study meant that it was not possible to measure volumetric changes in FPI, which would give a better insight into the scale of sand use in Cambodia.

In Singapore, the population increased by a factor of three in 50 years, it was this that resulted in large scale infrastructure development. Due to the small land area of Singapore, land reclamation was carried out. This has increased the land area by more than 20% in the last 40 year, creating more land for development. Because Singapore does not have the natural sand resources that many of its neighbouring countries have, it has imported 517 million tonnes of sand in the last 20 years to feed construction and reclamation activity (Peduzzi, 2014). Singapore is now the largest importer of sand in the world, illustrating that the modern demand for sand has increased the value to make the international trade of this natural commodity economically viable and profitable.

2.7 Why alluvial sand?

Alluvial sand, that in particular from riverbeds, is especially desired because the flow of water eliminates weak materials through abrasion and attrition leaving the remaining durable high-quality sediment (Kondolf, 1994). The high demand for sand and gravel excavated from riverbeds was first documented in the United States by Bull & Scott, because of the high quality of the aggregate. They also introduced the idea of river sediment being a convenient source of aggregate for the construction industry, as developments would often be situated on the floodplain close to a river which would reduce travel costs (Bull & Scott, 1974). Therefore, sediment excavation will be focused closest to the development occurring in urban areas of big, expanding cities. However, as the value of sand increases, for example the case of Singapore, the exports can become economically viable and the convenience of sand plays less of a part. Sand has become a commodity fuelling global construction development and reclamation efforts, with fluvial sediment a highly desirable source of aggregate. It is important to understand the uses of sand in order to reduce the demand and lower the economic value of sand, as this will ultimately facilitate sustainable management of sand mining more effectively than previously failed bans.

2.8 Methods in measuring demand for sand

The trade of sand in South East Asia has been widely reported, including research into the drivers of rising demand, to the rates of sediment extraction. Volumes of sediment extraction have been estimated by Dung for a 20km section of the Cau River in Northern Vietnam, which revealed the scale of illegal sand mining operations, as only 7 permits for mining had been issued meaning 85% of operations were illegal (Dung, 2011). However due to a lack of resources, Dung's research had limited site area, so without replicated research in other sections of rivers it is hard to definitively make sweeping comments of sand mining operations across Vietnam and the wider region. Bravard's later calculations of sediment extraction were funded by the WWF enabling surveys which spanned the whole MRB. The upscaling to a basin-wide survey gave the first quantitative figures of the volumes of sand extracted from the Mekong River. However, due

to the questionnaire style research errors stemmed from under reporting volumes, and a lack of repeat surveys meant there was no temporal range (Bravard et al, 2013).

Accurately measuring the scale of sand mining operations has been limited by the underreporting of data, as operations try to hide from quotas and bans that are in place, and illegal operations can be too dangerous to approach. Misreporting of data has also been discovered within international trade of sand by Peduzzi. By looking at differences between the volumes Singapore have imported, and the volumes of four neighbouring countries (Indonesia, Malaysia, Thailand, and Cambodia) have reportedly exported to Singapore. Over the past 20 years Singapore reportedly imported 517 million tonnes of sand, however four neighbouring countries reported exporting a total volume of sand 120 million tonnes more to Singapore (Peduzzi, 2014). Peduzzi concluded that this variation highlights the need for better monitoring of trade, as previous methods failed to investigate and clearly describe the reasons behind such differences. It is likely that as these records are from 1995 onwards Indonesia, Malaysia, Thailand and Cambodia were all eager to report volumes exported to show economic development through international trade before bans were put in place. The figure in Peduzzi's paper shows that after 2006, when bans started to be placed on sand exports in the four countries, Singapore began to report larger imported volumes than exports from the four exporters (Peduzzi, 2014). Although Peduzzi failed to explain this trend, the graph shows this which not only shows the importance of accurate reporting of volumes, but also the importance of enforcing trade bans accurately.

International trade figures are also limited as they do not include any national sand trade and usage. In the MRB in 2011, Cambodia was the largest excavator of sediment from the Mekong River (Bravard et al, 2013). Since then Mialhe has investigated how the capital, Phnom Penh, has developed between 1973 and 2015 and how sand has been utilised in this. Mialhe used supervised classifications of Landsat Imagery, combined with on field reference points to measure the growth of developments within the capital from 30km^2 to 250km^2 over the 42-year study period (Mialhe et al, 2019). The use of remote sensing techniques enabled Mialhe to cover a larger study area than Dung's on field

research with significantly fewer resources required (Dung, 2011). Mialhe also measured for the first time the scale of infilling Phnom Penh's wetlands, which rose from 4.3 km^2 to 46.2 km^2 in just 25 years (Mialhe et al, 2019). However, the surface area of lake and wetland infill does not show the volume of sand which would have been used. In order to calculate this, bathymetric survey data of such water bodies would have been needed before infill activities had begun. This limitation is also the case for the surface area measurement of development, which could have utilised DEM's to measure elevation differences to calculate volume changes in sites of interest, such as FPI. Studying the volumes of sand used at a larger scale across Cambodia is therefore something that would greatly benefit academia and policy makers in their understanding of the demand, use and excavation of sand in Cambodia. Outlined below are some of the key papers which have completed research related to measuring the demand for sand (Table 2-2).

Table 2-2: Key studies over time which have measured the scale of the demand for sand, including the location, key drivers, results, methods, and limitations.

Region/ Country	Activity/ Operation	Volumes of sand	Methods	Limitations	References
Bac Ninh Province, Northern Vietnam	FPI and construction industry creating demand for river sand caused by growth in construction industry and FPI	Estimated extraction from the Cau River on a 20km downstream section increased from 500-800 m^3/day up to 2005 to 1000-3000 m^3/day, with over 85% of surveyed extraction sites illegally operating	Field observations and focus groups of sand mining in the Cau River to understand the current situation of sand mining, combined with the collection of secondary data	The scale of the research was limited to a 20km section of the Cau River, no measurements were made meaning estimates were derived from qualitative observations	Dung, 2011
Mekong River, South East Asia	Sand Mining (extraction)	Estimated 34,446,983m^3yr^{-1} extracted in 2011	Systematic survey using questionnaires at extraction sites, at minimum recording the volume and category of sediment extracted	Questionnaire's relied on honest reporting of data, unable to measure illegal operations and limited temporal range	Bravard et al, 2013
Singapore	Singapore's sand imports, also compared to exports to Singapore from Indonesia, Malaysia, Thailand and Cambodia	Singapore imported 517 million tonnes of sand in the last 20 years, however exports from neighbouring countries to Singapore are 120 million tonnes greater	Utilising reported data on UNComTrade, and analysing it graphically	Limited reliability of the volumes reported, although that is used to make a point about how these countries are trying to cover up some of this activity	Peduzzi et al, 2014
Phnom Penh, Cambodia	The spatial growth and urbanisation of Phnom Penh from 1973 to 2015, predominantly through construction and different types of infill	The urban footprint of Phnom Penh went from 30km^2 to 250km^2, including wetland reclamation for urban development which rose from 4.3 km^2 to 46.2 km^2 between 1990 and 2015, such as lake infill	Remote sensing techniques, utilising supervised classification of Landsat Imagery which was enhanced by field observations	Wetlands can be hard to define, particularly if imagery has been collected during different seasons	Mialhe et al, 2019

2.9 DEM Differencing

DEM differencing is a remote sensing technique which has been widely used to measure changes in elevation of the land surface over time, from the date of collection of one dataset to another. Such methods have been commonly used in the cryosphere, where change in the elevation occur relatively quickly, meaning they can be measure in annual timesteps. For example, this allowed Berthier to measure elevation changes of glaciers in the Himalayas between 2000 (SRTM) and 2004 (SPOT5 satellites optical images). In this research the standard deviation of elevation points surrounding the glacier were minimised to improve the accuracy of the elevation measurements of the glacier. This is a particularly useful method as the surrounding mountain would have been stable over the four-year study period. By measuring the volume of the glacier Berthier was able to calculate that the mass balance was between -0.7 and -0.8 m/a, however the difference in data collection between SRTM and SPOT5 increased the uncertainty. This means that in the future it would be better for similarly collected and processed datasets to be compared (Berthier et al, 2007).

As new DEM missions are carried out and new datasets are released, differencing methods have started to be used to measure volumetric changes of other processes which change the earth's surface (Bagnardi et al, 2016; Purinton & Bookhagen, 2018). Bagnardi compared pre-eruptive topography from TanDEM-X DEM with the post-eruptive Pleiades-1 DEM to calculate mean estimates of the volume of lava flow, demonstrating how this method can be used to measure process which rapidly alter the land surface (Bagnardi et al, 2016). TandDEM-X DEM was also used by Purinton & Bookhagen to calibrate SRTM data for differencing to measure landslides in south central Andes. They acknowledged that TanDEM-X as a new high accuracy dataset which can be used to calibrate long standing biases in SRTM in order to measure elevation changes at smaller magnitudes from river processes. Calibrating the two datasets was the main focus and success of this paper and allowed comparisons and measurements to be made. The conclusion was that average rates of elevation changes in gravel-bed rivers were of 0.2 to above 0.5 m yr^{-1} (Purinton & Bookhagen, 2018). However, there are still limitations with the application of DEMs in this study site due to the reduced accuracies stemming from the steep

slopes and heavy vegetation in the Andes. This study aims to develop the capabilities of TanDEM-X and SRTM by reducing the relative differences between the datasets to measure land surface changes for low relief surfaces at a higher degree of accuracy than has previously been possible, before the release of TanDEM-X.

2.10 Justification of differencing

DEM differencing has been shown to be useful for measuring natural processes that alter the land surface elevation. This is particularly notable within the recent production of the TanDEM-X DEM which has been successfully calibrated with SRTM and Pleiades-1 DEMs (Bagnardi et al, 2016; Purinton & Bookhagen, 2018). However, such differencing has not been used to measure anthropogenic process as the differences are usually too small to measure or occur over a longer time period than the ~13 years between SRTM and TanDEM-X. FPI is likely to be an exception to this due to its industrial scale in the MRB over the past couple of decades (Bravard et al, 2013), which means that large areas of low-relief land surfaces are available for these comparisons. Therefore, this thesis will aim to utilise TanDEM-X and SRTM (NASADEM) DEM datasets to produce a first insight into the scale of FPI in Cambodia. The availability and near global coverage of the DEM datasets used in this method is a key benefit. As previously acknowledged, there are uncertainties in elevation measurements. But the relative differences between datasets have been reduced in this research by using bare earth comparison methods to determine a regional offset between NASADEM and TandDEM-X.

2.11 Research objectives

The overarching aim of this thesis is to improve the understanding of the volumes of sand used in Floodplain Infill (FPI) activities in Cambodia, as previously stated. To achieve this, applying DEM differencing methods, a number of objectives for this research project have been laid out:

- Identify unchanged bare earth control sites to assess systematic offsets and thereby calibrate NASADEM (2000) and TanDEM-X (2013) for accurate inter-comparisons.
- Identify and record areas of FPI within the study site in Cambodia, focusing on those with low relief surfaces.
- Measure the volumetric changes in the areas of FPI between NASADEM and TanDEM-X.
- Use annual high-resolution photos to determine when FPI occurred for each study site.

In addition, it is an aim of this research to understand the likely source of sand used in FPI activity in Cambodia. This will be addressed with the following objectives:

- Identify the closest likely fluvial source for any FPI material.
- Identify and measure the volumes of alternative local sources of sediment from nearby quarries and floodplain mining.
- Investigate and analyse Cambodia's natural sand trade data, for imports and exports that can be considered along with FPI.

This paper aims to improve the understanding of the scale of FPI activity in Cambodia since the turn of the century. This can then be used in to inform future policy and decision making within the LMB.

3. Methods

3.1 DEM preparation

NASADEM, developed from the original SRTM in 2000 and TanDEM-X were the main DEM datasets used in this research. The updated NASADEM, created by NASA derived from the original SRTM telemetry data, was also downloaded for the study area in Cambodia. Surface elevation measurements were improved in the final NASADEM product using ground control points from ICESAT, and comparisons with ASTER (USGS, 2020).

NASADEM was projected from the provided EGM96 MSL reference to a common EGM2008 geoid MSL reference, allowing for direct comparisons with TanDEM-X. The difference between Geoid and Ellipsoid can be seen spatially in Figure 3-1. The geoid is determined by the earth's gravity and approximated from the Mean Sea Level (MSL), whereas the ellipsoid shape was calculated based on the hypothetical equipotential gravitational surface (ESRI, 2003). The difference between the heights of the ellipsoid and geoid is the geoid height (N) (Figure 3-1).

The NASADEM (SRTM) is the most recent floating-point reprocessed release, with 1 arc second resolution (~ 30 m). The non-void filled (SRTM-only) version was chosen to ensure consistency of the data sources, such that only sites with actual radar elevation data were included in the analysis. Therefore, this research version of NASADEM uses data solely from the SRTM mission in February 2000, rather than being void filled from other data sources such as ASTER, which would have differing dates of collection and processing methods (Purinton & Bookhagen, 2018). Both NASADEM and TanDEM-X used active radar techniques to produced global coverage DEMs, and differencing methods using the two datasets have shown to be very effective in measuring changes in the earth's surface from human and natural processes (Grohmann, 2018; Purinton & Bookhagen, 2018).

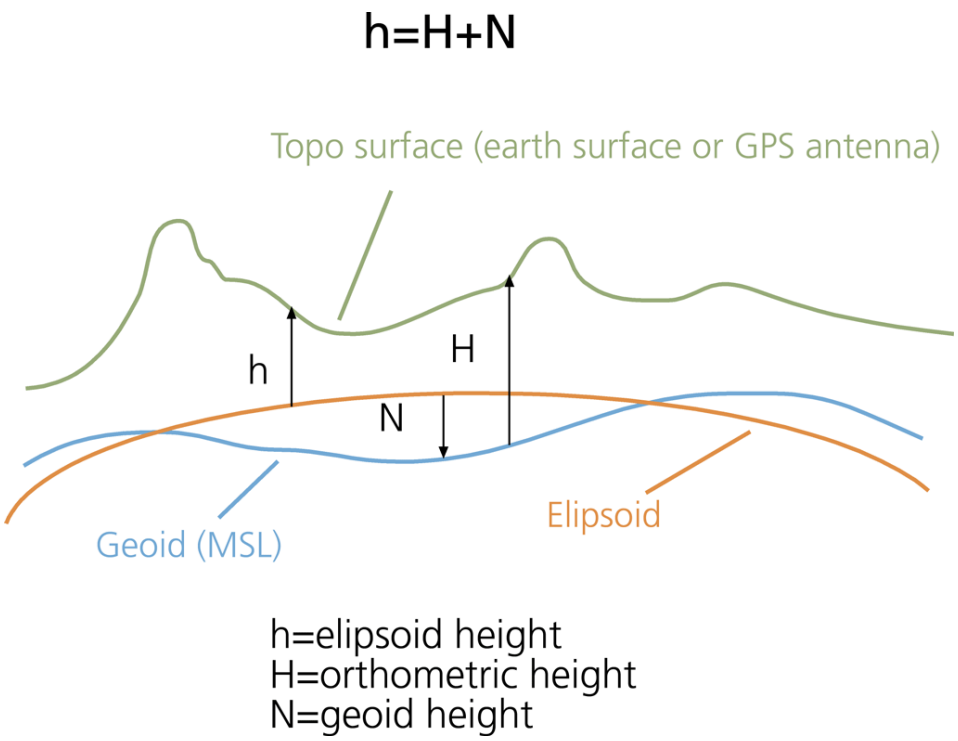

Figure 3-1 - The difference between Geoid and Ellipsoid (ESRI, 2003).

NASADEM (SRTM) was collected during the dry season in between 11th and 22nd of February 2000 (USGS). In February the Mekong water level is relatively low, therefore the extent of surface water was relatively small (Figure 3-2). NASADEM was therefore collected at a time of year to get the best look at the surface of the earth in Cambodia, as radar techniques are far less accurate over water bodies (Zandbergen, 2008).

All TanDEM-X satellite bistatic scenes were collected between December 2010 and January 2015. Importantly, the acquisition layer metadata revealed that the dates of data capture were between December 2010 and July 2013 for this study area. By noting the dates of the first, second, additional, first crossing and second crossing acquisitions (of which the ones that actually have data for a specific area), provides exact dates that TanDEM-X data was collected for the specific study sites. This therefore narrowed the temporal window of TanDEM-X for the study, by providing a more accurate end date of data collection. There is also additional uncertainty from water bodies during the dates of TanDEM-X collection, which could provide random relief due to low backscattering and

temporal de-correlation (Wendleder et al, 2012). The water layer TanDEM-X provided had a larger extent than from SRTM and was useful for avoiding areas which would have been affected by water on the earth's surface.

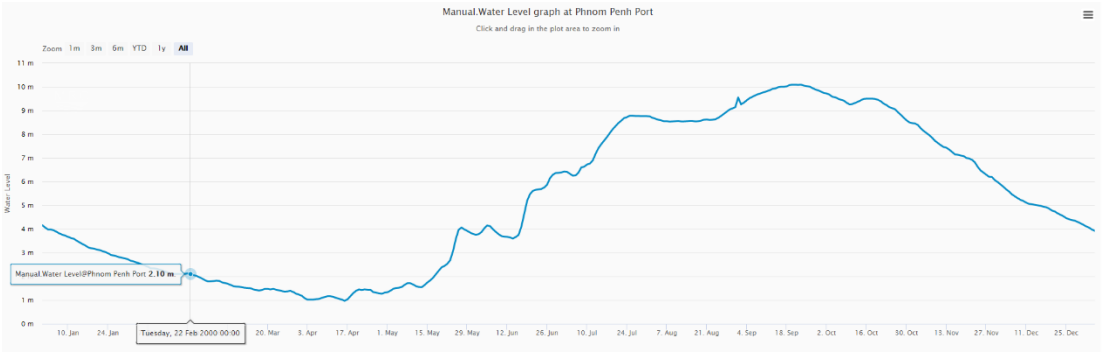

Figure 3-2 – Water level at Phnom Penh Port at during time of SRTM collection compared to the rest of 2000 (MRC, 2020).

Both NASADEM (SRTM) and TanDEM-X datasets were collected using Synthetic aperture radar (SAR) techniques, that use radar instruments on satellites to form high resolution radar images (Purinton & Bookhagen, 2018). In general, the primary limitation of InSAR is due to the scattering properties of the earth's surface. This is because the relative movement of these scatters, cause the scatter contribution to sum differently, known as decorrelation, depicted in Figure 3-3 (Zebker and Villasenor, 1992; Hooper et al, 2012).

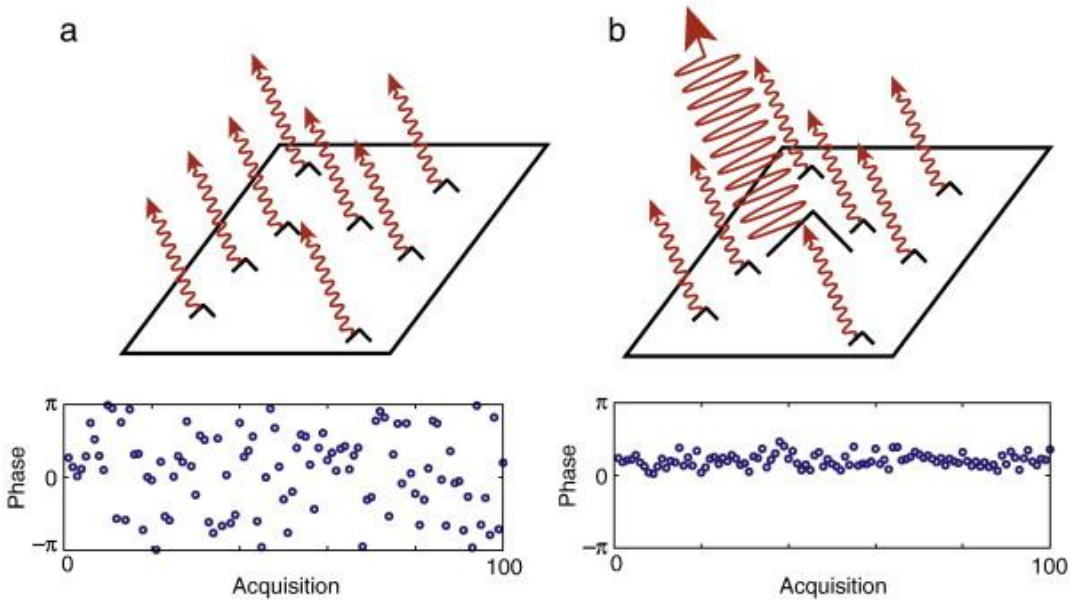

Figure 3-3 - The scatterers contributing to pixel and the plots below show simulations of the phase for 100 acquisitions. The brighter scatterer in b is three times brighter than the sum of the smaller scatterers (Hooper et al, 2012).

12m resolution DEM data was supplied by TanDEM-X, following their approval and order process. Raw heights are reported with respect to the WGS84 spheroid and were projected MSL elevations with respect to the best-available EGM2008 geoid. Both TanDEM-X and NASADEM were supplied referenced to WGS84 (Purinton et Bookhagen, 2018). They were then both adjusted to EGM2008 by subtracting the geoid deviation from the WGS84 (NGA). All computations were performed with Tide-Free version of EGM2008 to degree 2190, using point values of free-air Gravity Anomalies and Deflection of Vertical components. In this process the WGS84 constants, gravity field and geoid undulations were used to define the reference ellipsoid (NGA). EGM2008 is a spherical harmonic model of the Earth's gravitational potential, having both datasets refenced to EGM2008 ellipsoid allows comparisons (Pavlis et al, 2012).

TanDEM-X was supplied with additional layers which were used to validate the quality of the data spatially. The main layers used were the water mask (WAM) and Height Error Model (HEM), as it was collected over multiple years the areas of surface water would have altered tremendously (Appendix A). The coverage map (COV) and consistency map (COM) were also used to validate the quality of data in areas for this study, and remove areas where uncertainty was excessive. A NASA-determined water layer was also used to verify the NASADEM, by ensuring all areas of interest in this study were not covered by surface water at the time (unlikely, given the season). Assessing the potential existence of surface water is important as radar-determined elevations of water bodies are far less accurate than terrestrial areas (Zandbergen, 2008).

Both datasets were averaged for each study site, because averaging SRTM (NASADEM) data has been proven to reduce phase-noise error and therefore improve elevation height estimation (Zandbergen, 2008). NASADEM was averaged to 3 arc-seconds and TanDEM-X was averaged to 1.5 arc-seconds improving the quality of the datasets, to prepare for differencing. To limit the effects of edge noise, areas of interest were drawn away from steep changes in elevation due to land cover change. For example, borders next to forested areas, or buildings which RMS values greater than 1.25m were buffered inwards by at least one cell.

The DEMs were then differenced using raster calculator by subtracting the older NASADEM dataset from the most recent TanDEM-X. The resulting raster showed the change in elevation throughout the study area, with positive numbers showing an increase in elevation, and negatives showing a lowering of the land surface between 2000 and 2013. Previously, NASADEM and TanDEM-X data has been differenced to measure vertical elevation changes in the south-central Andes by correcting long standing errors in the NASADEM dataset using the TanDEM-X as a control surface (Purinton et Bookhagen, 2018). This research also ties the two datasets together, but using a different approach presented in sections 3.4: identifying stable bare earth areas that have not changed during the study period to demonstrate that there is a consistent regional offset between the two DEM datasets.

3.2 Historical imagery

Landsat 5 imagery was downloaded from February 2000 to get a clear image of the land surface at the time of SRTM collection, Landsat 7 was unavailable until later that year. Landsat 8 imagery from the latter period of TanDEM-X collection in 2013 was also obtained. Imagery was collected between these dates for the whole study period, between September and October during the wet season in Cambodia. If needed August and November were downloaded when cloud cover was too great in the earlier months. Water level is highest in these months, ensuring bare earth areas later identified were not seasonally flooded. Landsat 7 and 8 imagery were pansharpened using the panchromatic band to improve the resolution from 30m to 15m.

Satellite imagery from the rainy season was used to ensure the water level and therefore flood extent would be at its greatest, leaving areas which do not seasonally flood. The maximum observed flood extent was a useful tool identifying areas which were no longer seasonally flooding, which could indicate FPI had potentially occurred in that area. Fortunately, SRTM was collected during the dry season of 2000, which means that the areas that would seasonally be flooded, and therefore desirable areas to be infilled, were not inundated during SRTM collection (Figure 3-4). Using imagery from the rainy season also ensures

that the reference stable bare earth areas that were seasonally flooded, which would affect the quality of the inter-calibrations.

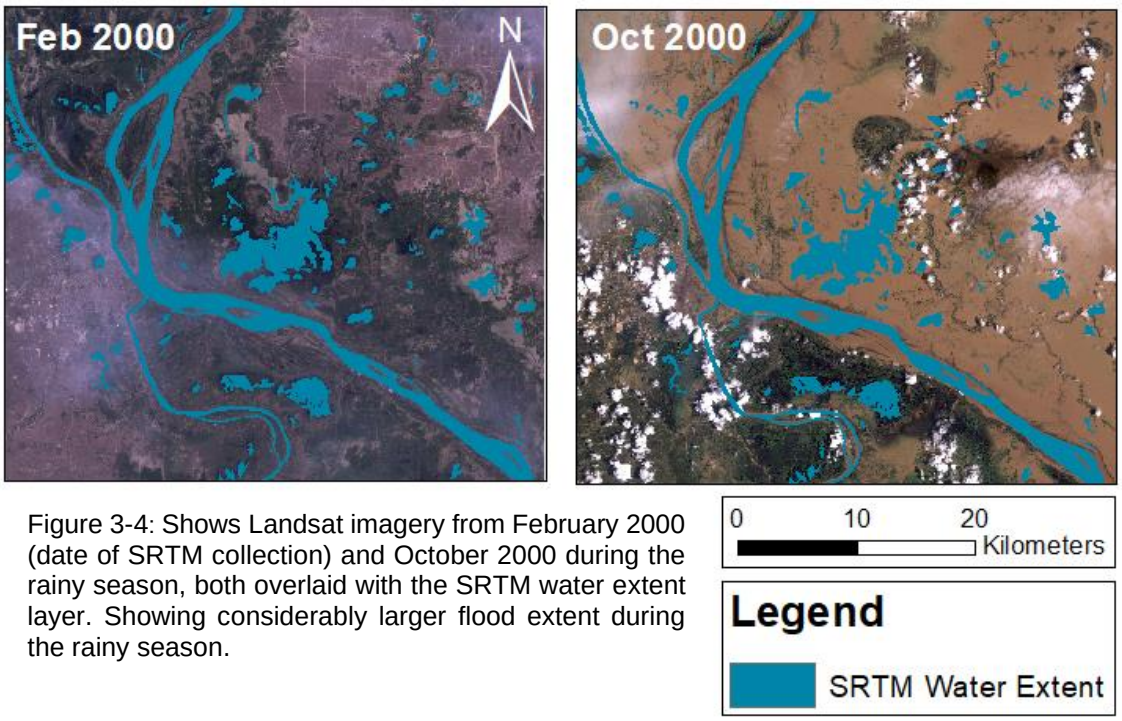

Figure 3-4: Shows Landsat imagery from February 2000 (date of SRTM collection) and October 2000 during the rainy season, both overlaid with the SRTM water extent layer. Showing considerably larger flood extent during the rainy season.

In addition, GoogleEarthPro historical imagery was used, primarily for the high-resolution imagery in recent years, to add another layer of validation for areas identified. Most of the imagery on GoogleEarthPro was collected in December, during the early dry season for each available year. The higher image quality in GoogleEarthPro made it possible to clearly see the FPI activity as well as barges used for sand mining on the Mekong River. It was also possible to digitise shapefiles directly in GoogleEarthPro, facilitating the establishment of a spatial dataset of FPI location and extent for area.

3.3 UNComtrade

The United Nations Comtrade (UN Comtrade) database offers free access to annual international trade data, provided by over 170 reporter countries. This database is detailed by the commodity or service category as well as the partner country. Exports of natural sand from Cambodia were downloaded from this database. Natural sand is defined as: ‘Sands; natural, silica and quartz sands, whether or not coloured’ (United Nations, 2019). This would include river sediment, and other natural sources of sand in Cambodia, which is fit for purpose in this research which is to understand the scale of natural sand exports over time. First the natural sand exports from Cambodia were downloaded, as reported by Cambodia from 2000 to 2013. Then for comparison the natural sand imported from Cambodia as reported by the importing country between 2000 and 2013. Annual totals were produced to analyse the data for any discrepancies in the volumes reported in the sand trade out of Cambodia.

3.4 Stable bare earth identification

Landsat imagery and GoogleEarthPro were used to identify areas around the study sites that were undisturbed bare earth throughout the entirety study period, from NASADEM data collection to the end of TanDEM-X (2000 to 2013). In this study stable bare earth areas are defined as not containing tall vegetation or human built infrastructure, and that have had no visible change in land use for each year during the study period (generally these are grazed fields, in some cases near airport runways – but not paved surfaces because these do not measure well with radar). Areas that were seasonally flooded were avoided as annual flood deposits may have built up over the 13-year period, increasing the elevation. This methodology assumes that the elevation in these areas has not changed between SRTM collection in 2000 and ending TanDEM-X in 2013, so further uncertainties will come from any possible changes in elevation which have not been accounted for. Areas were also checked to verify they had RMS less than 1.5m in both NASADEM and TanDEM-X datasets, ensuring there were no steep or dissected terrains that could cause inaccuracies between the datasets (Purinton et Bookhagen, 2018). STD calculations were performed on NASADEM

and TanDEM-X, identifying the difference between largest and smallest value of the cells in a neighbourhood that are likely to have been cause by a slope, dissection, infrastructure, or vegetation. In addition, checks were made to verify that bare earth areas were outside of the SRTM (NASADEM) water layer and any problematic zones identified using the TanDEM-X WAM, HEM, COV and COM layers.

In this study elevation change values were extracted using fishnet points with the grid size of the DEM of difference resolution (~30m), to ensure the elevation change for each pixel was recorded. This is the same resolution as the NASADEM dataset. Fishnet grids were clipped to fit to each bare earth area, and the same methodology was carried out consistently with the areas of interest described. Once extracted the mean elevation difference between NASADEM and TanDEM-X was calculated for each bare earth area, in order to determine the local offset, which could be compared against other bare earth areas to identify any consistent values and related statistics.

Mean elevation change for the 10 bare earth areas used to bind the two datasets together, reducing the relative differences, without improving the absolute accuracy. The results indicated a consistent average offset that TanDEM-X was ~1.24m higher in elevation compared to NASADEM (Figure 3-5). The range of difference was between 1.1 and 1.5 and the median was below 1.2, less than the conservative mean which was used (Figure 3-5). The bare earth areas were identified to have a clear spatial distribution across the study area, to limit biases from uncertainties in sections of the radar coverage. Bare earth inter-calibration is an important step because it means that the results do not include consistent elevation offsets between NASADEM and TanDEM-X, which in this case would have overestimated the volume of infill in Cambodia. Following this offset correction, the differencing estimates presented in the rest of the study would likely be somewhat less than the actual measured differences, so all volumetric calculations presented hereafter would be conservative underestimates.

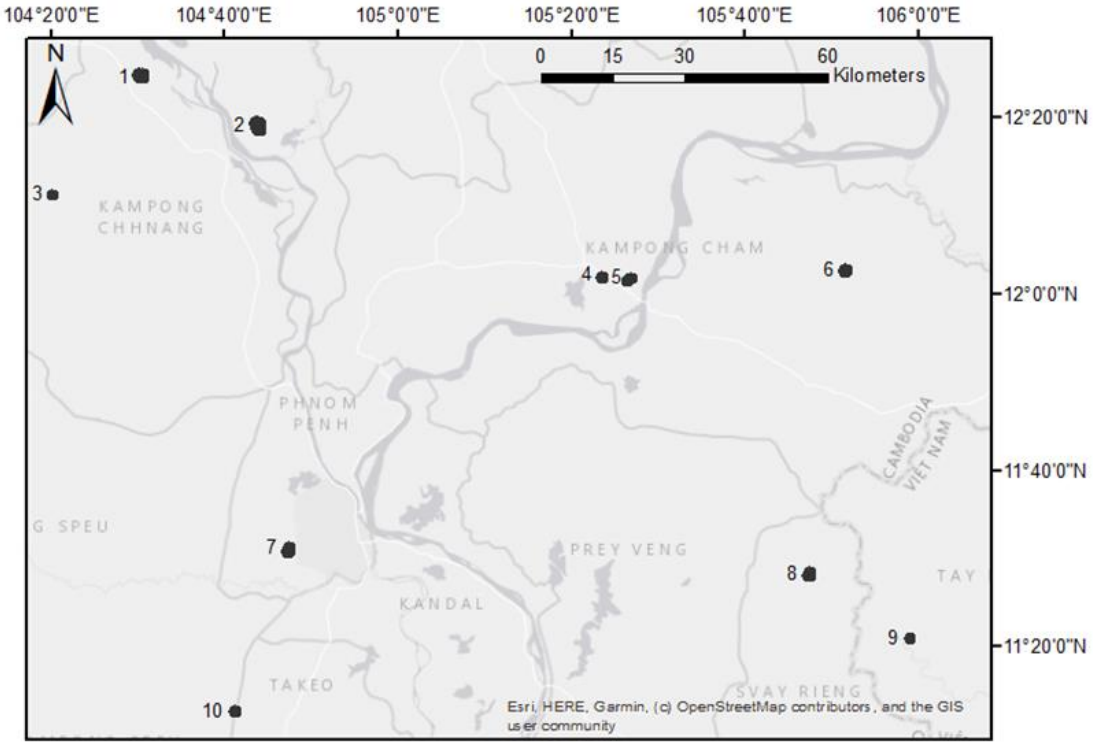

No.	Elevation Difference (m)
1	1.15
2	1.19
3	1.23
4	1.11
5	1.49
6	1.14
7	1.15
8	1.41
9	1.40
10	1.15
Mean	1.24

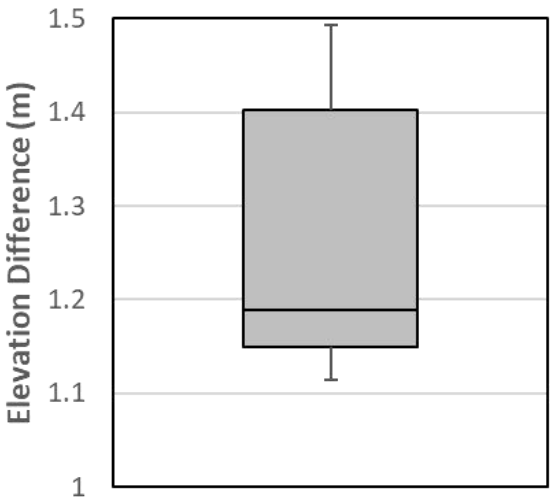

Figure 3-5: The map shows the location of the 10 bare earth areas identified in this study, the polygon border for each area has a buffer to make them easily visible at this scale, therefore sizes are not accurate. The table shows the average elevation for each of the numbered bare earth sites, which is also represented in the box plot.

3.5 Bare earth offset

Stable bare earth areas have been identified to measure the relative difference between NASADEM and TanDEM-X for the study area in Cambodia. The mean of this difference (1.24m) is much less than the absolute error associated with the two datasets. The quality of the DEMs is expected to be higher on the floodplain as they perform better over flat sparsely vegetated areas (Wessel et al, 2014). Validation of the original SRTM (from which NASADEM is derived) using extensive global ground truths, showed that the absolute height error in Eurasia is generally between 6-9m (Rodriquez et al, 2006). For the more recent TanDEM-X the absolute height error for moderate terrain, such as the floodplain, can be stated as being below 2m (Wessel et al, 2014). However, for local comparisons the relative error is often much lower, although this must be confirmed for each research site.

The bare earth areas identified in this research are a novel way of further tying the two datasets together such that the relative error is minimized. The absolute height error is not vital for measuring volumetric changes between the two datasets, as long as the two datasets are inter-calibrated as closely as possible for the research site(s). Because this error in relative differences is known from the analysis in section 3.4, the standard deviation of the difference in stable bare earth areas can be used to represent the uncertainty in the difference between NASADEM and TanDEM-X. The standard deviation for this is equal to 0.13, providing a quantified uncertainty for groups of cells differenced for the elevation change of ±0.13m (the uncertainty for individual cells would be higher, due to pixel-scale noise, but this averages out for areas of interest (AOIs) composed of hundreds of cells). This value represents the relative variance between the NASADEM and TanDEM-X datasets, which would also vary for other land covers due to the ground surface interactions of the radar.

This is therefore not representative of the full uncertainty but will be propagated into the average elevation changes measured for FPI AOIs later used for volumetric calculations to measure the uncertainty in the variance of the datasets relative to each other.

Additional uncertainty which is unquantified in this research but is important to understand, stems from the differences in backscattering between C-Band (SRTM/ NASADEM) and X-Band (TanDEM-X). Previous research has shown SRTM (C-Band) and datasets derived from X-Band (in this case DSM RAM) are similar in elevation (Figure 3-6) (Grohmann, 2015). This shows SRTM, later processed to NASADEM is better for comparisons with TanDEM-X than ASTER DEM. In general, SRTM elevations are slightly lower, as might be expected due to the smaller wavelength of X-Band which can detect more particles. TanDEM-X uses 3.1 cm wavelength X-Band compared to 5.6 cm wavelength in C-Band SRTM used in NASADEM (Purinton & Bookhagen, 2018).

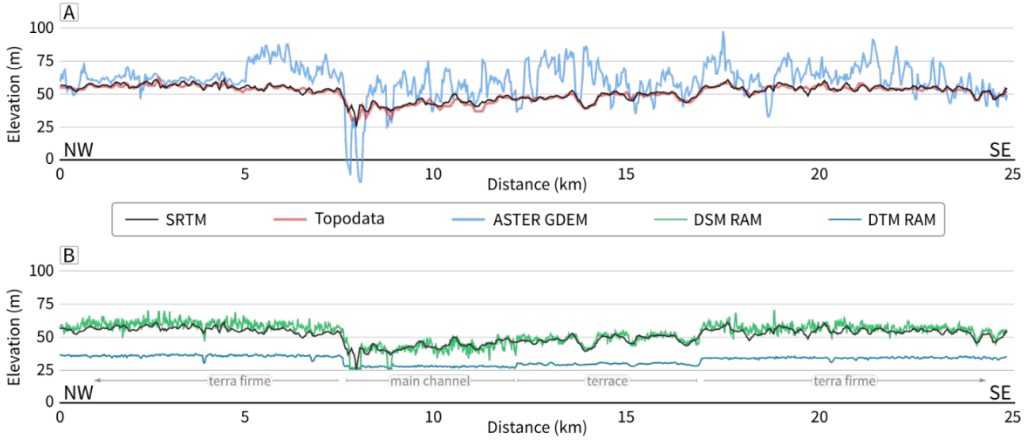

Figure 3-6 - Compares topographic profiles of different data sources in the Amazon (Grohmann, 2015).

3.6 Floodplain infill identification

Landsat imagery combined with GoogleEarthPro was used to identify areas of simple FPI between 2000 and 2013 in the study site. Areas of FPI for this study were identified as areas on the floodplain that show visible evidence of infilling used to raise the elevation of the land between 2000 and 2013, but that have not also been developed with houses, so as not to overestimate the volumes of infill (Figure 3-7).

Figure 3-7: Example floodplain infill area shown in 2013 Google Earth imagery, as well as streetview images from the same year to show on the ground perspective (Google, 2020).

SRTM (NASADEM) was collected in February 2000, the dry season in Cambodia, which means the flood extents were around their minimum, meaning that the water surface would have affected the quality of a smaller surface area. Therefore, elevation differences between NASADEM and TanDEM-X of areas that have been infilled to no longer be seasonally flooded, would not have been inundated in either collection periods, so the elevation data is more reliable (Figure 3-4 above). If for example NASADEM was collected during the peak rainy season when flood extents were at their greatest, this would make the elevation data from 2000 unreliable for a large proportion of the study area.

To help identify areas of infill, unsupervised classifications were created using imagery from the rainy season in 2000 and 2014 and then differenced to highlight areas that were no longer submerged by water in the wet season. Because the aim of floodplain infill is to raise the land above the highest flood level for protection, that was a logical and effective method to produce a guide for areas to start the search for FPI. Following this, ultimately the whole study area was investigated - in total 176 areas of infill were identified across the study site (section 4.1).

The digitised AOI for each FPI site was further refined by removing pixels that included infrastructure and clear areas of vegetation, this ensured that the elevation change was not overestimated by including the heights of such objects (Figure 3-8). Other changes in the surrounding areas due to vegetation and construction were not measured within the areas of infill. Such changes are visible around the outside of the fishnet in Figure (Figure 3-8). The measurements of FPI therefore only represent areas of bare earth infill, and not areas that have since been developed or vegetated, as this would falsely exaggerate elevation changes. The mean elevation increase of the FPI areas was nearly 2.8m, which is over 1.5m greater than the mean elevation change of the consistent (2000-2013) bare earth control areas in comparison. This method is inherently conservative because it is not measuring any FPI activity that has since been built upon or had trees planted. However, by producing a reliably conservative estimate the resulting data will give a robust insight into the minimum possible volume of floodplain infill.

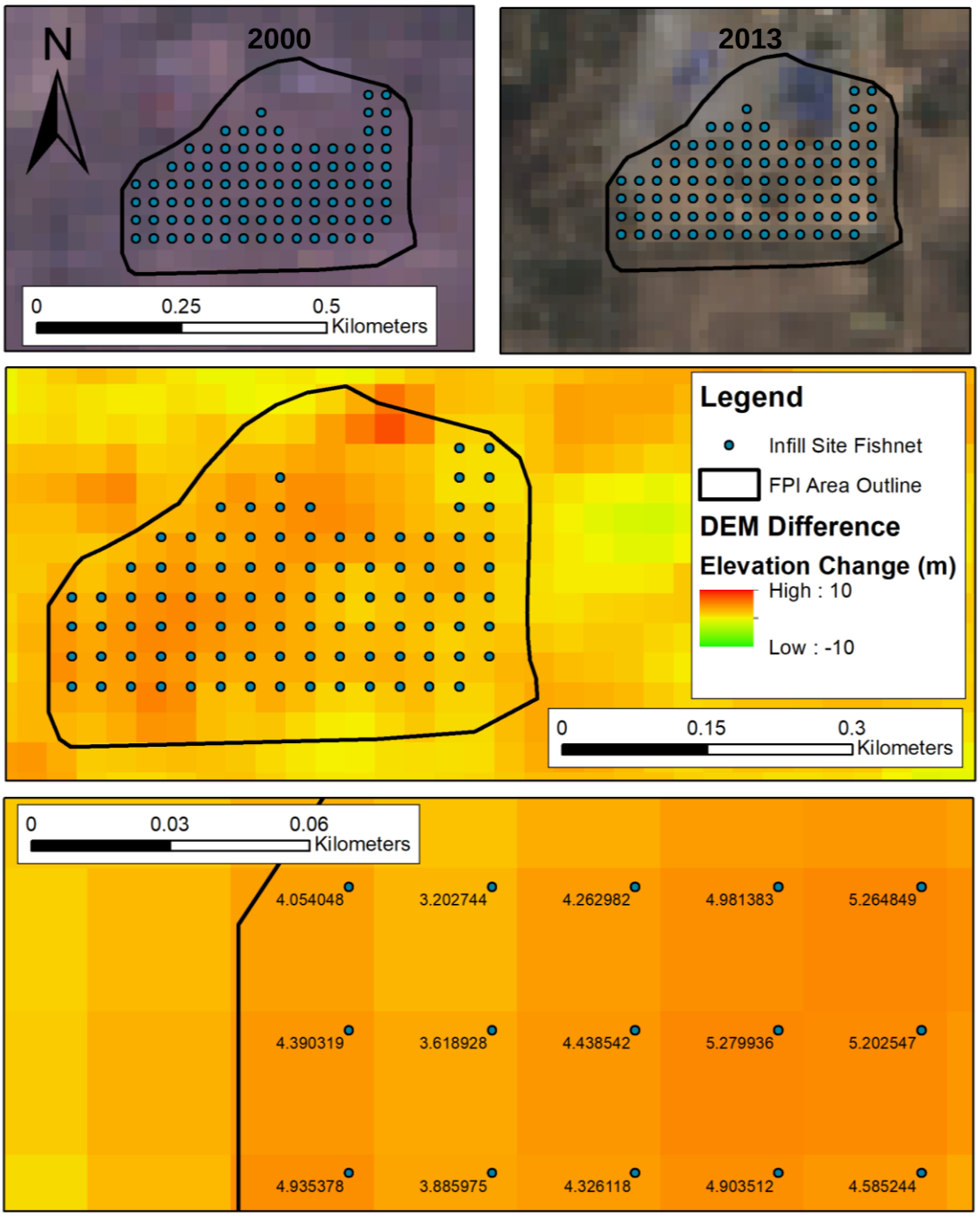

Figure 3-8: Shows the fishnet methodology for an example FPI site. With the initial outlined FPI area in black, and then cropped individual points to disregard buildings and trees, Points were used to extract the elevation change in the DEM of difference between NASADEM and TanDEM-X.

Additionally, it is interesting to consider the erosion and depositing along river banks. In these areas, natural processes of erosion or deposition will be greatest, and the rivers banks are also a key location for development (particularly near Phnom Penh). Because the river could have migrated somewhat during the study period, water could have disrupted the quality of the radar DEMs, so it is beyond the remit of this study to measure changes on the banks – though with additional analysis of riverbank images such comparison could be made in future research.

Information about each infill site was also recorded to enable further temporal and spatial analysis. For the temporal images, the year was logged for each site that infill first appeared, and also the year infill activities finished, with the resultant years of infill calculated. Spatial information recorded for each FPI site were the closest river channel (selected between The Mekong, Tonle Sap and Bassac), the river distance downstream for that the closest point to that channel, and the political province.

3.7 Volumetric calculations

Areas of interest were delineated and further checked against the additional SRTM water layer and TanDEM-X WAM and HEM layers. The surface area of each polygon was measured, and the value for each pixel (elevation change) from the DEM of difference was extracted (after correcting for the 1.24m difference between the two datasets determined by the stable bare earth areas). The volume was then calculated by multiplying the mean elevation change by the surface area. The resultant volumes of infill calculated for each FPI area were summed to produce the total volume of infill for the study area between 2000 and 2013. The data was also analysed temporally and spatially, using the information collected on the location of each infill site and the start and finish years of visible infill activity.

$$FPI\ \ (m^3) = \ Surface\ Area\ (m^2) \times (Average\ Elevation\ Difference\ (m) - Calibration\ (m))$$

Once volumes were calculated, masses were then calculated by assuming a sand density of 1,600 kgm^{-3}, to facilitate comparisons with other results (eg., Hackney et al, 2020).

3.8 Spatial patterns of infill

The position of each area of infill was noted to show its river kilometre distance with respect to the closest point of one of the three main river channels in the study area (Mekong, Tonle Sap and Bassac). In the few cases where FPI was close to multiple channels, the calculated volume of infill was divided evenly between the channels. This enabled the spatial analysis of FPI trends by quantifying the volume of FPI closest to section(s) along the river(s) from where it likely was extracted. Each channel was binned into large increments of at least 10kms, that were then used for averaging calculations. With the aim of highlighting hotspots and spatial patterns of FPI along the river channels between 2000 and 2013 rather that the exact locations of sediment extraction. This approach assumes that local sand dredging operations are unlikely to source material exceptional distances away from their ultimate delivery destination, because of the considerable time and fuel required. This averaging technique also enables this research to analyse the spatial patterns of FPI within Cambodia relative to the main watercourses, where most of the sediment would have likely been sourced (Bravard et al, 2013).

3.9 Temporal trends of infill

While the spatial resolution of NASADEM and TanDEM-X allows trends of FPI to be analysed spatially, it is not inherently possible to analyse detailed temporal trends with the DEM's used on their own, as there were only two dates. Previous studies have given average annual rates of elevation change of the lands surface from landslides and other natural processes (Grohmann, 2018; Purinton & Bookhagen, 2018). However, this study uses a new approach of obtaining satellite imagery to identify periods of infill at each site, providing significantly better constraints for the temporal trends within the period of data collection of NASADEM and TanDEM-X, providing near-annual temporal resolution from 2000 to 2013.

In this research the year of infill starting and ending (as seen in the imagery) was recorded, so that the number of years of infill could be calculated and used to split the total volume of infill evenly between these years. Although this is limited because it still only divides the volume of FPI recorded in each area equally between the times infill activities appear to be present in that specific area, it excludes years where infilling does not occur. The averaged FPI from each site was then summed for each year through the study from 2000 to 2013, to provide a temporal framework for the measured FPI. This method appears to work well for determining temporal trends in the changing rates of FPI in Cambodia. However, the methodological assumptions (FPI was divided each site) means there is uncertainty in the partitioning between individual adjacent years. To show such long-term trends, the volumes of FPI were grouped into 4 time periods where trends of FPI were alike.

3.10 Combining spatial and temporal

The spatial and temporal information was combined for the FPI dataset allowing the analysis of the locations of the greatest volumes of infill over time. The spatial data was divided into larger 20km sections and then the temporal information for each infill site was used to divide the study period into 4 sections for times where FPI activity was alike. The relevant volumes for each sub-section nearest to the riverbank for each time period were subsequently summed, with the data being shown in proportional circles on a map for each of the time periods (section 4.6). This allows spatial patterns to be observed over time periods of three to four years within the dates of collection of SRTM (2000) and TanDEM-X (2013), improving the spatial resolution, adding an entirely new edge to DEM differencing from combing observations in satellite imagery.

3.11 Lake infill

Lakes, defined as areas of water all year round, were identified that were visible in 2000 but had been infilled by 2013. Lake infill is common in areas of Cambodia where land is valuable for development, meaning they were often easily identified with the construction of new infrastructure by 2013. Where the lake had been

infilled by 2013 the TanDEM-X data was not affected by surface water, however SRTM data was not accurate for areas covered in water, and bathymetric data of lakes before they were filled was not available.

Therefore to estimate the average depth of the lake bed in 2000, the elevation of the low bare earth bank around each lake was measured and a depths of 0.5m, 1.0m and 1.5m were assumed for the average depth based on observations of some shallow floodplain lakes near Phnom Penh by Prof. Rolf Aalto. These estimated bed elevations were then differenced, with the measured elevation infilled land covering these areas recorded in the TanDEM-X DEM. This method is limited because the depth data are not available for specific lakebed elevations in 2000. However, it does give plausible estimates for the range volumes of lake infilling that were observed to have occurred between 2000 and 2013.

3.12 Alternate sources of sediment

Aggregate can also be sourced from outside the river, although this requires considerably more effort and fuel to first extract the hard or cohesive material, and then to transport it to the FPI location by lorries, which are vastly more costly than river barges. Alternatives to river sediment were investigated as sources of potential aggregate excavation within Cambodia - these were identified with the aim of measuring possible contributions to the volumes of FPI from sources other than river sand. Quarries were identified in highland areas near the FPI sites, and sediment excavation pits were located on the floodplains more locally (Appendix D). The relatively adjusted DEM of difference was then used to calculate the volume of material excavated, replicating the same method used for measuring FPI to allow direct comparison of the results. This is an important step to quantitatively assess potential sediment sources for FPI other than the riverbed sands. Although infill has been identified as the largest consumer of sediment from the riverbed, being able to quantify the volumes produce by on land mining operations will further advance the understanding of the other sources of infill material (Bravard et al, 2013).

4 Results

The following section will illustrate and describe the volumes of FPI in Cambodia, as well as equivalent weights assuming a sand density of 1,600 kgm^{-3} to allow comparisons with other research (Hackney et al, 2020). First, results will be presented for the volumes of FPI between 2000 and 2013 in Cambodia. To help understand the source of sediment, alternative sources of sand will be investigated, namely imported sand and quarried material. Then temporal trends of FPI will be explored, followed by spatial patterns. Finally, the spatial and temporal analysis will be combined to see if hotspots of FPI have altered overtime.

4.1 Scale of FPI

The total volume of FPI measured in Cambodia between 2000 and 2013 was 183±18 $x10^6$ m^3 (Figure 4-2) (Data from each FPI site presented in Appendix B). The uncertainty relating to the variance between the datasets stems from the standard deviation in the bare earth relative difference reduction results, which equates to ±0.13m of elevation change per each cell. The FPI total is an underestimate due to the several conservative assumptions presented earlier, both for the differencing offset and the exclusion of many FPI areas that were vegetated or had buildings (Section 3). Even this conservative volume is enormous, to put this into context it would fill over 73,000 Olympic size swimming pools. This volume equates to a mass of sand equivalent to 292±29 $x10^6$ tonnes (assuming a sand density of 1,600 kgm^{-3}). Highlighting the mass industrial scale of FPI operations in Cambodia since the turn of the century up to the end of TanDEM-X collected in 2013.

Table 4-1: Key volumes (m^3) of FPI measured between SRTM (2000) and TanDEM-X (2013), including estimates of lake infill volumes at different average depths of the infilled lakes.

Infill activity from 2000 to 2013	**Volume ($x10^6$ m^3)**
Lake infill (0.5m depth)	32.49
Lake infill (1.0m depth)	36.04
Lake infill (1.5m depth)	39.60
FPI Total	**183.11 ± 17.58**
FPI Total plus Lake infill (1.0m)	**219.15 ± 21.14**

The vertical topology of FPI at individual sites is shown in Appendix C, using transect data to show the changes in elevation along a cross section of the identified site (Figure 4-1) (additional examples in Appendix C). These figures illustrate the FPI processes occurring at individual sites that sum up the enormous total volumes in Table 4-1. This thesis will mainly focus on the combined volumes of all of the FPI sites identified between 2000 and 2013, by location and time, to better understand the average scale of operations during this period in the Mekong Basin in Cambodia.

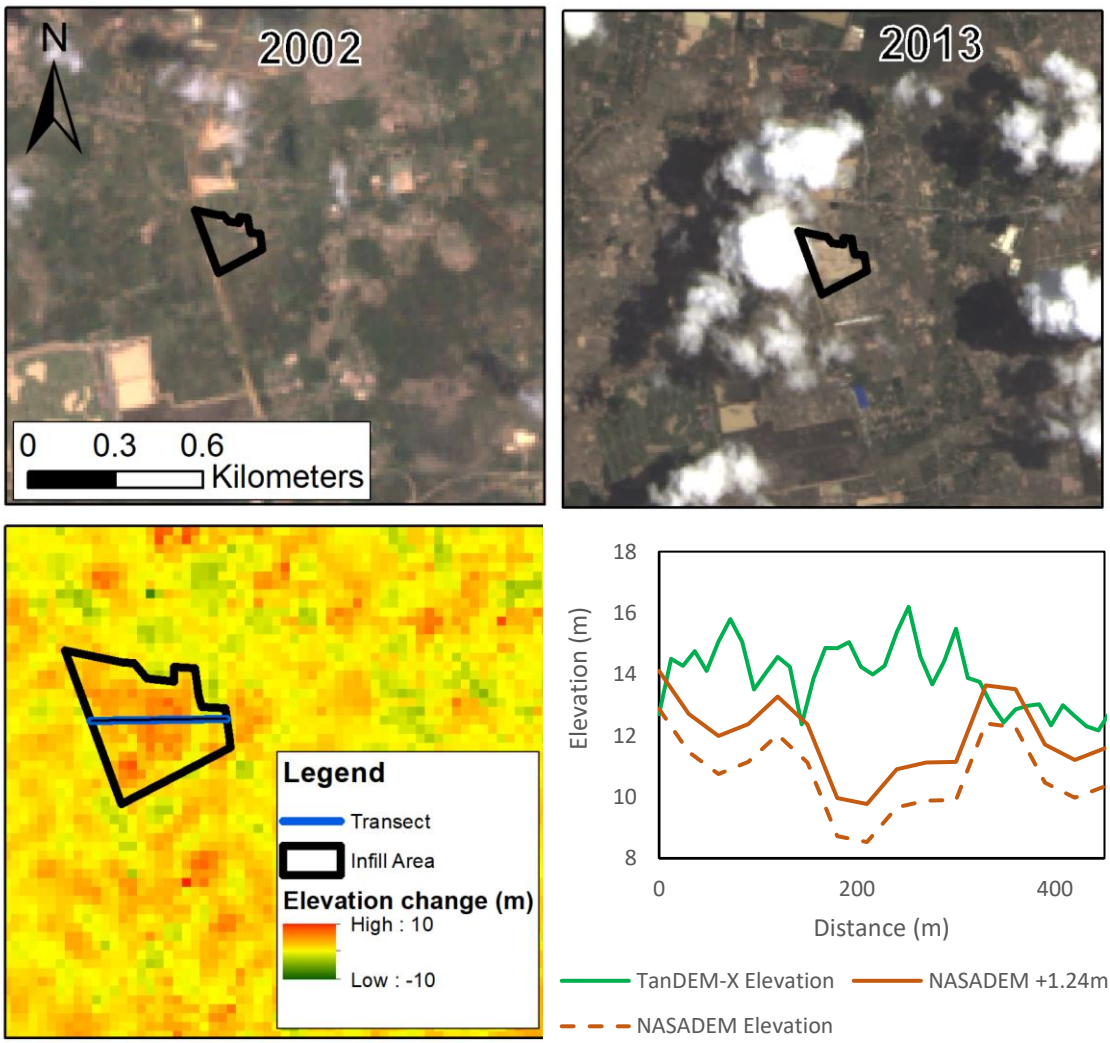

Figure 4-1: Elevation change of a FPI site identified. With cross sectional data showing the elevation of NASADEM (2000) and TanDEM-X (2013).

With the addition of lake infill the volume of infill between 2000 and 2013 is likely to increase by around 36±4 $x10^6$ m^3, assuming an average lake depth of 1m. Significant volumes would therefore have been used to infill the 7 lakes in Cambodia during the study period. However, there is a large degree of uncertainty in lake infill volumes because of the range of average depths used. Therefore, the volume of FPI which excludes lake infill will be carried forward throughout the results. It is important to state that lake infill made a significant contribution to the volume of sediment used for infill, however until further information on lake depths is available, these volumes will not be included. This does however highlight scope for future investigation into the volumes of sediment used in previous lake infill activities, and it is also recommended to carry out bathymetric surveys of lake which still exist in main urban areas in case of future lake infill.

4.2 Cambodia's international trade of sand

The UNComtrade data shows that Cambodia reported importing just under 0.5 $x10^6$ kg of natural sand between 2000 and 2016, which equates to less than 300m^3 when a sand density of 1600 kg/m^3 is applied (United Nations, 2019) (Table 4-2). Importantly this shows that Cambodia has not been importing sand in order to fuel the large scale FPI activity during this period. In fact, in addition to national uses of sand, Cambodia has exported large volumes of natural sand in this time.

Between 2000 and 2016 Cambodia underreported the volume of sand exported by over 44 $x10^6$ m^3, by nearly 6 times the volume that countries had reported as imported from Cambodia. Discrepancies between the volume of natural sand reportedly exported by Cambodia and the volume imported from Cambodia by the rest of the world started in 2009. In this year Cambodia reported exporting nearly half the sand that reported imported from Cambodia (Figure 4-2). This paper will later explore why Cambodia have reported exporting sand at a much lower rate, than countries worldwide have reported imported from Cambodia.

Table 4-2: Natural sand trade data from 2000 to 2016 for Cambodia (United Nations, 2019).

Trade Flow (2000-2016)	Natural sand ($x10^6$ kg)	Volume ($x10^6$ m^3)
Imported by Cambodia	0.47	0.00
Cambodia's Reported Exports	14,458.98	9.04
Imported from Cambodia	85,311.92	53.32

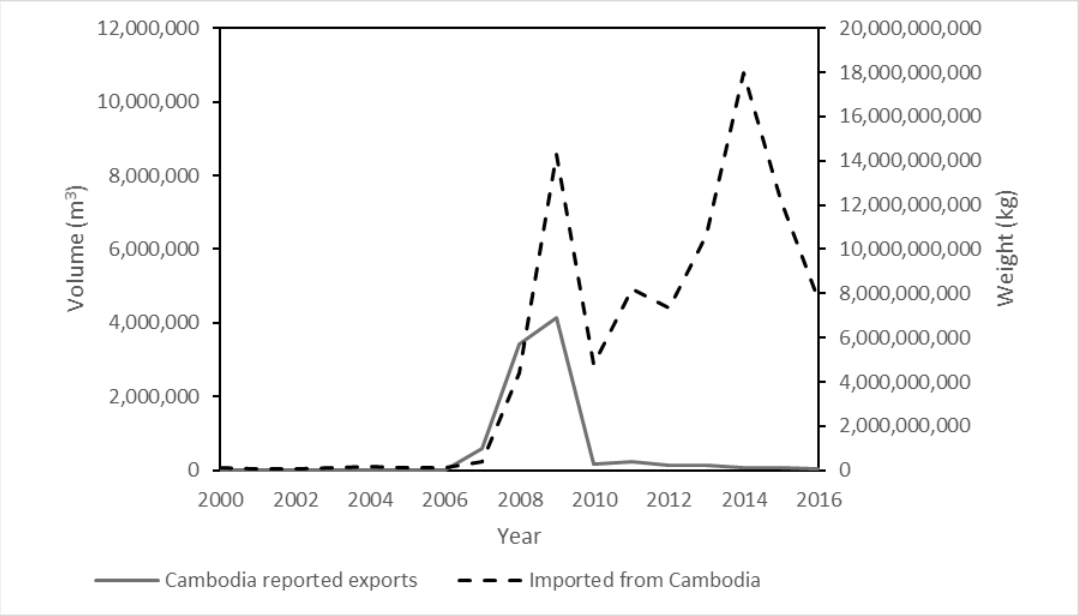

Figure 4-2: UnComtrade natural sand import and export data relating to Cambodia, as reported by Cambodia and alternately by the rest of the world. Volume on the primary axis and the converted weight in kilograms on the secondary axis (United Nations, 2019).

Singapore was by far and away the biggest importer of natural sand from Cambodia, importing over $50x10^6$ m^3, which equates to over 93% of the total sand trade imported from Cambodia (United Nations, 2019). Vietnam, a much closer neighbour, was the second largest importer of natural sand, but imported less than $2x10^6$ m^3 in the same period from Cambodia (United Nations, 2019). It is clear that the main international demand for sand from Cambodia comes from Singapore. Although in total the volumes measured in FPI nationally within Cambodia over doubled the volumes reported to have been exported from Cambodia (United Nations, 2019).

4.3 Alternative sources of sediment

The combined volume of sediment removed from highland quarries and floodplain excavation sites between 2000 and 2013 was nearly 24±1.03 x10^6 m^3 (Figure 4-4). Seven quarry sites and 17 floodplain excavation sites were identified (Appendix D), but some quarry sites in the study area would inevitably have been missed, so this is regarded as an underestimate. The uncertainty from the bare earth relative difference reduction standard deviation was applied to both types of quarry volumes. There is also additional uncertainty relating to the floodplain extraction data as many of the extraction sites contained water during the dates of TanDEM-X collection, which could provide random relief due to low backscattering and temporal de-correlation (Wendleder et al, 2012). The uncertainty propagated from the bare earth standard deviation is relatively lower for the highland quarry data because the quarries were both dry, and tens of metres deeper from removal than floodplain quarries (Appendix D). Therefore, the uncertainty of ±0.13m for each pixel was proportionally much smaller compared to the elevation change between NASADEM and TanDEM-X.

Table 4-3: Key volumes (m^3) measured between SRTM (2000) and TanDEM-X (2013). Including major sources of quarried material, as well as estimates of lake infill volumes.

Source of Sediment	**Volume (x10^6 m^3)**
Highland Quarries	13.59±0.07
Floodplain Extraction	10.24±0.96
Quarry Total	23.83±1.03
FPI Total	**183.11 ± 17.58**
FPI Total plus Lake infill (1.0m)	**219.15 ± 21.14**

The total volume of quarried material measured in the study area between 2000 and 2013 is only enough to make up around 12-14% of the volume of FPI. Furthermore, it seems unlikely that expensive hard rock from highland quarries would be transported significant distances for simple use as fill, rather than used for more suitable purposes such as road base or riprap. Even so, approximately 86-88% of the FPI material is unaccounted (88-90% including lakes) and must be sourced from rivers, as Cambodia have not been importing aggregate (United

Nations, 2019). Therefore, most of the material used for FPI would necessarily have been extracted from the Mekong, Tonle Sap and Bassac. When the 183±18 $x10^6$ m^3 of FPI (without lake infill) is combined with the $30x10^6$ m^3 of natural sand exported by Cambodia between 2000 and 2013 (United Nations, 2019). This would leave 190±19 $x10^6$ m^3 of sand unaccounted for when volumes of unidentified quarried material were subtracted, that most likely would have come from the rivers.

To help explain the source of this sediment, it has been reported that raising natural depression above flood levels in the districts near The Mekong and Bassac Rivers has consumed the largest volumes of sediment from the riverbeds, as it is a convenient source of high-quality, durable aggregate (Bravard et al, 2013; Kondolf, 1994). Having shown that alternative sources of sediment could not supply the volume of sand used in international trade and in national FPI, with evidence from Bravard it is clear the Mekong river system has been the greatest source of aggregate within the study period. Therefore, this research will now investigate the temporal and spatial patterns of FPI within Cambodia from 2000 (SRTM) to 2013 (TanDEM-X), in relation to the river system throughout the study area in Cambodia.

4.4 Temporal trends of FPI in Cambodia

The rates of annual FPI were consistently greater than the volumes of natural sand exported by Cambodia every year from 2000 to 2013, showing a vastly larger consumption nationally than international demand for sand from Cambodia. Even in 2009 when sand trade is at its greatest at $8x10^6$ m^3, the FPI activity in Cambodia was over twice in volume at $20±2x10^6$ m^3 (Figure 4-3). This indicates that FPI is a huge domestic usage and therefore local demand for sand within Cambodia.

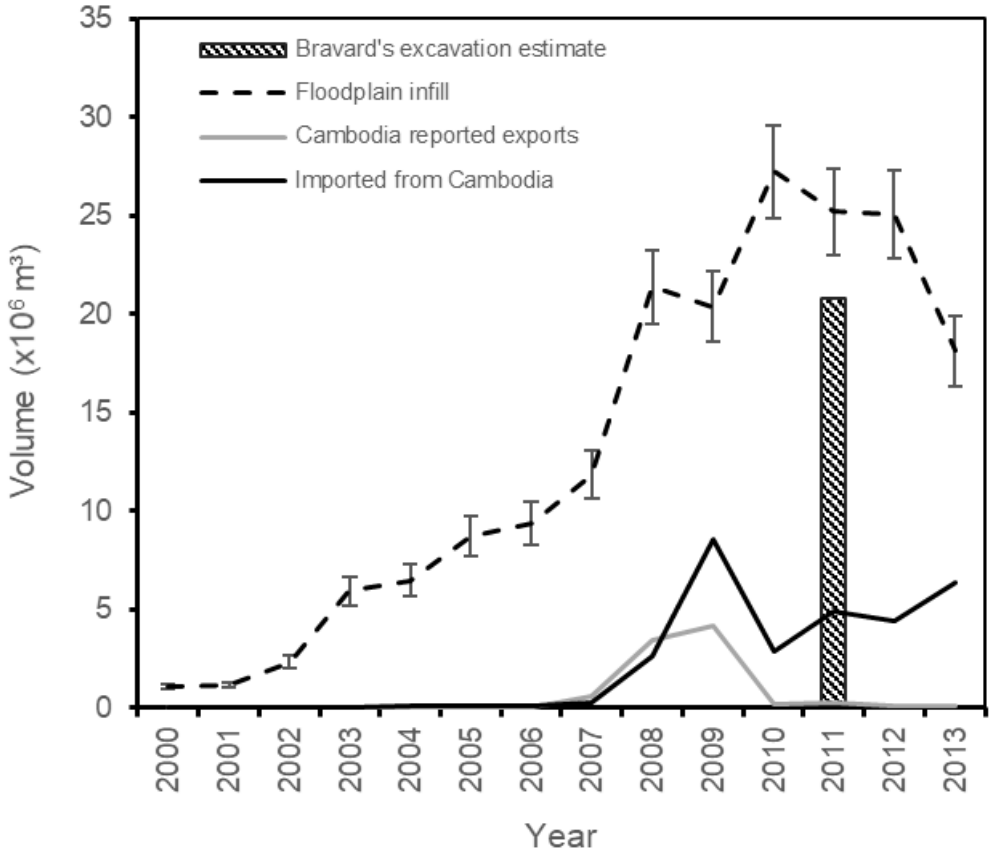

Figure 4-3**:** Temporal rates of FPI and UNComtrade data from 2000 to 2013 (United Nations, 2019). The long dashed lines represents FPI, with error bars to show the margin of uncertainty from bare earth relative difference reduction. Grey line is sand volume (m^3) Cambodia reported exported, black line is sand reported imported from Cambodia (from other countries). Yearly infill data is shown in Appendix E.

Changes in the rates of FPI over the study period portray how FPI activity has increased since the turn of the century. Rates of infill have risen steadily from 2000 to 2007, when FPI rates exceeded $10x10^6$ m^3 annually for the first time (Figure 4-3). This first half of the study period can be defined as the period of steady expansion of FPI activity. Since 2008 the volume has consistently exceeded $17x10^6$ m^3, showing a large difference between the first half of the study period and the second.

From 2007 up until the peak rates of FPI recorded in 2010, there is a sharp upwards trend, at a steeper gradient to the expansion than seen earlier in the decade (Figure 4-3). The steepest change in FPI rates occurs between 2007 and

2008, where rates nearly double from 12±1 $x10^6$ m^3 in 2007 to 21±2 $x10^6$ m^3 in 2008. This interval can be identified as the period of rapid industrial expansion of FPI activity in Cambodia. FPI rates continue to rise, peaking around 2010 at 27±2 $x10^6$ m^3. After this peak in 2010 rates slowly decrease through to 2013, with volumes still around 50% more of that in 2007. This final period of study still shows large volumes of FPI activity, can be defined as the post-peak period.

The highest volume of infill of just over 27±2 $x10^6$ m^3 is experienced in 2010, with following two years slightly over 25±2 $x10^6$ m^3, meaning this period showed the greatest volume of FPI activity. In general, the largest rates of FPI were recorded between 2008 and 2012, where the volume of infill was greater than $20x10^6$ m^3, falling only slightly in 2013 to around 18±2 $x10^6$ m^3. Unfortunately, the DEM data used in this research limits the temporal range of this study, so it is impossible to say how trends of FPI activity have continued after 2013. Future research with new DEMs could be used to investigate FPI activity after 2013.

Previously, Bravard had estimated $20x10^6$ m^3 of sediment was extracted from the Mekong River in Cambodia per year in 2011 (Figure 4-3). However, the estimated volume of FPI from this study in the same year was roughly 30% greater. Bravard highlighted various limitations which made the figures an underestimate by an unknown factor. Now, the direct measurements of FPI made in this study support the previous interpretation that Bravard's results were an underestimate, because just the single sediment consumer of FPI exceeds these rates in 2011 in Cambodia (Figure 4-3). This insight into the scale of FPI in Cambodia between 2000 and 2013 is therefore also an eye opener for the scale of sediment use, demand, and resources in the LMB.

Uncertainty bars in the yearly rates of FPI have been calculated using the standard deviation in the bare earth relative difference (0.13m). A long with this uncertainty in calculated volumes, there is uncertainty in the exact timing of each infill operation. Because of this uncertainty between years, it is best for understanding multi-year trends in infill, with a slightly lower temporal resolution than presented.

4.5 Spatial patterns of FPI in Cambodia

FPI activity was analysed in relation to the downstream position of the nearest main river channel within the study area; The Mekong, Tonle Sap and Bassac. Of these the largest volumes of infill were recorded closest to the main Mekong channel, totalling roughly 109±11 $x10^6$ m^3 (Appendix E). FPI activity near the other two channels combined is still less than the total FPI that was measured closet to the Mekong main stem. With the FPI located near the other two channels as follows, the Tonle Sap at 46± $6x10^6$ m^3 and Bassac: 28± $1x10^6$ m^3.

FPI near the Tonle Sap is more intermittent, with most activity focused in and around the main cities and towns, such as Krong Kampong Chhnang, the capital city of the Kampong Chhnang Province. To the south of Phnom Penh along the Bassac River there is evidence for FPI adjacent to each 10km stretch of the river. However, 84% of the volume of FPI near the Bassac is focused within 20km of Phnom Penh (Figure 4-4). Further south along the Bassac channel significantly less FPI is recorded, under $1x10^6$ m^3 per section as the river travels towards the Vietnamese border. Similarly, to the Cambodian study area, in the lowland areas of Vietnam FPI has been widely used to reclaim and elevate land above flood level (Bravard et al, 2013).

The biggest hot spots of FPI are in the areas to the north and south of Phnom Penh (Figure 4-4). The largest volumes of floodplain infill occurred upstream of Phnom Penh, nearest to the Mekong and Tonle Sap rivers where volumes of 34±$5x10^6$ m^3 and 29±$4x10^6$ m^3 were recorded respectively between 2000 and 2013 (Figure 4-4). This hotspot of development adjacent to both river channels accounts for over a third of the total volume of FPI recorded in Cambodia between 2000 and 2013. This indicates that the Urban areas in Phnom Penh have continued to expand outwards in all directions, particularly to the north where the largest infill growth areas have been recorded.

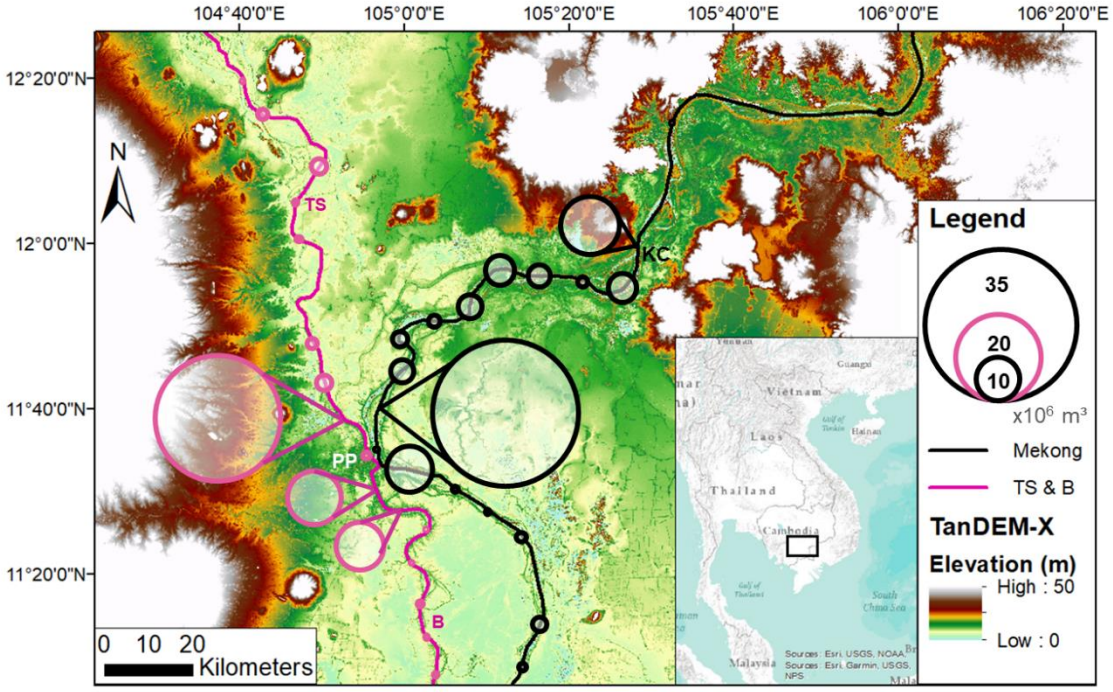

Figure 4-4: Spatial summary of floodplain infill (FPI). Circles depict measured volumes of infill (2013 – 2000) summed as 10km river increments (referenced to nearest channel).

Further upstream the Mekong, an 80km stretch from Phnom Pen to Kampong Cham indicates large volumes of FPI between 2000 and 2013, where the channel is free alluvial (Gupta & Liew, 2007). This section has experienced the largest volume of FPI outside of the two major cities, accounting for over 20% of the total FPI measured (Figure 4-4).

FPI activity near Kampong Cham is on the largest scale outside the area of Phnom Penh, with over $13\pm2x10^6m^3$ recorded between 2000 and 2013. Kampong Cham appears to be an area of development and was the only other place in the study area where lake infill was discovered. This means even greater volumes of infill would have taken places between 2000 and 2013, as lake infill was not quantified the volumes reported above. There is a distinct lack of infill activity upstream of Kampong Cham along the Mekong main stem, where the valley is most narrow with the smallest areas at risk of flooding (Figure 4-4). Local infilling has been observed around homes and roads for many locations in this region

(Rolf Aalto personal communication), but this is not possible to quantify using the research techniques of this study.

Measurements just over 2±1x10^6 m^3 of infill close to the centre of Phnom Penh is because most of this area had already been developed by the start of the study period in 2000. This meant new areas of FPI between 2000 and 2013 were rare and difficult to identify (Figure 4-4). However, central Phnom Penh was where 6 of the 7 infilled lakes in the study area were observed. This would have contributed an estimated extra 36±4 x10^6 m^3 which is not represented in this figure due to the considerable uncertainty with the lake infill volumes. If these estimates of lake infill were added it would mean central Phnom Penh would have experience similar scale infill between 2000 and 2013 as the section with the largest volumes of infill just north of Phnom Penh.

4.6 Spatial and temporal analysis

Combining the temporal and spatial data allows the trends of FPI in Cambodia to be shown across time and space. Interestingly, along the Bassac the highest rates of infill occurred near Phnom Penh between 2005 and 2007, then have been reducing ever since. However, further downstream towards the Vietnamese border, rates of FPI have been continuously increasing for each successive time period. Although continuing to increase in scale downstream, FPI activity is still greatest near Phnom Penh in the latest period (2011-2013). Representing the start of a slow shift of additional FPI activity occurring outside the capital, but the majority still in close proximity to the high value land in Phnom Penh.

Along the Tonle Sap River, FPI is greatest between 2008 and 2010 (15.5±2 x10^6 m^3) focused to the north of Phnom Penh, with FPI near the centre of Phnom Penh much less (Figure 4-5). Along the rest of the Tonle Sap further north there is little FPI activity, although it is gradually increasing, also indicating infill activities are increasing in all areas not just major cities. These areas go from less than 1 x10^6 m^3 of FPI between 2000 and 2004, to nearly 4±1x$10^6$$m^3$ from 2011 to 2013. Although these volumes are only around 15% of the volumes recorded in Phnom Penh, they do show rapid growth having quadrupled in just over a decade.

Along the Mekong main stem since 2000 FPI has been greatest near Phnom Penh and Kampong Cham, along this 150km stretch is also where the greatest increase in rates of FPI have occurred. Intriguingly the section north of Phnom Penh along the Mekong main stem, is largest between 2008 and 2010 (15.5±2 $x10^6$ m^3), and then reduces in scale by nearly 3 $x10^6$ m^3 between 2011 and 2013 (Figure 4-5). However, for the downstream section of Phnom Penh FPI rates continue to increase, reaching a maximum of 10±1 $x10^6$ m^3 between 2010 and 2013. Indicating the sprawl of the capital city is increasing in rates to the south, although the scale of FPI is still greater to the north.

FPI activity around Kampong Cham up to 2007 was relatively small, with just over 3 $x10^6$ m^3 measured in the eight years from 2000 up to and including 2007 (Figure 4-5). More than double this volume of FPI activity is then recorded in the three-year period of 2008, 2009 and 2010. Then, in the more recent section from 2011 up to and including 2013, over 3 $x10^6$ m^3 of infill was measured. This upward trend of infill around Kampong Cham highlights expanse of FPI activity outside of the capital city in Cambodia. Further monitoring and measuring of FPI activity is therefore vital.

Since the turn of the century the scale of FPI has continued to grow in Cambodia, to the point where 183±18 $x10^6$ m^3 of FPI was recorded between 2000 and 2013, not counting sediment used to infill seven lakes. This trend has grown both over time and space. Major cities, such as Phnom Penh and more recently Kampong Cham are major hotspot for FPI activity. Importantly, this research has highlighted that FPI activity is now also spreading farther away from these major cities.

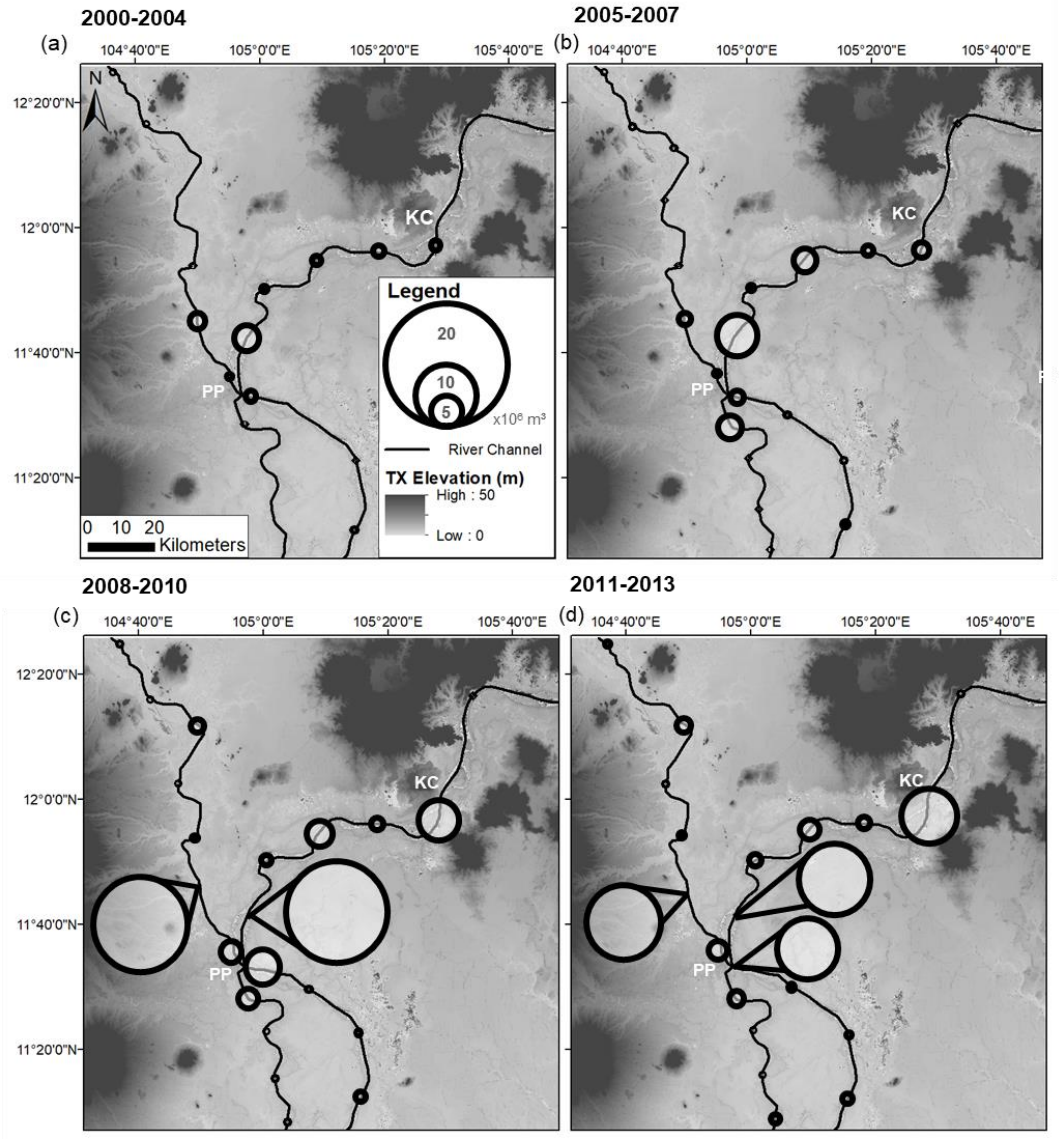

Figure 4-5**:** FPI distribution at 20km increments for 4 temporal intervals, in the LMB, Cambodia.

5. Discussion

5.1 FPI in Cambodia

FPI has been prevalent in Cambodia since introduced in the 1860's by French colonials who expanded the city of Phnom Penh out from the Mekong across the seasonally flooded floodplains (Doyle, 2012). This research has measured that 183±18 $x10^6$ m^3 of material had been built up in FPI activity between 2000 and 2013 in Cambodia. Revealing mass, industrial scale of FPI activity in this time equivalent to 292,971$x10^6$ kg of sand (assuming a sand density of 1,600 kgm^{-3}). To assess the scale of FPI activity within Cambodia it can be compared to the volume of sediment imported from countries worldwide from Cambodia during the same period. The volume exported by Cambodia in between 2000 and 2013 was 53$x10^6$ m^3 or 85,311$x10^6$ kg (sand density of 1,600 kgm^{-3}) which is nearly 3.5 times less than the scale of national FPI (United Nations, 2019).

This study is the first to quantitatively measure the FPI in Cambodia, and in doing so has revealed the major scale of FPI activity in the country. The relative difference of the SRTM to TanDEM-X was used to nullify the absolute height errors in the two datasets, and uncertainties from the standard deviation of bare earth areas have been propagated throughout. This relative difference reduced distance of elevation change measured, ensuring volumes were not overestimated. Although not quantified in this research, using data collected using InSAR techniques has limitations from the scattering properties of the earth's surface, known as decorrelation (Hooper et al, 2012). Therefore, uncertainty mentioned in this discussion results from differences in the bare earth measurements and is not an estimate of the uncertainty originating from the datasets. In addition, where possible conservative approaches were taken in the methodology, which means overall the values of FPI are underestimates by an unknown factor.

FPI activity has been a major demand for sediment from 2000 and 2013. Although this study is limited by temporally by the flight dates of SRTM and TanDEM-X, it shows the importance of continuing research on the demand and source of sediment within the MRB. Mialhe's study showed how the urban area of Phnom Penh has increased up to 2015, with infill of wetland areas a major process in

this expansion (Mialhe et al, 2019). FPI activity will continue to expand as long as there are additional landowners who can afford to infill their land above flood levels to protect their property and increase the value up to five time (Pierdet, 2008). Although there are clear benefits from FPI to the individual socially and economically, the environmental threat from unsustainable sourcing of sediment in the main concern, as well as having knock on impacts of flooding downstream (Kondolf, 1994; Houng & Pathirana, 2013). Therefore, further research into FPI activity, as well as sources of sediment will be crucial in enabling authorities to begin to regulate the sustainable development of the Mekong Basin.

5.2 FPI over time

The scale of FPI was smallest at the start of the study, between 2000 and 2001, where less than $2x10^6$ m^3 per year of sediment was estimated to have been used. Although these volumes are overshadowed by the exponential growth in FPI activity in Cambodia that occurred after, it is important not to understate the scale of activity at this time; equivalent to around 800 Olympic size swimming pools per year. Annual rates of FPI during this period equate to the weight of sand equivalent to $3.2x10^6$ tonnes yr^{-1}. With river sediment identified as likely main source of sediment, it is concerning that this volume equates to roughly half of the total sand flux entering the Mekong delta of $6.18 \pm 2.01x10^6$ tonnes yr^{-1} (Hackney et al, 2020).

Since 2001 the rates of FPI have exponentially grown up until 2010, where rates of infill peak at around $28 \pm 2x10^6$ m^3. This rapid increase in FPI activity reflects the average economic growth rate of 7% since 2001 in Cambodia, as FPI projects have become economically viable and more widely accessible (Mialhe et al, 2019). Another indicator of this expansion is the six-fold increase in the construction industry between 2003 and 2008, which would be a huge demand for aggregate itself (Nam, 2017). FPI is intertwined with the expansions of construction industry as infilled land provides areas for development.

Sediment excavated from The Mekong river has been identified as the main source of aggregate used in FPI activity in Cambodia, by ruling out importing of sand and on land quarries. This allows comparisons to be made between the

volumes of sediment excavated from the Mekong River and the related volumes of FPI. Such comparisons can be made with Bravard's estimate of just under $21x10^6$ m^3 of sediment excavated in Cambodia in 2011, with the FPI estimate from the same year, which is around $25\pm2x10^6$ m^3. The FPI measurements in this thesis, which is only one use of the sediment excavated, are therefore estimated to be $4\pm2x10^6$ m^3 greater in the same year. This is because of the underreporting of results questionnaires and surveys carried out by Bravard (Bravard et al, 2013). Bravard explained that the estimated volumes excavated were likely to be underestimates, as the mining operators would have benefited from lower fees by underreporting. The next step is to make direct measurements of the Mekong riverbed, in order to quantify excavation with lower levels of uncertainty than produced from questionnaire methods.

Unpublished research by Vasilopoulos is working to calibrate bathymetric datasets of the Mekong River from 1998 and 2013, in order to make direct measurements of sediment excavation (Vasilopoulos, personal communication). Previous research by Brunier assessed incision along relatively smaller sections along the channels of the Mekong delta (Brunier et al, 2014). To further this the bathymetric datasets in Vasilopoulos' work cover from north of Kampong Cham to the Vietnamese border, so will be able to quantify excavation at a greater scale (Vasilopoulos, personal communication). Similarities in the study area and time periods will allow for comparisons with the volumes of FPI calculated in this research, which will be carried out on the completion of Vasilopoulos' work.

The rates of FPI in 2010 and onward calculated in this research, combined with Bravard's estimate of excavation also illustrate the failings in enforcing the ban on dredging in 2009 after international pressure (Bravard et al, 2013). Shown with the largest volumes of FPI, which relies on nearby river sediment, and Bravard's estimate of sediment excavation occurring after 2009. Since then bans on sand mining have only really focused on exports, which were banned permanently in Cambodia in 2017 (BBC, 2017). However, the results of this study show that exports of sand are nearly 3.5 times less than the volumes of sediment used in FPI activity nationally within Cambodia, meaning the largest demand for sand is not addressed with a ban on exports (United Nations, 2019). Clearly more is needed to be done to truly allow the sustainable and safe development of

Cambodia's floodplains, without inducing detrimental effects elsewhere in the Mekong Basin.

It is important to continue to research the scale and trends of FPI in Cambodia and across the LMB. Since 2013, the date of TanDEM-X collection, in recent imagery on Google EarthPro there are numerous barges visible in the Mekong River (Figure 5-1). Near Phnom Penh ongoing FPI activities are still prevalent in the imagery and have been seen by various academics working in the field (personal communication, Prof. Rolf Aalto). Comparison of an area to the south east of Phnom Penh from 2013 to 2020 show continued industrial scale FPI (Figure 5-1). As land continues to increase in value, developers will take greater risks with FPI projects. This has been seen before with the infilling of lakes in Phnom Penh, some of which were retention reservoirs, which is likely to increase flood risk (Schneider, 2011). In the 2020 imagery, although unclear what the reclamation efforts will be used for, there is another example of ambitious uses for sediment to raise up land for development, this time within the river (Figure 5-1). This may be a harbour, but further development along the banks of the Mekong will put more stress on the river. With climate change expected to result in more frequent higher discharges events during the monsoon season, flood risk will be exacerbated in the basin from continued FPI development (Hoang et al, 2016; Pokhrel, 2018).

Figure 5-1 – Comparisons of the Mekong River Bank near Phnom Penh from 2013 and 2020 (Google, 2020).

5.3 Spatial FPI trends

FPI activity between 2000 and 2013 was predominantly focused in and around Phnom Penh, and Kampong Cham. The largest volumes of FPI occurred within 10km north of Phnom Penh, an area which has previously been recognised as having the largest infill growth areas since 2002 (Mom & Ongsomwang, 2016). Previous studies have analysed this area using satellite imagery, but the use of DEM differencing methods used in this research reveals that over $60x10^6$ m^3 of FPI activity has occurred between 2000 and 2013 in the area north of Phnom Penh. Similar spatial trends have been observed by Mailhe, where growth occurs most rapidly post 1990 when the Cambodian- Vietnamese War ended, then since the turn of the century expansion has been even more rapid (Figure 5-2) (Mialhe et al, 2019). Since 2000 the urban footprint of Phnom Penh has been expanding in all directions, most rapidly in Northern areas. FPI is needed in these areas of natural depression to raise the land above flood levels to protect infrastructure. In Cambodia FPI has been identified as the largest consumer of sand from riverbeds, making the scale of FPI measured in this thesis greatly concerning (Bravard et al, 2013).

Such urban development increases the flood risk due to local hydrological changes and higher concentration of people and assets, likely to be made worse my climate change. An example of this is infilling of lakes, which makes urban areas more densely populated and developed increasing impacts, as well as the removal of key retention reservoirs which is likely to increase flood likelihood (Schneider, 2011). Development will also impact further downstream by increasing the flow in the Mekong Delta, which combined with rising sea levels have modelled a significant increase in flooding in large cities on the delta (Huong & Pathirana, 2013). Therefore, future developments need to consider possible impacts the basin to avoid such adverse effects.

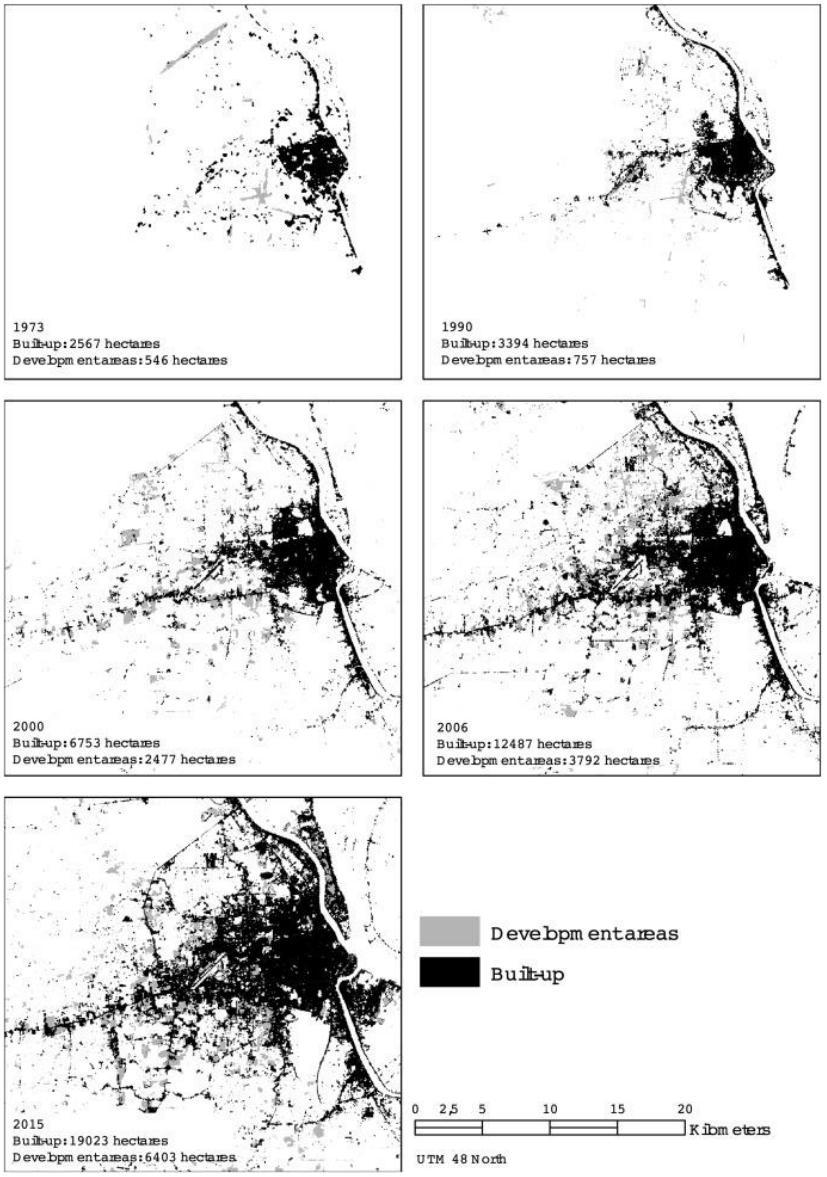

Figure 5-2: The expansion of urban areas in Phnom Penh between 1973 to 2015 (Mialhe et al, 2019).

While economic growth dictates where FPI activity can occur, geomorphology is another control on the spatial trends of FPI. This is most evident upstream of Kampong Cham along the Mekong River where the channel has been defined as structure-guided alluvial, within a narrower valley (Gupta & Liew, 2007). In this area the Mekong is less able to migrate and there are less depressions in the floodplain, explaining why the lowest volumes of FPI were identified in this stretch.

In this research the average distance from the centre of one of the main river channels (Mekong, Bassac or Tonle Sap) to each of the 176 infill sites identified was under 7km. FPI activity has been commonly associated with occurring near river channels, as the rivers provide a convenient source of high-quality aggregate (Kondolf, 1994). The largest volumes of infill were adjacent to the Mekong main stem, with over 60% of the total infill estimate occurring closest to the Mekong main channel, indicating the Mekong would have been the main source of sediment in this time. To reduce the cost of transport, it is likely sediment would have been extracted from the nearest river channel, meaning sediment excavation fuelled by FPI activity would have been widespread through Cambodia. Bravard's research revealed Cambodia was the largest extractor of sediment from the Mekong between 2011 and 2012, with sediment additionally being extracted in Laos, Thailand and Vietnam (Figure 5-3) (Bravard et al, 2013).

Figure 5-3: Sand mining 'pumping dredge' boats on the Mekong main stem in Cambodia (left) and Bassac in Cambodia (right) (Bravard et al, 2013).

In the centre of Phnom Penh minimal volumes of FPI were recorded in this research, due to the methods used and the study period. In the centre of Phnom Penh there has been a long history of FPI activity, dating back to the 1860's, meaning central urban area had largely already been developed by 2000 (Doyle, 2012; Mialhe et al, 2019). The capabilities of the methods applied in this research was also limited, meaning areas of infill which had since been developed were not measured. In Phnom Penh infrastructure was built quickly and densely on areas of FPI, therefore a limited area of infill which were measurable with this technique, which is a limitation. Other limitations stem from inaccuracies from

backscattering over waterbodies in the DEM datasets, that meant it was not possible to measure the volumes of sediment used to infill the seven lakes that were infilled in the study area between 2000 and 2013. Of these lakes six where situated in central Phnom Penh, where the value of land is greatest, which means the estimated volume of FPI is largely underestimated in the centre of Phnom Penh. Rough estimations were made based on the surface area of the lakes and applied a conservative average depth, which was estimated to be around 36±4 $x10^6$ m^3, however this value was not represented in this figure due to the considerable uncertainty as depth information was not available for the lakes.

5.4 Lake infill

As the value of land has increased Cambodia's urban areas, infill activity has increased. In Phnom Penh this includes the filling of urban lakes, described by Mialhe as a 'typical example of infilling' (Mialhe et al, 2019). This study identified six cases of lake infill in Phnom Penh, in many cases there were considerably large water bodies which would have used an enormous amount of sediment to infill (Figure 5-4). One example of Lake infill was also discovered in Kampong Cham, which is a worrying sign that lake infill may become more widespread throughout Cambodia in the future, as the economy continues to grow.

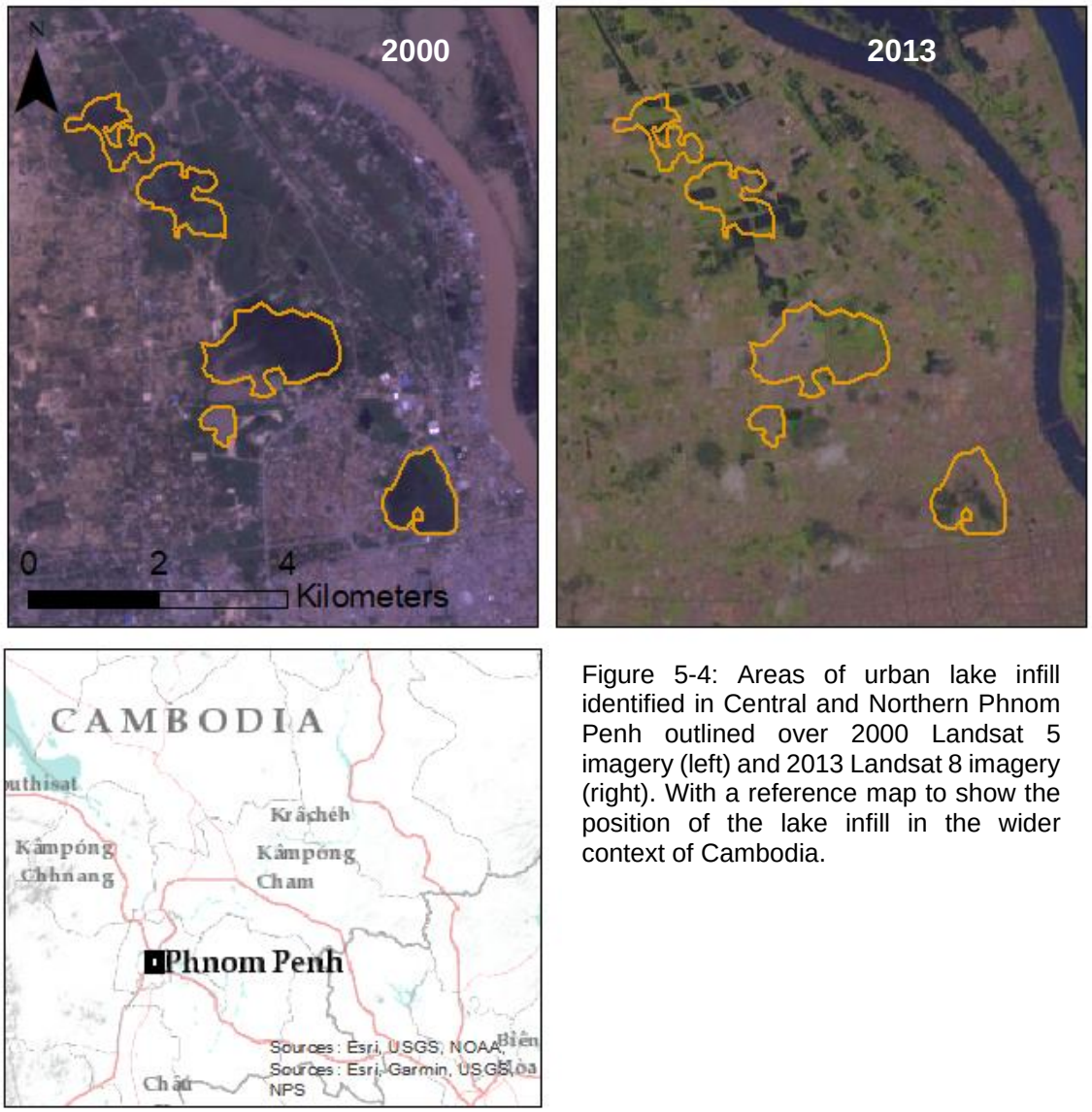

Figure 5-4: Areas of urban lake infill identified in Central and Northern Phnom Penh outlined over 2000 Landsat 5 imagery (left) and 2013 Landsat 8 imagery (right). With a reference map to show the position of the lake infill in the wider context of Cambodia.

The filling of water bodies such as these lakes in urban areas will put the inner-city area at higher risk of flooding. Boeng Kak Lake in the main inner-city area of Phnom Penh is an example of a retention reservoir which has been infilled with the aim of construction profitable real estate projects. The loss of water storage in the urban area from infilling this lake, and similar lakes nearby, increases the risk of flooding, and it is anticipated that the effects of climate change will increase this risk further (Schneider, 2011). Social issues also arise from lake infill projects such as Boeng Kak Lake, when the poor urban residents are evicted by force (Mgbako, 2010; Schneider, 2011). It would be beneficial for further research to accurately quantify the volumes of sand used in lake infill, to draw further attention

to the issue of the extreme demand for sand in Cambodia. But it is also clear that regulations need to be put in place immediately to limit the spread of lake infill projects in Cambodia, saving them from repeating the same upward trend of FPI after the turn of the century.

5.5 Spatial variations over time

By combining the spatial information collected from the DEM differencing and timescales of FPI from satellite imagery, this research was able to analyse the spatial patterns of FPI with finer temporal resolution. Due to the uncertainty associated with the start and end times of FPI activity at each site observed in the satellite imagery, the study period (2000-2013) was split into 4 periods (2000-2004, 2005-2007, 2008-2010 and 2011-2013), so that average volumes of FPI located closest to each section of main river channel could be analysed over time.

FPI activity between 2000 and 2004 was focused almost completely on areas from Phnom Penh to Kampong Cham, with scarce examples occurring in other regions. The spatial trends are similar again between 2005 and 2007, with activity beginning to increase around Phnom Penh and Kampong Cham, but still at a considerably smaller scale. The most noticeable change occurs in the period between 2008 and 2010, where volumes of infill in and around Phnom Penh over doubled. Phnom Penh has remained the epicentre of FPI activity in Cambodia, followed by Kampong Cham. But the increases in FPI throughout the country from 2000 to 2013 are an indicator of how wealth has growing outside of the major cities. Cambodia's economic growth since the turn of the century has resulted in the scale of FPI activity grow over time, and over space, as it become economically viable to development land further from the main urban centres (Pierdet, 2008; Mialhe et al, 2019).

This study shows that Phnom Penh and then Kampong Cham have had the largest rates of FPI from 2000 to 2013. This highlights them as areas of focus for resource management which will ultimately protect the rivers from the effects of sediment excavation (Kondolf 1994: Bravard et al, 2013). The capital city, Phnom Penh consistently had the highest volumes of FPI activity throughout the study period. In the area surrounding Kampong Cham where the scale of FPI has

shown the largest growth from with rates of FPI increasing by more than nine times from the start of the study period in 2000 to 2013. Follow on research will be needed to measure and monitor FPI activity in Kampong Cham, as well as other similarly large cities which my potentially have the largest potential for FPI activity growth.

The development of Cambodia is important and the economic growth the country has achieved since the turn of the century has been very exciting. However, fluvial sand resources have become unsustainable due to the industrial scale of FPI and exports driving excavation (Lamb et al, 2019). This is because local resource management committees have lost their ability to regulate or stop sand mining, and therefore lost their credibility, with illegal sand mining carried out without consequence (Marschke, 2017). Therefore, to enable sustainable development in Cambodia, there needs to be better enforcement of regulations. In addition, innovative alternatives need to be introduced which can satisfy the demand for aggregate from FPI and construction, while limiting the impacts on the Mekong River system.

Although rates of FPI to the north of Phnom Penh started to reduce after 2011, it was still the largest hotspot of FPI activity. To the south of Phnom Penh and around Kampong Cham FPI activity continued to increase right up to the end of the study period in 2013. This indicates FPI is showing no signs of slowing down or stopping, but in fact it is likely that the focus of the largest volumes may shift spatially over time. Kampong Chhnang to the North, and Prey Veng to the South are examples of cities which have shown increase in FPI activity since 2007, although currently at a much smaller scale, they have potential to be future hotspots of FPI activity. It is important to understand areas where FPI activity has been increasing in scale most recently, as they are areas where ideas around sustainable development have the best opportunity of being implemented effectively, without limiting or restricting the opportunities for development in those areas.

5.6 Sand trade

From 2000 to 2016 Cambodia imported less than 300 m^3 of natural sand, meaning that almost all of the 183±18 $x10^6$ m^3 of FPI would definitely have been sourced nationally (United Nations, 2019). In 2016 the global sand industry was valued at US$1.71 billion, with sand being extracted at a rate that exceeds natural renewal worldwide, making it unsustainable (Peduzzi, 2014; Sutherland et al, 2017). Cambodia has been proven to be no exception to this, fuelled by a growing demand from FPI. The source of sediment in FPI activity is vital in understanding sustainability and if future actions are required.

Sand trade data also illustrates how trustworthy reporting of data is needed to better understand the scale of the sand problem in Cambodia. To understand the true scale of exports from Cambodia, the reported imports of sand from countries across the globe were analysed, which were nearly six times greater between 2000 and 2016 than the volumes Cambodia had reported exporting (United Nations, 2019). It appears underreporting of sand has been used to cover up the scale of the problem since 2009, when the Cambodian Prime Minster officially forbade exporting natural sand exports from rivers to Singapore (Franke, 2014; Koehnken & Rintoul, 2018). More recently, in 2017, Cambodia and Vietnam officially banned exports again. However, in 2018 Mekong River Sand was still advertised for sale online, emphasising the lack of enforcement of such embargos (Koehnken & Rintoul, 2018).

Although the volumes of sand exported by Cambodia since the turn of the century are nearly 3.5 times smaller than volumes of FPI measured between 2000 and 2013, they are still significant volumes which contribute to the increase of demand for sand. Additional demand from the construction industry makes sand a widely sought-after commodity, increase pressure on excavation and mining processes. Singapore is the biggest importer of sand globally, and Cambodia has been the largest exporter to Singapore from 2007 to 2016 (Figure 5-5) (Lamb et al, 2019). This is a cross border issue, effecting multiple countries across the transboundary MRB. Vietnam is the second largest exporter to Singapore (Figure 5-5), likely much of this sediment would also have been sourced from the Mekong (Lamb et al, 2019). Demonstrating that sand excavation is an issue outside of the study are in Cambodia. Bravard estimated the majority of sand extracted from the

Mekong River was in Cambodia, with annual extraction rates of $21x10^6$ m^3 in 2011. On top of this Vietnam extracted nearly $8x10^6$ m^3, then Thailand at around $5x10^6$ m^3 and Laos just over $1x10^6$ m^3, all annually within the same time period (Bravard et al, 2013). All indication an abundance of river channel sediment mining throughout the MRB.

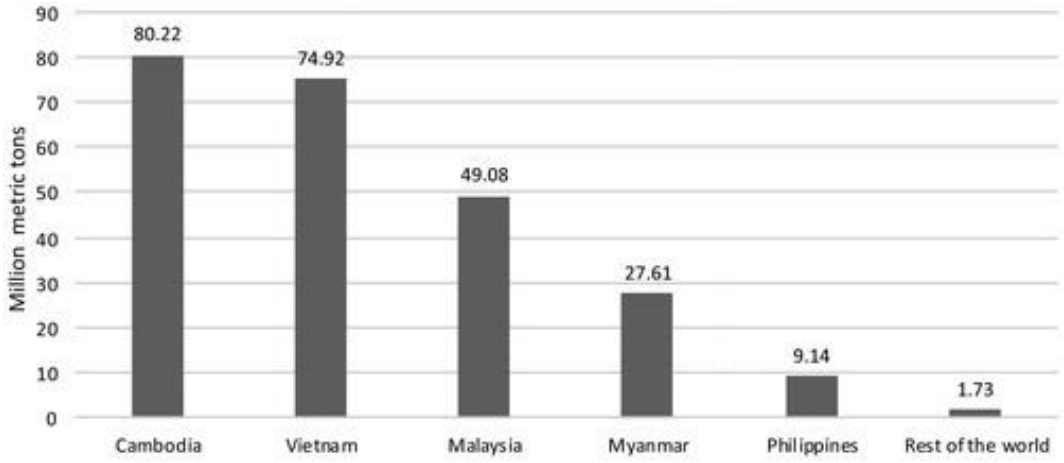

Figure 5-5: Singapore sand imports, as reported on UNComtrade, from 2007 to 2016 (Lamb et al, 2019)

5.7 Sources of sediment

Understanding the main source of sediment that has supplied FPI activity in Cambodia is pivotal in addressing the impacts of such a large-scale industry. FPI has already been recognised as being the largest consumer of sand excavated from riverbeds in the Mekong Basin (Bravard et al, 2013). In this study to address the possibility of alternative sources of sediment suppling the FPI activity measured in Cambodia, this research has analysed sand imports and quarry volumes. Cambodia importing sand, discussed above, can be quickly discounted as a major supplier of sand for FPI activity, as it makes up just over 0.0001% of the volume of FPI recorded from 2000-2013 (United Nations, 2019).

Another possible alternative source of sediment addressed was quarried material. Areas of quarried land on the floodplain and in the highlands of Cambodia were identified and then volumes of sediment excavated were calculated using the DEM differencing methods. The volumes of quarried material

were only equal to around 12-14% of the total volume of FPI recorded in the same period (2000-2013). It is also unclear what material was being mined at each site identified, and it is unlikely valuable hard rock from highland quarries would be transported long distances to the sites of FPI. Therefore, it is almost certain that some of the mines were not quarrying material for FPI and therefore would have contributed even less to the 183±18 $x10^6$ m^3 of FPI.

Beaches are also a source of sand in many countries, especially in Myanmar (Lamb et al, 2017). Off the coast of Cambodia, two activists were arrested and convicted of 'violation of privacy' for filming illegal sand mining in 2017, showing that laws surrounding sand mining are not being enforced correctly (Larson, 2018). Beach sediment were not measured using volumetric difference methods as there would be very high uncertainty due to natural sediment transport processes. There were also no beaches within the study area of this research, the closest being roughly 150km from Phnom Penh. It is therefore assumed that due to the long distance between beaches and the main urban centres in the study area, sediment would have more likely been sourced from the more conveniently located Mekong River.

Another source of sediment witnessed in this study was from on-site excavation, which most commonly was associated with expanses in the road network across the floodplain. In this instance, sediment was excavated from either side of the road and used to build up the road deck. As road network infill was too narrow to measure with the 1 arc-second resolution NASADEM dataset (roughly 30m), it was not measured in this thesis. The wide use of sediment for infill of road and levee to raise above flood levels, across the lowland areas of the LMB, has been quoted as a reason why the economic demand for sand in Cambodia and Vietnam is high (Bravard et al, 2013). With future improvements in DEM resolution, such as TanDEM-X, it may eventually be possible to measure the infill of road networks.

Having addressed the main alternative sources of sediment, it is clear that none of the alternatives are as convenient or high quality as river sediment, nor have the capacity to meet the demand of FPI from 2000 to 2013. This is evident in Google streetview imagery in Phnom Penh near the banks of The Mekong River, where the infrastructure is built on raised land adjacent to the river banks with

lorries of sediment and mining barges visible in the Mekong River (Figure 5-6). Therefore, supported by Bravard who reported FPI is the largest consumer of sand excavated from riverbeds in the Mekong Basin, it is determined that river sediment is the source of the majority of sediment used in FPI activity from 2000-2013 with a good degree of confidence (Bravard et al, 2013).

Figure 5-6: Images from Google Streetview showing sediment being transported and stored next to the bank of The Mekong River in Phnom Penh, Cambodia (Google, 2020).

5.8 Mekong River sand mining

The economic demand for sand from infill activity, construction and exports is not only very high in Cambodia, but throughout the entire LMB. FPI activity in Cambodia has been identified as the process which consumes the largest volumes of sand which have been directly drawn from riverbeds in the Mekong Basin (Bravard et al, 2013). When industrial-scale dredging began along the lower Mekong, it was focused around Phnom Penh, to supply infill of the floodplains, wetlands and channel banks, to improve the flood resilience of capital (Pierdet, 2008). This relates to some of the earliest concepts of river sediment being a convenient source of high-quality aggregate for construction as Phnom Penh as also the location of the largest scale FPI measurements (Newport, 1974; Kondolf, 1994). It has also been reported that the number of mining operations along the Lower Mekong River had risen from 15 in 2001 to 70 in 2011, an increase likely fuelled by the increasing demand for sand from FPI (Figure 4-3) (Hackney et al, 2019). As FPI has expanded spatially in Cambodia, spreading from Phnom Penh to other urban centres, sand mining activity appears to have followed. An example of this along the Mekong River at Kampong Cham, where large barges can be seen near the riverbanks, directly opposite to the site of lake infill (Figure 5-7). As economic development continues, it is likely FPI and lake infill will be widespread economically viable throughout more cities and towns in Cambodia, and sand mining will follow.

Figure 5-7: Boeng Snay in Kampong Cham shown in 2003 and ten years later in 2013 when lake infill had largely been completed. Sand mining barges are visible on the Mekong River in close proximity to the site of lake infill.

5.9 Impacts to river system

FPI activity creates the largest demand for sand in Cambodia, with most sourced from the Mekong River as it is a convenient source of high-quality sediment (Kondolf, 1994; Bravard et al, 2013). It is therefore important to look at the impacts sediment removal has on the Mekong River system. However, it is impossible to assign complete causation of such impacts to the Mekong River to solely sand mining, as there are many factors which combine within the basin. The MRB is subject to change from large scale sand mining, as well as sediment trapping from hydropower dams and irrigation, which combined amplify the detrimental effects of each other (Bravard et al, 2013; Kondolf et al, 2014). However, by looking at previous case studies which observe similar direct impacts it enables greater confidence in understanding the impacts relating directly from sand mining.

5.10 Geomorphic impacts

Geomorphic impacts of sand mining primarily come from excavating directly changing the shape and depth of the riverbed. The lowering of riverbeds due to sediment excavation has been witnessed to cause bank instability in rivers across the world for decades (Kondolf, 1994). In the Tuscon River, United States this caused potential undermining of bridges, where the sandy gravel bed of the river was lowered by around four metres (Bull & Scott, 1974). Without mitigation it is possible for large scale sand mining operations, similar to that along the Mekong River to cause costly structural damage to infrastructure.

The Mekong River bed has already shown average bed deepening of 1.3m in the Mekong and Bassac channels on the delta, which results in increased bank instability as well as shoreline erosion of the delta (Kondolf, 1994; Brunier et al, 2014; Vasilopoulos, personal communication). Increased bank instability and erosion has been seen in many cases along the Mekong river, and has started to impact infrastructure along the rivers banks (Figure 5-8) (Miyazawa et al, 2008; Bravard et al, 2013; Brunier et al, 2014; Hackney et al, 2020). If such bank erosion increases, more infrastructure along the Mekong Riverbanks will become

vulnerable, which could have large economic impacts (Kondolf, 1997; Padmalal et al, 2008). This is of greatest concern in urbanised areas, where sand mining often takes place for convenience, with particular focus on Phnom Penh, where the largest increase in average width of the channel increased by over 40m from 1996 to 2016 (Kondolf 1994; Bird, 2018).

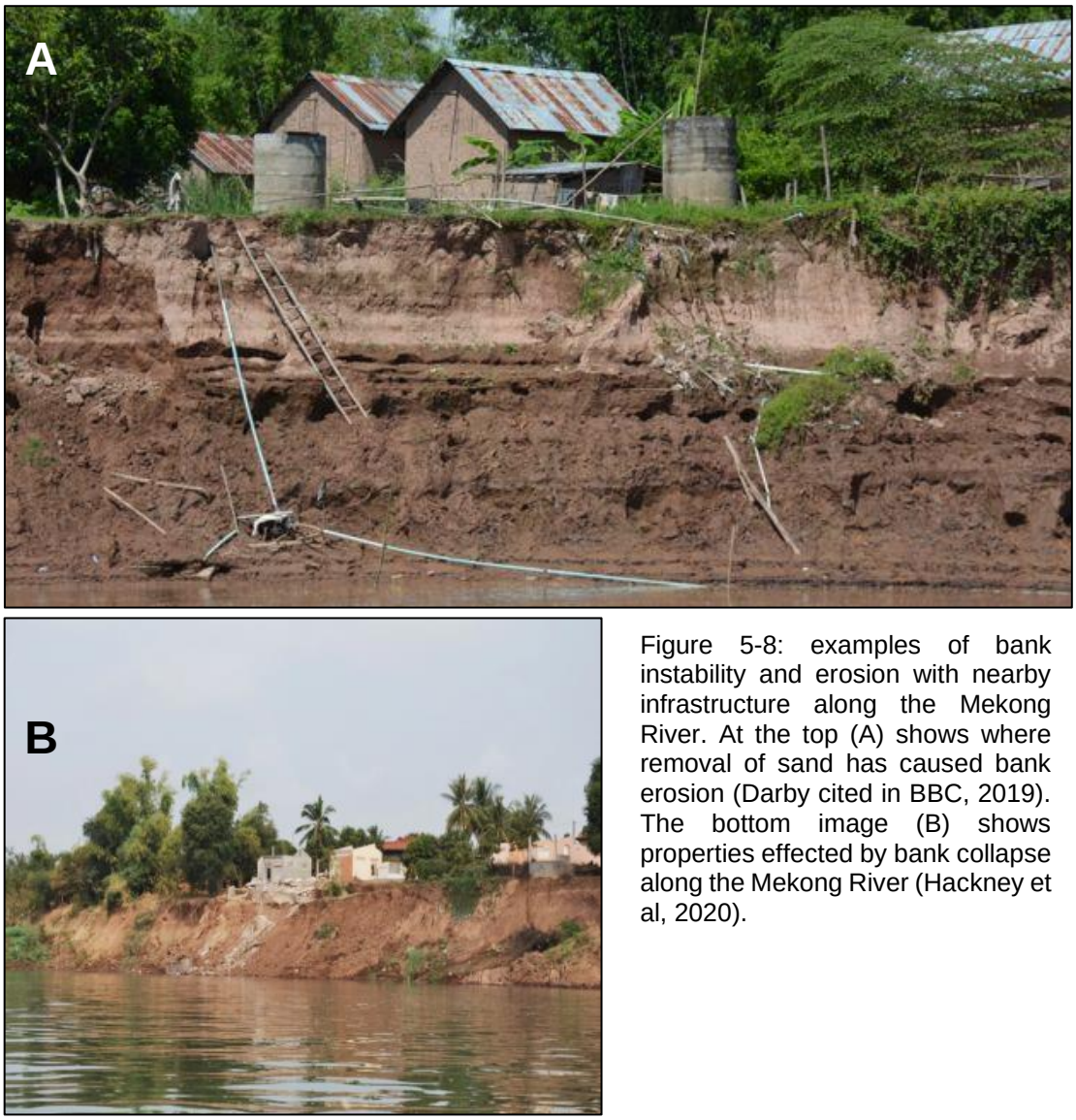

Figure 5-8: examples of bank instability and erosion with nearby infrastructure along the Mekong River. At the top (A) shows where removal of sand has caused bank erosion (Darby cited in BBC, 2019). The bottom image (B) shows properties effected by bank collapse along the Mekong River (Hackney et al, 2020).

Sediment extraction from the Mekong river has been shown to be between five and nine times greater than the natural supply of sand. This creates a large deficit in the sediment supply which can have severe consequences for the delta system (Hackney et al, 2020). In addition to this the delta is vulnerable to changes in sea-

level and sediment trapping from dams. Under a ‘definite future’ scenario of 38 dams which are built or under construction, would reduce the cumulative sediment supply to the delta by 51% (Kondolf et al, 2014). The Mekong delta is now in a phase of exacerbated vulnerability from a combination of; sediment supply reduction, due to sand mining and dams; and coastal erosion increases from sea level rise. Which threatens the future stability of the Mekong Delta and the assurance of its ecosystem services, impacts that will be extremely difficult to reverse (Brunier et al, 2014).

5.11 Environmental impacts

Sand dredging licences in Cambodia have made concessions within protected areas, which are home to internationally significant habitats and ecosystems, including endangered species (Global Witness, 2010). Anthropogenic pressures on the Mekong River upstream of the study site have also caused habitat loss and fragmentation which has led to the Irrawaddy dolphin being classified as critically endangered (Beasley et al, 2013). Further habitat loss also effects even the most abundant of fish stocks and crabs, which local fisherman have attributed to the introduction of dredging vessels (Global Witness, 2010). All impacts to the environment within the LMB will have knock of effects to the human populations which call the LMB home.

5.12 Human impacts

Sand extracted from the Mekong river causes changes to the instream and riparian habitats, which effect fish stocks and in turn the food security of fishermen and farmers who reply on the river ecosystem for their livelihoods (Padmalal et al, 2008; Ziv et al, 2012). Impacts to the Mekong River have the ability to affect a large majority of the 70 million people that live within the LMB (Piesse, 2016). With 80% of the households within the region directly dependent on the river for their food and livelihoods (Piesse, 2016). Additionally, the vulnerabilities of the delta will be a direct threat to the 20 million habitants, which may lead to environment change refugees (Orr et al, 2012).

Insufficient regulation of illegal sand mining along the Mekong River has resulted in corruption and gang involvement, which puts public guards at threat as well as citizens who may get caught up in such activity (Nguyen, 2011; Bravard et al, 2013). Ignoring the environmental and human impacts of sand mining caused by poor environmental management practices of the sand mining industry, is a violation of Cambodia's national legislation, commitment to human rights, and obligations to conserve biodiversity (Global Witness, 2010).

5.13 Unsustainable sand extraction

The array of impacts caused by sediment excavation from the Mekong River demonstrate how the industrial scale of mining is unsustainable. Showing that change is needed now, before detrimental, irreversible impacts take place. Previous shortcomings from legislative action and bans on excavation and exports, due to failure to implement such schemes effectively means that sand excavation continues to be unsustainable in Cambodia (Bravard et al, 2013). Currently rates of extraction from the Mekong River exceed the sediment supply from upstream, which will impact bank stability and retreat susceptibility of the delta (Hackney et al, 2020).

FPI was measured at being roughly 183±18 $x10^6$ m^3 in the study area in Cambodia from 2000 to 2013, such an enormous scale of infill will have created a gigantic demand for sand from the Mekong River. This has brought great benefit to land and properties owners, reducing flood risk to their properties, and increasing the value by up to five times (Pierdet, 2008). However, large scale FPI would have contributed to the fact Cambodia had the largest extraction rates of any country in the MRB during 2011 and 2012 (Bravard et al, 2013). Therefore, the demand for sand caused by FPI developments needs to be regulated to preserve long-term sustainability of sediment resources in the MRB (Hackney et al, 2020).

5.14 Legislation

Across the MRB efforts have been made to try and implement bans of sand exports and well as excavation from rivers. In 2009 Cambodian Prime Minster officially forbade exporting natural sand exports from rivers to Singapore. However, Singapore has reported importing over $25x10^6$ m^3 of natural sand from Cambodia since then, from 2010 to 2016 (Franke, 2014; Koehnken & Rintoul, 2018; United Nations, 2019). In 2017 Cambodia and Vietnam officially banned exports again, however in 2018 Mekong River sand was still advertised for sale online, emphasising the lack of enforcement of such embargos (Koehnken & Rintoul, 2018). Illegal sand mining still has a constant presence throughout the MRB, and with no effective legislation to control volumes and methods of extracting, such activity will continue to negatively impact the river (Nguyen, 2011; Bravard et al, 2013). Therefore, it is important that such bans are effectively enforced with regulatory frameworks to ensure sand is no longer exported at an industrial scale (United Nations, 2019).

This paper shows that FPI activity within Cambodia is the largest consumer of sand, demonstrating there needs to be a focus on reducing the demand for sand from FPI. Previous bans on sand mining have been ineffectively enforced, with the excavation activity continuing at an industrial scale driven by the demand and resultant economic benefit. It would be unfair to put a ban on FPI, as it is an effective way of protecting people's properties and livelihoods. However, guidance and innovation is needed to ensure FPI and associated materials are carried out sustainably.

5.15 Actions for sustainable sand

To successfully make sand sustainable in the MRB, it is important to understand the drivers of the industry as a whole, in order to effectively reduce the negative impacts without reducing the benefits. Sand mining from the Mekong River occurs because of a high demand for sand mostly nationally but also from Singapore and neighbouring countries (Bravard et al, 2013; United Nations, 2019). Therefore, it is vital for the sand used in FPI activity to be addressed as well as placing bans on exports.

It would not be effective to simply recommend reducing the volumes of aggregate used. As quotas and bans have proven before, the economic demand and opportunity will overcome inadequately enforced quotas (Bravard et al, 2013). In the construction industry, ideas around reducing the amount of sediment required by using more efficient building materials. These include concrete blocks and construction panels with hollow cores which could be used to reduce the demand for sand, and hopefully be adapted to reduce the demand from FPI (Bendixen et al, 2019).

Further ideas around the innovative alternative sources of sediment from industrial water, crushed rock and even recycled plastic would lessen the demand for fluvial sediment. This includes reusing sand-based materials where possible, for example demolition waste being crush down and reused for areas where lower quality aggregates are needed (Bendixen et al, 2019). Although it will be very difficult, the key is finding an alternative high-quality source of aggregate which can compete economically with natural fluvial sand. Although the convenient of fluvial sediment means it is unlikely such alternatives will be cost effective

This research has brought a first insight into the scale of FPI and the strain this has put on the Mekong River due to increase demand for sand driving sediment excavation. However, monitoring will need to continue, spanning the entire MRB, and looking at the global supply of sand to ensure sustainability. Ultimately, although previous government bans have failed, it is imperative that a new style of legislation is enforced to establish a regulatory framework that limits extraction rates by identifying viable alternative sources of sediment to the FPI industry (Hackney et al, 2020). FPI plays an important role in protecting people's properties and livelihoods throughout the floodplains of Cambodia and Vietnam, bringing many benefits across the basin. However, the unsustainable sourcing of sediment is needed to reduce the impacts of sand mining.

By identifying FPI as the largest consumer of sediment from the Mekong River, it gives a focus of efforts to reduce the demand for sand in the region (Bravard et al, 2013). The scale of FPI in Cambodia creates the demand for sand mined from the Mekong River. It is therefore imperative that all of the above ideas are introduced in order to educate and support the sustainable extraction and FPI activities in the basin (Bendixen et al, 2019). With supporting frameworks,

monitoring can be carried out to ensure there is a sustainable balance between the extracted volumes of sediment and the natural supply (Hackney et al, 2020). This level of innovative support is needed to maintain current levels of development, while also monitoring and regulating the long-term sustainability of the sediment source and mean sufficient volumes of sand are delivered to the delta (Hackney et al, 2020). Such ideas should be applied to all fluvial systems across the world to ensure the supply of sand is sustained to the levels of demand for future generations.

6. Conclusion

The LMB is home to over 70 million people, with 80% of this population relying on the river for food and livelihoods (Piesse, 2016). Economic development within the region, which has supported urban expansion has led widespread FPI activity in the LMB, where sediment is used to fill land above flood levels in the low lying floodplains and on the delta (Pierdet, 2008; Nam, 2017; Mailhe et al, 2019). This study revealed that from 2000 (NASADEM) to 2013 (TanDEM-X) $183 \pm 18 \times 10^6$ m^3 of sediment was used to raise the elevation of identified FPI sites in the MRB in Cambodia. Roughly 80% of this FPI was recorded within a 20km area around Phnom Penh, highlighting the capital as a hotspot for FPI activity during this period. Worryingly, the above FPI measurements do not include sediment used to infill lakes in Cambodia, which was particularly evident in the Capital where six lakes had been infilled during the study period. Lakes were infilled to produce new, high value land for development, but will likely increase the flood risk for the surrounding area (Scheider, 2011). As Cambodia's economic growth continues, at a rate of 7% since the turn of the century, FPI activity began to be witnessed along all stretches of the Mekong, Tonle Sap and Bassac Rivers (Mailhe et al, 2019). From Kampong Cham in the Lower Mekong Basin the river channel is free alluvial, surrounded by depressions in the floodplain, so FPI is an effective way of raising land above flood levels, increasing the resilience of developments (Gupta & Liew, 2007; Doyle, 2012). As FPI becomes economically viable for more people, the expanse of activity has been witnessed across Cambodia in smaller towns in addition to the major cities.

As part of this assessment, the scale of alternative sources of sediment were investigated to understand the likely source of the majority of sediment used in the measure FPI activity in Cambodia from 2000 to 2013. The scale of quarried material in the study area only equated to around 12-14% of the volume of FPI measured during the same period. Cambodia also imported less than 300 m^3 of natural sand since the turn of the century, showing the sediment must have been nationally sourced (United Nations, 2019). These figures meant that it can be said with more confidence that the main source of sediment for FPI was from the Mekong River and adjoining channels. Supported by Bravard's previous statement that FPI was the largest consumer of sand from the Mekong riverbed,

as it is a convenient source of high quality sediment (Kondolf, 1994; Bravard et al, 2013).

The peak years of FPI identified were since 2008, where volumes started exceeding $20\pm2x10^6$ m^3 annually, eventually peaking in 2010 and 2011 above $25\pm2x10^6$ m^3yr^{-1}. FPI, the main consumer of sand from riverbeds in the MRB, exceeded Bravard's earlier underestimate of sediment excavation from the Mekong in Cambodia in 2011 by around $4\pm2x10^6$ m^3 (Bravard et al, 2013). This demonstrates the benefits of making measurements of the landscape to calculate volumes of sand activity in Cambodia, not relying on honesty from those excavating sand, who would benefit from underreporting their figures (Bravard et al, 2013).

Misreporting of data was also noticed in the UNComtrade data of Cambodia's trade of natural sand (United Nations, 2019). Since 2009 Cambodia's reported exports have been well below the volumes reportedly imported from Cambodia by countries worldwide, notably Singapore (United Nations, 2019). This follows a ban on sand exports placed in Cambodia in 2009, however the data shows major failings, revealing exports continued but were falsely reported (Peduzzi, 2014).

There are many impacts from the supply chain of FPI, driving fluvial sand mining in the LMB. With the transboundary river subject to a cumulation natural and anthropogenic forcing's throughout the basin (Bravard et al, 2013; Kondolf et al, 2018). Bravard's underestimate of the volume of sand extraction from the Mekong alone equates to roughly half of the sand flux entering the Mekong delta, which is exacerbated by dam sediment retention (Kondolf et al, 2018; Hackney et al, 2020). Unfortunately, there is a sediment supply deficit to the delta, which has been seen to cause retreat of the delta coastline (Anthony et al, 2015; Kondolf et al, 2018). These impacts will be intensified by climatic changes to rainfall and sea level rise, which has been seen to increase flood risk in Vietnam on the Mekong delta (Huong & Pathirana, 2012). Overall, these forcing's have increased the vulnerability of the 20 million people who call the Mekong Delta home, and has already been seen to cause outmigration of residents (Szabo et al, 2016).

Industrial scale sand mining form the Mekong River, fuelled by FPI, impacts the geomorphology, environment, and people throughout the LMB. Sand mining from

the riverbed creates pits which propagate up and downstream, witnessed in the Mekong River channel using bathymetric data (Kondolf, 1994; Brunier et al, 2014; Vasilopoulos, personal communication). Such deepening has caused bank instability, and along the Mekong bank erosion has started to impact infrastructure, which can have large economic impacts (Miyazawa et al, 2008; Padmalal et al, 2008). Geomorphic changes can have knock on impacts to people and the environment, including destruction of habitat which effects fish stocks (Padmalal et al, 2008). This puts stress on the food security for the more than 55 million people who rely on the Mekong River for food and their livelihoods (Piesse, 2016).

It is vital that future policies are effectively applied to reduce sand mining in the MRB. To achieve this it is important to understand the main cause of the demand for sand in Cambodia, which has been identified in the paper as floodplain infill (FPI). While FPI brings many benefits to people living in the LMB, by increasing the flood resilience of developments which have been raised above flood levels. It is vital that the aggregate used in this process is sustainably sourced, because of the negative impacts it can otherwise have throughout the basin. At the moment large-scale extraction of sand from the Mekong river is unsustainable, as estimations of sediment extraction exceed the total sediment flux reaching the delta by over $40x10^6\,yr^{-1}$ (Hackney et al, 2020). With the Mekong River in a sediment deficit, sediment extraction needs to be reduced, in order to reduce the long-term impacts to the basin and the delta.

The scale of FPI in Cambodia between 2000 and 2013 has been revealed to be the largest demand for sand in Cambodia by this research, driving sediment excavation from river channels in the Mekong Basin. FPI benefits many building owners in the Lower Mekong Basin, so to put a ban or quota on infill activity would likely be hard to enforce and ineffective (Doyle, 2012). Therefore, it is crucial to ensure the aggregate used in FPI activity is sustainable, which will reduce the demand for fluvial sediment, eventually benefiting the health of the whole river system. To achieve a sustainable balance between the volumes of sand mined and the natural supply of sediment, it is not enough to simply apply a ban, as bans on exports have shown to be ineffective (United Nations, 2019). Instead innovative alternative sources of sediment will need to be utilised. With new styles

of supportive legislation effectively enforced, and ongoing monitoring to ensure the Mekong is not starved of sediment (Bendixen et al, 2019; Hackney et al, 2020).

Appendices

Appendix A: TanDEM-X WAM and HEM data

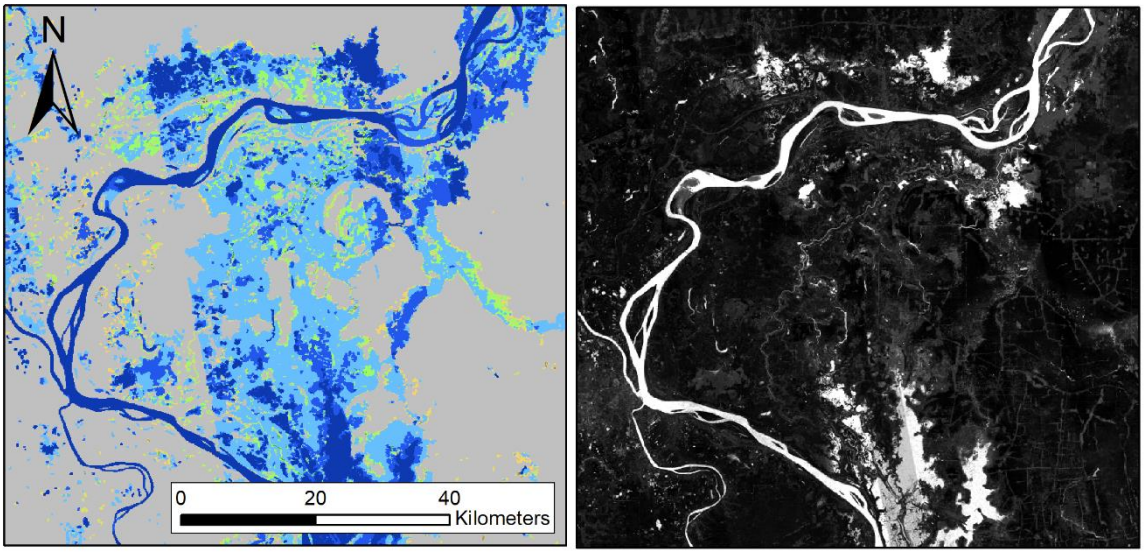

Appendix A: TanDEM-X WAM layer on the left, dark blue shades show areas where surface water is likely to have affected the quality of the DEM data. On the right is the HEM layer, with lighter colours showing lower quality, and darker higher confidence in quality of data.

Appendix B: FPI site data

Infill site No.	Area (km^2)	Nearest River	Distance downstream (km)	Average Elevation Difference (m)	Calibrated Elevation Difference (m)	Adjusted Volume (m^3)	Year FPI started	End of FPI (by 2013)	Years of infill	Volume/year (m^3)
1	0.34	M	24	3.73	2.48	844,088.88	2005	2010	6	140,681.48
2	0.08	M	35	2.83	1.58	132,503.01	2011	2013	3	44,167.67
3	0.52	M	66	1.49	0.24	126,049.43	2011	2013	3	42,016.48
4	0.15	M	78	3.33	2.08	303,872.27	2006	2012	7	43,410.32
5	0.29	M	78	2.42	1.17	339,093.30	2010	2013	4	84,773.32
6	0.38	M	102	1.86	0.61	233,877.57	2011	2013	3	77,959.19
7	1.69	M	104	2.71	1.46	2,457,527.55	2000	2010	11	223,411.60
8	0.43	M	107	5.26	4.01	1,721,271.10	2010	2013	4	430,317.78
9	1.56	M	107	3.79	2.54	3,963,061.97	2007	2013	7	566,151.71
10	1.11	M	108	2.49	1.24	1,381,709.27	2007	2013	7	197,387.04
11	1.13	M	108	3.87	2.62	2,949,143.51	2007	2013	7	421,306.22
12	0.93	M	108	2.25	1.00	926,356.31	2003	2010	8	115,794.54
13	0.13	M	115	2.01	0.76	98,396.30	2010	2013	4	24,599.08
14	0.14	M	116	3.27	2.02	291,668.31	2003	2010	8	36,458.54
15	0.50	M	117	2.88	1.63	810,453.57	2003	2010	8	101,306.70
16	2.58	M	118	3.31	2.06	5,316,300.75	2010	2013	4	1,329,075.19
17	1.08	M	121	3.02	1.77	1,913,850.35	2010	2013	4	478,462.59
18	0.81	M	125	2.05	0.80	646,613.73	2000	2006	7	92,373.39
19	0.58	M	130	2.62	1.37	795,478.67	2004	2013	10	79,547.87
20	0.24	M	135	2.31	1.06	258,379.08	2004	2012	9	28,708.79
21	0.21	M	136	2.21	0.96	201,498.81	2004	2012	9	22,388.76

22	7.66	M	138	1.76	0.51	3,905,437.96	2002	2011	10	390,543.80
23	1.69	M	146	2.27	1.02	1,722,998.75	2003	2010	8	215,374.84
24	2.50	M	147	2.43	1.18	2,948,208.59	2005	2012	8	368,526.07
25	0.35	M	148	2.02	0.77	267,772.13	2010	2013	4	66,943.03
26	0.39	M	148	2.71	1.46	569,686.45	2006	2012	7	81,383.78
27	1.67	M	148	2.04	0.79	1,323,519.25	2005	2012	8	165,439.91
28	0.30	M	154	2.36	1.11	332,072.64	2000	2010	11	30,188.42
29	0.61	M	155	1.91	0.66	404,592.01	2006	2013	8	50,574.00
30	5.93	M	155	1.97	0.72	4,257,023.18	2003	2013	11	387,002.11
31	0.87	M	159	1.80	0.55	476,209.64	2010	2013	4	119,052.41
32	0.35	M	160	2.07	0.82	287,659.47	2010	2013	4	71,914.87
33	0.25	M	162	1.91	0.66	163,608.65	2002	2007	6	27,268.11
34	0.37	M	162	2.11	0.86	317,215.02	2000	2012	13	24,401.16
35	0.50	M	164	1.47	0.22	112,019.30	2006	2013	8	14,002.41
36	0.28	M	167	2.09	0.84	231,154.29	2000	2010	11	21,014.03
37	0.33	M	167	2.32	1.07	351,550.03	2010	2013	4	87,887.51
38	0.67	M	168	2.91	1.66	1,115,126.02	2010	2013	4	278,781.51
39	0.06	M	169	2.39	1.14	68,614.88	2000	2003	4	17,153.72
40	0.10	M	170	3.67	2.42	238,121.03	2010	2013	4	59,530.26
41	0.57	M	170	2.22	0.97	549,582.49	2007	2013	7	78,511.78
42	0.96	M	171	1.79	0.54	514,616.71	2003	2010	8	64,327.09
43	0.04	M	172	3.37	2.12	84,667.48	2002	2010	9	9,407.50
44	0.32	M	173	1.92	0.67	215,822.33	2002	2010	9	23,980.26
45	0.81	M	173	2.79	1.54	1,245,515.06	2002	2010	9	138,390.56
46	0.25	M	175	3.76	2.51	628,901.70	2010	2013	4	157,225.43
47	0.08	M	179	1.46	0.21	16,564.16	2006	2010	5	3,312.83
48	0.10	M	181	2.56	1.31	128,938.93	2008	2012	5	25,787.79
49	0.49	M	182	2.15	0.90	438,875.63	2010	2013	4	109,718.91
50	0.39	M	182	1.87	0.62	243,615.25	2010	2013	4	60,903.81
51	0.52	M	185	2.20	0.95	496,713.95	2008	2013	6	82,785.66
52	0.47	M	185	3.44	2.19	1,029,364.15	2003	2010	8	128,670.52
53	0.19	M	186	2.17	0.92	175,149.58	2010	2013	4	43,787.39
54	1.08	M	187	3.92	2.67	2,880,921.94	2003	2010	8	360,115.24
55	4.95	M	190	2.93	1.68	8,299,939.72	2007	2013	7	1,185,705.67
56	0.19	M	192	3.28	2.03	384,887.34	2003	2010	8	48,110.92
57	1.02	M	193	3.08	1.83	1,869,891.19	2003	2010	8	233,736.40
58	5.27	M	198	2.27	1.02	5,354,255.80	2003	2006	4	1,338,563.95
59	0.40	M	198	4.55	3.30	1,318,006.30	2007	2013	7	188,286.61
60	2.41	M	198	2.15	0.90	2,179,740.78	2007	2013	7	311,391.54
61	3.04	M	209	4.32	3.07	9,323,270.02	2010	2013	4	2,330,817.51
62	0.09	M	209	2.95	1.70	153,147.12	2010	2013	4	38,286.78
63	0.15	M	209	1.88	0.63	94,756.00	2007	2012	6	15,792.67
64	0.88	M	209	2.60	1.35	1,187,318.62	2008	2013	6	197,886.44
65	0.28	M	209	3.11	1.86	515,581.44	2008	2013	6	85,930.24
66	0.55	M	210	5.48	4.23	2,340,169.19	2002	2013	12	195,014.10
67	0.13	M	210	3.33	2.08	270,025.21	2010	2013	4	67,506.30
68	0.08	M	210	4.35	3.10	248,184.22	2006	2013	8	31,023.03
69	0.16	B	210	2.27	1.02	163,115.55	2005	2013	9	18,123.95
70	0.74	B	210	2.23	0.98	725,453.06	2000	2010	11	65,950.28
71	2.09	M	211	2.36	1.11	2,313,363.53	2002	2013	12	192,780.29
72	0.13	B	211	3.27	2.02	267,866.13	2005	2013	9	29,762.90
73	1.07	B	212	3.45	2.20	2,360,867.33	2005	2013	9	262,318.59
74	0.77	B	212	2.07	0.82	632,468.54	2008	2013	6	105,411.42
75	0.35	M	213	4.07	2.82	991,675.43	2000	2011	12	82,639.62
76	0.04	M	213	3.11	1.86	74,461.17	2000	2008	9	8,273.46
77	0.16	B	213	3.16	1.91	305,663.57	2008	2013	6	50,943.93

78	0.09	M	214	3.23	1.98	178,084.16	2010	2013	4	44,521.04
79	0.54	M	214	3.55	2.30	1,233,574.19	2004	2010	7	176,224.88
80	0.16	B	214	3.47	2.22	355,982.47	2007	2013	7	50,854.64
81	1.84	B	214	3.23	1.98	3,638,059.77	2005	2008	4	909,514.94
82	0.19	B	214	2.81	1.56	295,851.39	2008	2013	6	49,308.56
83	0.09	M	215	2.71	1.46	131,321.18	2010	2013	4	32,830.29
84	0.19	B	215	2.76	1.51	286,710.72	2008	2013	6	47,785.12
85	0.19	B	215	3.30	2.05	388,914.39	2009	2013	5	77,782.88
86	0.22	B	216	2.22	0.97	212,449.53	2009	2013	5	42,489.91
87	0.08	B	218	3.97	2.72	217,993.57	2010	2013	4	54,498.39
88	0.41	M	220	2.91	1.66	679,176.48	2007	2013	7	97,025.21
89	0.77	M	222	1.78	0.53	406,874.67	2012	2013	2	203,437.34
90	0.49	M	223	1.61	0.36	174,252.76	2012	2013	2	87,126.38
91	0.34	M	225	3.06	1.81	621,517.65	2005	2008	4	155,379.41
92	0.29	B	225	3.51	2.26	654,203.29	2007	2013	7	93,457.61
93	0.11	B	227	2.66	1.41	154,694.06	2007	2013	7	22,099.15
94	0.31	M	230	2.84	1.59	496,191.24	2006	2013	8	62,023.90
95	0.20	M	232	3.91	2.66	532,666.21	2009	2013	5	106,533.24
96	0.03	M	235	1.80	0.55	16,412.90	2007	2011	5	3,282.58
97	0.05	M	237	2.54	1.29	64,689.19	2007	2011	5	12,937.84
98	0.03	M	238	2.86	1.61	48,195.59	2008	2011	4	12,048.90
99	0.21	M	241	1.93	0.68	143,035.80	2010	2013	4	35,758.95
100	0.27	M	244	2.61	1.36	365,011.42	2002	2008	7	52,144.49
101	0.07	M	247	8.80	7.55	528,788.31	2002	2013	12	44,065.69
102	1.15	M	247	2.41	1.16	1,336,980.41	2007	2013	7	190,997.20
103	0.44	B	258	2.87	1.62	709,306.42	2008	2012	5	141,861.28
104	1.02	M	263	3.72	2.47	2,529,974.48	2003	2013	11	229,997.68
105	0.92	B	263	1.98	0.73	674,496.96	2011	2013	3	224,832.32
106	0.13	M	265	4.02	2.77	372,232.58	2003	2013	11	33,839.33
107	0.45	M	268	2.33	1.08	489,683.23	2003	2013	11	44,516.66
108	0.59	M	273	4.37	3.12	1,839,305.47	2007	2013	7	262,757.92
109	0.59	B	273	2.23	0.98	578,125.40	2005	2013	9	64,236.16
110	0.15	B	274	2.23	0.98	147,030.05	2005	2013	9	16,336.67
111	0.15	B	274	1.56	0.31	46,058.78	2011	2013	3	15,352.93
112	0.24	B	276	2.06	0.81	193,458.79	2011	2013	3	64,486.26
113	0.84	B	281	2.02	0.77	649,490.75	2009	2013	5	129,898.15
114	0.23	B	281	1.81	0.56	131,199.88	2009	2013	5	26,239.98
115	0.21	T	8	2.24	0.99	208,744.22	2013	2013	1	208,744.22
116	0.20	T	11	3.02	1.77	354,318.20	2010	2013	4	88,579.55
117	0.12	T	11	2.60	1.35	162,291.56	2000	2013	14	11,592.25
118	0.13	T	17	3.10	1.85	240,072.25	2005	2013	9	26,674.69
119	1.06	T	20	2.44	1.19	1,261,764.75	2001	2013	13	97,058.83
120	0.86	T	22	2.14	0.89	765,410.44	2003	2009	7	109,344.35
121	0.21	T	24	3.05	1.80	378,465.40	2003	2009	7	54,066.49
122	1.88	T	44	2.47	1.22	2,301,309.11	2008	2013	6	383,551.52
123	1.70	T	44	1.63	0.38	648,913.83	2005	2013	9	72,101.54
124	0.96	T	44	1.76	0.51	493,506.79	2007	2010	4	123,376.70
125	0.59	T	50	2.05	0.80	473,184.71	2010	2013	4	118,296.18
126	0.36	T	53	2.50	1.25	446,407.15	2010	2013	4	111,601.79
127	0.13	T	56	1.99	0.74	96,738.98	2010	2013	4	24,184.74
128	0.21	T	56	2.29	1.04	217,364.59	2000	2013	14	15,526.04
129	0.36	T	60	2.45	1.20	431,346.91	2007	2013	7	61,620.99
130	0.48	T	63	2.39	1.14	545,700.07	2011	2013	3	181,900.02
131	0.69	T	63	1.67	0.42	288,454.03	2006	2010	5	57,690.81
132	0.08	T	65	1.60	0.35	29,005.67	2010	2013	4	7,251.42
133	0.14	T	65	1.83	0.58	80,269.78	2010	2013	4	20,067.44

134	0.15	T	65	1.27	0.02	3,016.54	2006	2011	6	502.76
135	0.40	T	79	1.29	0.04	15,105.56	2007	2013	7	2,157.94
136	0.05	T	86	1.41	0.16	7,842.24	2005	2013	9	871.36
137	0.06	T	87	2.27	1.02	61,493.25	2007	2013	7	8,784.75
138	0.47	T	90	1.56	0.31	146,277.88	2008	2012	5	29,255.58
139	0.24	T	90	2.80	1.55	368,306.88	2008	2012	5	73,661.38
140	0.16	T	93	2.55	1.30	211,339.70	2008	2013	6	35,223.28
141	0.14	T	93	3.04	1.79	245,625.42	2003	2010	8	30,703.18
142	0.16	T	93	1.89	0.64	102,097.38	2002	2010	9	11,344.15
143	0.34	T	94	2.27	1.02	342,737.77	2003	2010	8	42,842.22
144	0.07	T	94	1.92	0.67	46,621.58	2002	2010	9	5,180.18
145	0.27	T	98	1.88	0.63	169,048.59	2010	2013	4	42,262.15
146	1.24	T	98	1.92	0.67	828,578.78	2010	2013	4	207,144.69
147	0.05	T	100	2.29	1.04	52,055.74	2011	2013	3	17,351.91
148	0.61	T	103	3.14	1.89	1,149,933.14	2009	2013	5	229,986.63
149	0.10	T	105	1.40	0.15	14,558.35	2000	2008	9	1,617.59
150	0.09	T	109	3.79	2.54	228,182.74	2002	2008	7	32,597.53
151	1.93	T	109	2.32	1.07	2,068,437.32	2008	2013	6	344,739.55
152	11.89	T	110	3.68	2.43	28,897,443.56	2008	2012	5	5,779,488.71
153	0.31	T	110	2.57	1.32	414,151.08	2008	2013	6	69,025.18
154	0.16	T	112	3.43	2.18	352,346.38	2008	2012	5	70,469.28
155	0.79	T	113	1.45	0.20	158,572.48	2012	2013	2	79,286.24
156	1.36	T	113	2.18	0.93	1,264,073.52	2000	2008	9	140,452.61
157	0.31	T	114	3.71	2.46	750,016.89	2006	2012	7	107,145.27
158	0.30	T	115	2.52	1.27	379,597.56	2000	2008	9	42,177.51
159	0.73	T	115	2.96	1.71	1,250,715.87	2010	2013	4	312,678.97
160	0.22	T	116	3.51	2.26	496,369.65	2006	2010	5	99,273.93
161	3.19	T	117	3.00	1.75	5,573,260.85	2008	2013	6	928,876.81
162	0.09	T	117	5.95	4.70	423,079.16	2004	2010	7	60,439.88
163	0.28	T	117	3.37	2.12	596,438.83	2000	2006	7	85,205.55
164	0.18	T	117	2.81	1.56	280,449.17	2000	2010	11	25,495.38
165	0.22	T	118	4.90	3.65	802,565.65	2008	2013	6	133,760.94
166	0.47	T	119	3.41	2.16	1,017,957.04	2000	2010	11	92,541.55
167	0.88	T	119	2.32	1.07	944,446.96	2000	2008	9	104,938.55
168	0.06	T	122	12.69	11.44	686,163.98	2006	2012	7	98,023.43
169	0.19	T	124	2.24	0.99	187,821.19	2008	2013	6	31,303.53
170	0.17	T	127	6.03	4.78	812,062.97	2004	2008	5	162,412.59
171	0.37	T	127	2.39	1.14	418,168.81	2004	2013	10	41,816.88
172	0.08	T	127	3.01	1.76	140,907.06	2010	2013	4	35,226.77
173	0.27	T	128	2.47	1.22	329,366.13	2007	2012	6	54,894.36
174	0.03	T	128	2.27	1.02	30,641.42	2010	2013	4	7,660.36
175	0.83	T	129	6.89	5.64	4,690,830.92	2008	2013	6	781,805.15
176	0.23	T	129	2.86	1.61	375,888.54	2008	2013	6	62,648.09

Appendix C: Transect of NASADEM and TanDEM-X

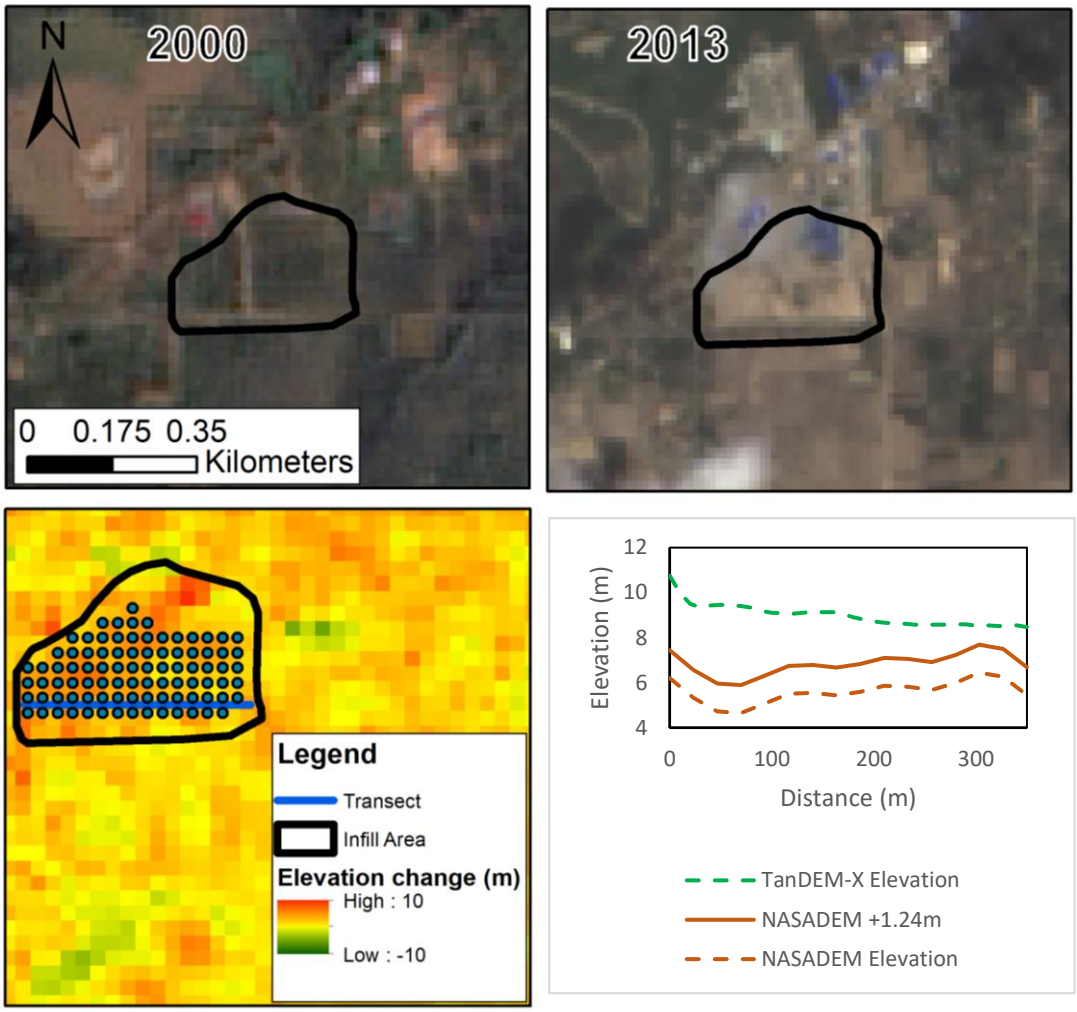


N
2000
2013
0 0.275 0.55
Kilometers

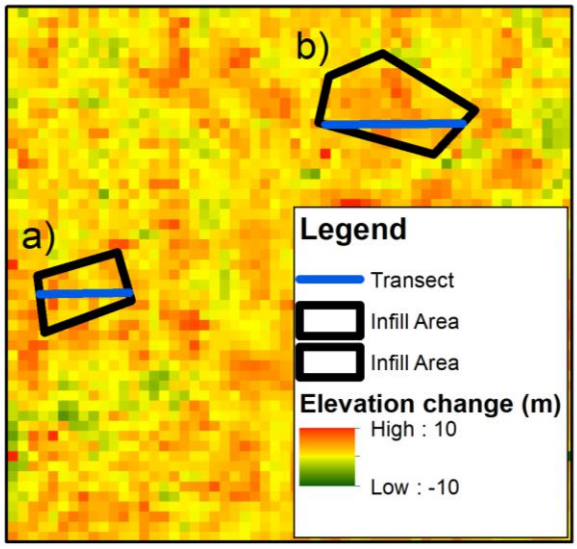
b)
a)
Legend
Transect
Infill Area
Infill Area
Elevation change (m)
High : 10
Low : -10

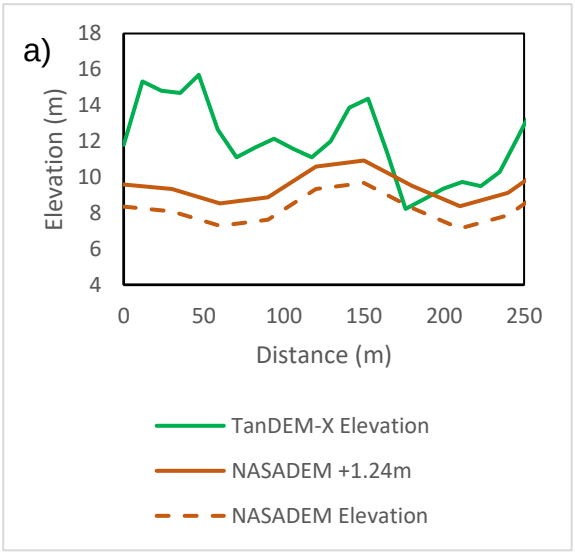
a)
Elevation (m)
18
16
14
12
10
8
6
4
0
50
100
150
200
250
Distance (m)
TanDEM-X Elevation
NASADEM +1.24m
NASADEM Elevation

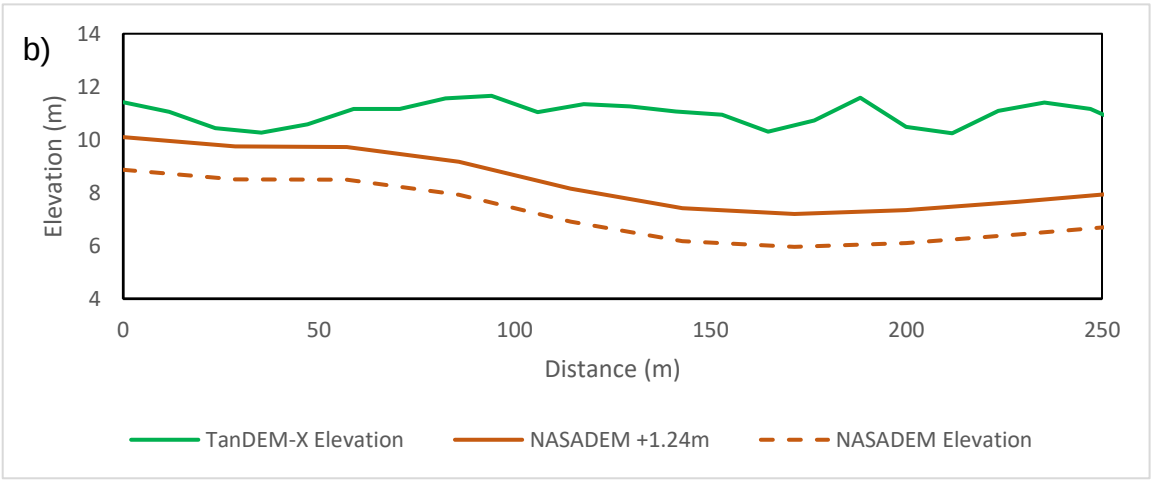
b)
Elevation (m)
14
12
10
8
6
4
0
50
100
150
200
250
Distance (m)
TanDEM-X Elevation
NASADEM +1.24m
NASADEM Elevation

Appendix D: Quarry and floodplain excavation sites

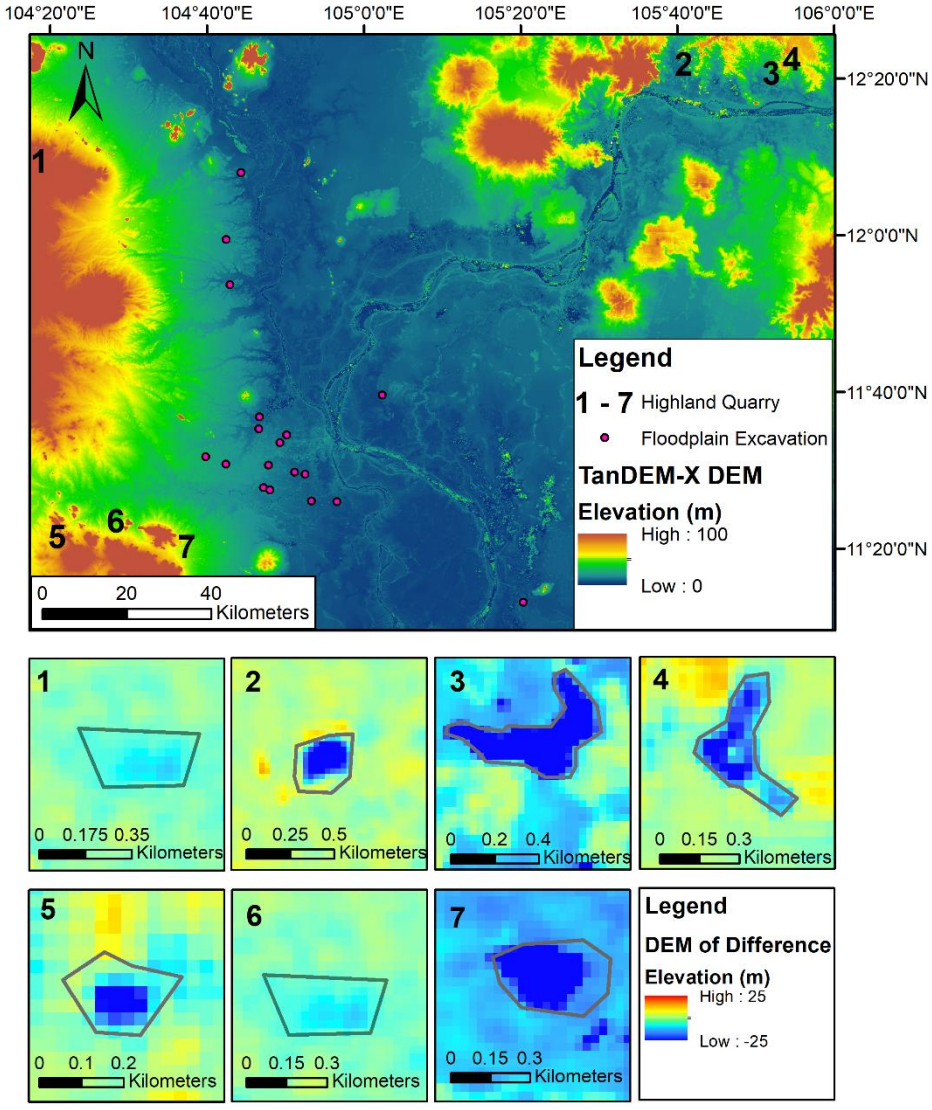

Appendix E: Infill volumes in relation to closest main river channel

River	Volume infill nearby 2000-2013 ($x10^6$ m^3)
Bassac	27.72±1.38
Mekong	108.96±10.53
Tonle Sap	46.43±5.67
Total	**183.11 ± 17.58**

Appendix F: Yearly FPI rates

Year	Volume of infill ($x10^6$ m3)
2000	1.01±0.12
2001	1.82±0.13
2002	2.30±0.31
2003	5.88±0.74
2004	6.43±0.78
2005	8.66±1.00
2006	9.31±1.07
2007	11.74±1.22
2008	21.24±1.87
2009	20.24±1.80
2010	27.06±2.35
2011	25.04±2.20
2012	24.91±2.22
2013	17.99±1.77

Bibliography

- Anthony, E.J., Brunier, G., Besset, M., Goichot, M., Dussouillez, P. and Nguyen, V.L., (2015) Linking rapid erosion of the Mekong River delta to human activities. *Scientific reports*, *5*(1), pp.1-12.
- Bagnardi, M., González, P.J. and Hooper, A., (2016). High-resolution digital elevation model from tri-stereo Pleiades-1 satellite imagery for lava flow volume estimates at Fogo Volcano. *Geophysical Research Letters*, *43*(12), pp.6267-6275.
- BBC (2017) Cambodia bans sand exports permanently (13 July 2017) [online]. Available at: <https://www.bbc.com/news/business-40590695> [Accessed 14 July 2020].
- BBC (2019) How the scramble for sand is destroying the Mekong (19 December 2019) [online]. Available at: <https://www.bbc.co.uk/news/business-50629100> [Accessed 14 July 2020].
- Beasley, I., Pollock, K., Jefferson, T.A., Arnold, P., Morse, L., Yim, S., Lor Kim, S. and Marsh, H., (2013) Likely future extirpation of another Asian river dolphin: The critically endangered population of the Irrawaddy dolphin in the Mekong River is small and declining. Marine Mammal Science, 29(3).
- Bendixen, M., Best, J., Hackney, C. and Iversen, L.L., (2019). Time is running out for sand.
- Berthier, E., Arnaud, Y., Kumar, R., Ahmad, S., Wagnon, P. and Chevallier, P., (2007). Remote sensing estimates of glacier mass balances in the Himachal Pradesh (Western Himalaya, India). *Remote Sensing of Environment*, *108*(3), pp.327-338.
- Bird, K.D.C (unpublished dissertation, University of Exeter, 2018). Remote Sensing analysis of morphological changes in the Cambodian Mekong River, since the introduction of in-channel sand mining.
- Brunier, G., Anthony, E.J., Goichot, M., Provansal, M. and Dussouillez, P., (2014) Recent morphological changes in the Mekong and Bassac river channels, Mekong delta: The marked impact of river-bed mining and implications for delta destabilisation. *Geomorphology*, *224*, pp.177-191.

- Bull, W.B. and Scott, K.M., (1974) Impact of mining gravel from urban stream beds in the southwestern United States. *Geology*, *2*(4), pp.171-174.
- Chen, Y., Zhang, G., Ding, X. and Li, Z., (2000). Monitoring earth surface deformations with InSAR technology: principles and some critical issues. Journal of Geospatial Engineering, 2(1), pp.3-22.
- Costa-Cabral, M.C., Richey, J.E., Goteti, G., Lettenmaier, D.P., Feldkötter, C. and Snidvongs, A., (2008). Landscape structure and use, climate, and water movement in the Mekong River basin. *Hydrological Processes: An International Journal*, *22*(12), pp.1731-1746.
- Crippen, R., Buckley, S., Agram, P., Belz, E., Gurrola, E., Hensley, S., Kobrick, M., Lavalle, M., Martin, J., Neumann, M. and Nguyen, Q., (2016). NASADEM global elevation model: methods and progress. Int Arch Photogramm Remote Sens Spat Inf Sci, 41, p.B4.
- Darby, S.E., Hackney, C.R., Leyland, J., Kummu, M., Lauri, H., Parsons, D.R., Best, J.L., Nicholas, A.P. and Aalto, R., (2016) Fluvial sediment supply to a mega-delta reduced by shifting tropical-cyclone activity. *Nature*, *539*(7628), pp.276-279.
- Díaz-Varela, R.A., De la Rosa, R., León, L. and Zarco-Tejada, P.J., (2015). High-resolution airborne UAV imagery to assess olive tree crown parameters using 3D photo reconstruction: application in breeding trials. Remote Sensing, 7(4), pp.4213-4232.
- Doyle, S.E. (2012) City of Water. Nakhara: Journal of Environmental Design and Planning, 8, pp.135-154.
- Du, J.L., Yang, S.L. and Feng, H., (2016) Recent human impacts on the morphological evolution of the Yangtze River delta foreland: A review and new perspectives. *Estuarine, Coastal and Shelf Science*, *181*, pp.160-169.
- Dung, N.M., (2011). *River sand mining and management: a case of Cau river in Bac Ninh province, Vietnam*. EEPSEA, IDRC Regional Office for Southeast and East Asia, Singapore, SG.
- EO (2020) TDX (TanDEM-X: TerraSAR-X add-on for Digital Elevation Measurement) [online]. Available at:

<https://earth.esa.int/web/eoportal/satellite-missions/t/tandem-x> [Accessed 12 June 2020].

- ESRI (2003) Mean Sea Level, GPS, and the Geoid [online]. Available at: https://www.esri.com/news/arcuser/0703/geoid1of3.html [Accessed 14/11/2020].
- Franke, M., (2014). *When one country's land gain is another country's land loss...: The social, ecological and economic dimensions of sand extraction in the context of world-systems analysis exemplified by Singapore's sand imports* (No. 36/2014). Working Paper, Institute for International Political Economy Berlin.
- Global Witness. (2010) Shifting sand: How Singapore's demand for Cambodian sand threatens ecosystems and undermines good governance. Global Witness, London, p.48.
- Google (2020) Google Earth Cambodia study area, range of scales [online]. Available at: <https://earth.google.com/web/> [Accessed 2019-2020].
- Gorokhovich, Y. and Voustianiouk, A., (2006) Accuracy assessment of the processed SRTM-based elevation data by CGIAR using field data from USA and Thailand and its relation to the terrain characteristics. Remote sensing of Environment, 104(4), pp.409-415.
- Grohmann, C.H., (2018). Evaluation of TanDEM-X DEMs on selected Brazilian sites: Comparison with SRTM, ASTER GDEM and ALOS AW3D30. Remote Sensing of Environment, 212, pp.121-133.
- Gupta, A. and Liew, S.C. (2007) The Mekong from satellite imagery: a quick look at a large river. Geomorphology, 85(3-4), pp.259-274.
- Hackney, C., Bendixen, M., Best, J. and Iversen, L., (2019). Time is running out for sand.
- Hackney, C.R., Darby, S.E., Parsons, D.R., Leyland, J., Best, J.L., Aalto, R., Nicholas, A.P. and Houseago, R.C., (2020) River bank instability from unsustainable sand mining in the lower Mekong River. *Nature Sustainability*, pp.1-9.

- Hayakawa, Y.S., Oguchi, T. and Lin, Z., (2008) Comparison of new and existing global digital elevation models: ASTER G-DEM and SRTM-3. *Geophysical Research Letters*, *35*(17).
- Hecht, J.S., Lacombe, G., Arias, M.E., Dang, T.D. and Piman, T., (2019) Hydropower dams of the Mekong River basin: A review of their hydrological impacts. *Journal of hydrology*, *568*, pp.285-300.
- Hoang, L.P., Lauri, H., Kummu, M., Koponen, J., Van Vliet, M.T., Supit, I., Leemans, R., Kabat, P. and Ludwig, F., (2016). Mekong River flow and hydrological extremes under climate change. *Hydrology and Earth System Sciences*, *20*(7), pp.3027-3041.
- Hooper, A., Bekaert, D., Spaans, K. and Arıkan, M., (2012). Recent advances in SAR interferometry time series analysis for measuring crustal deformation. Tectonophysics, 514, pp.1-13.
- Huong, H.T.L. and Pathirana, A., (2013). Urbanization and climate change impacts on future urban flooding in Can Tho city, Vietnam. *Hydrology and Earth System Sciences*, *17*(1), p.379.
- Jordan, C., Tiede, J., Lojek, O., Visscher, J., Apel, H., Nguyen, H.Q., Quang, C.N.X. and Schlurmann, T., (2019). Sand mining in the Mekong Delta revisited-current scales of local sediment deficits. *Scientific reports*, *9*(1), pp.1-14.
- S. M. Buckley, P. S. Agram, J. E. Belz, R. E. Crippen, E. M. Gurrola, S. Hensley, M. Kobrick, M. Lavalle, J. M. Martin, M. Neumann, Q. D. Nguyen, P. A. Rosen, J. G. Shimada, M. Simard, W. W. Tung (2020), NASADEM. [online]. Available at: <https://lpdaac.usgs.gov/documents/592/NASADEM_User_Guide_V1.pdf> [Accessed 08/11/2020].
- Koehnken, L. and Rintoul, M., (2018). Impacts of sand mining on ecosystem structure, process and biodiversity in rivers. *World Wildlife Fund International*.
- Kondolf, G.M. (1997) Profile: hungry water: effects of dams and gravel mining on river channels. Environmental management, 21(4), pp.533-551.

- Kondolf, G.M., (1994) Geomorphic and environmental effects of instream gravel mining. *Landscape and Urban planning*, *28*(2-3), pp.225-243.
- Kondolf, G.M., Rubin, Z.K. and Minear, J.T., (2014) Dams on the Mekong: Cumulative sediment starvation. *Water Resources Research*, *50*(6), pp.5158-5169.
- Kondolf, G.M., Schmitt, R.J., Carling, P., Darby, S., Arias, M., Bizzi, S., Castelletti, A., Cochrane, T.A., Gibson, S., Kummu, M. and Oeurng, C., (2018) Changing sediment budget of the Mekong: Cumulative threats and management strategies for a large river basin. *Science of the total environment*, *625*, pp.114-134.
- Kubo, S. (2008) Geomorphological features and subsurface geology of the Lower Mekong Plain around Phnom Penh City, Cambodia (South East Asia). *Rev. Geogr. Acad.* 2, 20–32.
- Kummu, M., Lu, X., Wang, J.J. and Varis, O., (2010) Basin-wide sediment trapping efficiency of emerging reservoirs along the Mekong. *Geomorphology*, *119*(3-4), pp.181-197.
- Lamb, V., Marschke, M. and Rigg, J., (2019). Trading sand, undermining lives: Omitted livelihoods in the global trade in sand. *Annals of the American Association of Geographers*, *109*(5), pp.1511-1528.
- Larson, C., (2018). Asia's hunger for sand takes toll on ecology.
- Leeuw, J., Shankman, D., Wu, G., de Boer, W.F., Burnham, J., He, Q., Yesou, H. and Xiao, J., (2009) Strategic assessment of the magnitude and impacts of sand mining in Poyang Lake, China. *Regional Environmental Change*, *10*(2), pp.95-102.
- Lillesand, T., Kiefer, R.W. and Chipman, J., (2015) *Remote sensing and image interpretation*. John Wiley & Sons.
- Magee, D., (2011). The dragon upstream: China’s role in Lancang-Mekong development. In *Politics and development in a transboundary watershed* (pp. 171-193). Springer, Dordrecht.
- Marschke, M., (2017). Exploring rural livelihoods through the lens of coastal fishers. In *The Handbook of Contemporary Cambodia* (pp. 121-130). Routledge.

- Mekong River Commission (MRC), (2011). Assessment of Basin-Wide Development Scenarios—Main Report. *Mekong River Commission (MRC), Vientiane, Lao PDR*.
- Mgbako, C., Gao, R.E., Joynes, E. and Cave, A., (2010). Forced eviction and resettlement in Cambodia: case studies from Phnom Penh. *Wash. U. Global Stud. L. Rev.*, *9*, p.39.
- Mialhe, F., Gunnell, Y., Navratil, O., Choi, D., Sovann, C., Lejot, J., Gaudou, B., Se, B. and Landon, N., (2019). Spatial growth of Phnom Penh, Cambodia (1973–2015): Patterns, rates, and socio-ecological consequences. *Land Use Policy*, *87*, p.104061.
- Minderhoud, P.S.J., Coumou, L., Erkens, G., Middelkoop, H. and Stouthamer, E., (2019). Mekong delta much lower than previously assumed in sea-level rise impact assessments. Nature communications, 10(1), pp.1-13.
- Miyazawa, N., Sunada, K. and Sokhem, P., (2008). Bank erosion in the Mekong River Basin: Is bank erosion in my town caused by the activities of my neighbours. *Kummu, M. et al.(eds.) Modern Myths of the Mekong. A critical review of water and development concepts, principles and policies. Water & Development Publications, Helsinki University of Technology*, pp.19-26.
- Mom, K. and Ongsomwang, S., (2016). URBAN GROWTH MODELING OF PHNOM PENH, CAMBODIA USING SATELLITE IMAGERIES AND A LOGISTIC REGRESSION MODEL. *Suranaree Journal of Science & Technology*, *23*(4).
- Musa, Z.N., Popescu, I. and Mynett, A., (2015) A review of applications of satellite SAR, optical, altimetry and DEM data for surface water modelling, mapping and parameter estimation. *Hydrology and Earth System Sciences*, *19*(9), p.3755.
- Nam, S., (2017). Urban speculation, economic openness, and market experiments in Phnom Penh. *positions: asia critique*, *25*(4), pp.645-667.
- Newport, B.D. (1974) State-of-the art: sand and gravel industry (Vol. 1). National Environmental Research Center, Office of Research and

Development, US Environmental Protection Agency; for sale by the Supt. of Docs., US Govt. Print. Off., Washington.

- NGA. EGM2008 - WGS 84 Version [online]. Available at: https://earth-info.nga.mil/GandG/wgs84/gravitymod/egm2008/egm08_wgs84.html [Accessed 12/12/2020].
- Nguyen M. D. (2011) River Sand Mining and Management : a Case of Cau River in Bac Ninh Province, Vietnam. Singapore, EEPSEA Research Reports, 61 p.
- Nguyen, V.L., Ta, T.K.O. and Tateishi, M., (2000) Late Holocene depositional environments and coastal evolution of the Mekong River Delta, Southern Vietnam. *Journal of Asian Earth Sciences*, *18*(4), pp.427-439.
- Ohimain, E.I., (2004). Environmental impacts of dredging in the Niger Delta. *Terra et Aqua*, *97*, pp.9-19.
- Orr, S., Pittock, J., Chapagain, A. and Dumaresq, D. (2012) Dams on the Mekong River: Lost fish protein and the implications for land and water resources. Global Environmental Change, 22(4), pp.925-932.
- Padmalal, D., Maya, K., Sreebha, S. and Sreeja, R. (2008) Environmental effects of river sand mining: a case from the river catchments of Vembanad lake, Southwest coast of India. Environmental geology, 54(4), pp.879-889.
- Pavlis, N.K., Holmes, S.A., Kenyon, S.C. and Factor, J.K., (2012). The development and evaluation of the Earth Gravitational Model 2008 (EGM2008). Journal of geophysical research: solid earth, 117(B4).
- Peduzzi, P., (2014). Sand, rarer than one thinks. *Environmental Development*, *11*, pp.208-218.
- Pierdet, C., (2008). Waterside Margins and Urban Policies in the Center of Phnom Penh (Cambodia). *Autrepart*, (1), pp.123-136.
- Piesse, M., (2016). Livelihoods and food security on the Mekong River. *Future Direction International, Strategic Analysis Paper,(May 26, 2016). Accessed June*, *13*.

- Pokhrel, Y., Burbano, M., Roush, J., Kang, H., Sridhar, V. and Hyndman, D.W., (2018). A review of the integrated effects of changing climate, land use, and dams on Mekong river hydrology. *Water*, *10*(3), p.266.
- Purinton, B. and Bookhagen, B., (2017). Validation of digital elevation models (DEMs) and comparison of geomorphic metrics on the southern Central Andean Plateau. *Earth Surface Dynamics*, *5*(2).
- Purinton, B. and Bookhagen, B., (2018). Measuring decadal vertical land-level changes from SRTM-C (2000) and TanDEM-X (~ 2015) in the south-central Andes. *Earth Surface Dynamics*, *6*(4), p.971.
- Rinaldi, M., Wyżga, B. and Surian, N., (2005) Sediment mining in alluvial channels: physical effects and management perspectives. *River research and applications*, *21*(7), pp.805-828.
- Rodriguez, E., Morris, C.S. and Belz, J.E., (2006). A global assessment of the SRTM performance. *Photogrammetric Engineering & Remote Sensing*, *72*(3), pp.249-260.
- Schneider, H., (2011) The conflict for Boeng Kak lake in Phnom Penh, Cambodia. *Pacific News, 36 (July/August), 4*, *10*.
- Steinberger, J.K., Krausmann, F. and Eisenmenger, N., (2010). Global patterns of materials use: A socioeconomic and geophysical analysis. *Ecological Economics*, *69*(5), pp.1148-1158.
- Stone, R., (2011). Mayhem on the Mekong.
- Stone, R., (2016). Dam-building threatens Mekong fisheries.
- Sutherland, W.J., Barnard, P., Broad, S., Clout, M., Connor, B., Côté, I.M., Dicks, L.V., Doran, H., Entwistle, A.C., Fleishman, E. and Fox, M., (2017). A 2017 horizon scan of emerging issues for global conservation and biological diversity. *Trends in ecology & evolution*, *32*(1), pp.31-40.
- Szabo, S., Brondizio, E., Renaud, F.G., Hetrick, S., Nicholls, R.J., Matthews, Z., Tessler, Z., Tejedor, A., Sebesvari, Z., Foufoula-Georgiou, E. and Da Costa, S., (2016). Population dynamics, delta vulnerability and environmental change: comparison of the Mekong, Ganges–Brahmaputra and Amazon delta regions. *Sustainability Science*, *11*(4), pp.539-554.

- Tachikawa, T., Kaku, M., Iwasaki, A., Gesch, D.B., Oimoen, M.J., Zhang, Z., Danielson, J.J., Krieger, T., Curtis, B., Haase, J. and Abrams, M., (2011). *ASTER global digital elevation model version 2-summary of validation results*. NASA.
- Torres, A., Brandt, J., Lear, K. and Liu, J., (2017). A looming tragedy of the sand commons. *Science*, *357*(6355), pp.970-971.
- Uhlemann, S., Kuras, O., Richards, L. A., Naden, E. & Polya, D. A. (2017) Electrical resistivity tomography determines the spatial distribution of clay layer thickness and aquifer vulnerability, Kandal Province, Cambodia. *J. Asian Earth Sci.* 147, 402–414.
- Un, K., (2011). Cambodia: Moving away from democracy? *International Political Science Review*, *32*(5), pp.546-562.
- UN. (2020) UN, Land deformation mapping using DInSAR. [online]. Available at: <https://un-spider.org/links-and-resources/data-sources/daotm-land-deformation> [Accessed 14 November 2020].
- United Nations. (2019) UN Comtrade. [online]. Available at: <https://comtrade.un.org/> [Accessed 19 October 2019].
- USGS (2020) NASADEM SRTM-only Height and Height Precision Product [online](PI: Sean Buckley). Available at: <https://lpdaac.usgs.gov/products/nasadem_shhpv001/> [Accessed 28 August 2020].
- USGS. USGS EROS Archive - Digital Elevation - Shuttle Radar Topography Mission (SRTM) 1 Arc-Second Global.
- Wendleder, A., Wessel, B., Roth, A., Breunig, M., Martin, K. and Wagenbrenner, S., (2012). TanDEM-X water indication mask: Generation and first evaluation results. *IEEE Journal of Selected Topics in Applied Earth Observations and Remote Sensing*, *6*(1), pp.171-179.
- Wessel, B., Gruber, A., Huber, M., Breunig, M., Wagenbrenner, S., Wendleder, A. and Roth, A., (2014) July. Validation of the absolute height accuracy of TanDEM-X DEM for moderate terrain. In *2014 IEEE Geoscience and Remote Sensing Symposium* (pp. 3394-3397). IEEE.
- Zandbergen, P. (2008) Applications of shuttle radar topography mission elevation data. *Geography Compass*, *2*(5), pp.1404-1431.

- Zhao, J.K., Chen, L. and Yang, Y.X., (2017) December. Effects of the human activities on the water level process of the Poyang Lake. In *IOP Conference Series: Earth and Environmental Science* (Vol. 100, No. 1, p. 012216). IOP Publishing.
- Ziv, G., Baran, E., Nam, S., Rodríguez-Iturbe, I. and Levin, S.A. (2012) Trading-off fish biodiversity, food security, and hydropower in the Mekong River Basin. Proceedings of the National Academy of Sciences, 109(15), pp.5609-5614.